

CEX-62.12

BC

AEC Category: HEALTH AND SAFETY

*See page 6  
General  
Comments*

# CEX-62.12

## OPERATION BREN

ENERGY AND ANGULAR DISTRIBUTION  
OF NEUTRONS AND GAMMA RAYS—  
OPERATION BREN

J. H. Thorngate, J. A. Auxier,  
F. F. Haywood, and S. Helf

**DISTRIBUTION STATEMENT A**  
Approved for Public Release  
Distribution Unlimited

20000912 087

LOVELACE FOUNDATION  
Issuance Date: February 1967  
DOCUMENT NUMBER

CIVIL EFFECTS TEST OPERATIONS  
U.S. ATOMIC ENERGY COMMISSION

DTIC QUALITY INSPECTED 4

Reproduced From  
Best Available Copy

JAN 12 1968

29657

## LEGAL NOTICE

This report was prepared as an account of Government sponsored work. Neither the United States, nor the Commission, nor any person acting on behalf of the Commission:

A. Makes any warranty or representation, expressed or implied, with respect to the accuracy, completeness, or usefulness of the information contained in this report, or that the use of any information, apparatus, method, or process disclosed in this report may not infringe privately owned rights; or

B. Assumes any liabilities with respect to the use of, or for damages resulting from the use of any information, apparatus, method, or process disclosed in this report.

As used in the above, "person acting on behalf of the Commission" includes any employee or contractor of the Commission, or employee of such contractor, to the extent that such employee or contractor of the Commission, or employee of such contractor prepares, disseminates, or provides access to, any information pursuant to his employment or contract with the Commission, or his employment with such contractor.

Printed in USA. Price ~~\$8.00~~. Available from the Clearinghouse for Federal Scientific and Technical Information, National Bureau of Standards, U. S. Department of Commerce, Springfield, Virginia 22151.

# ENERGY AND ANGULAR DISTRIBUTION OF NEUTRONS AND GAMMA RAYS— OPERATION BREN

By

J. H. Thorngate, J. A. Auxier,  
F. F. Haywood, and S. Helf

Approved by: L. J. DEAL  
Chief  
Civil Effects Branch  
U. S. Atomic Energy Commission

Health Physics Division  
Oak Ridge National Laboratory  
Oak Ridge, Tennessee

## NOTICE

This report is published in the interest of providing information which may prove of value to the reader in his study of effects data derived principally from nuclear weapons tests and from experiments designed to duplicate various characteristics of nuclear weapons.

This document is based on information available at the time of preparation which may have subsequently been expanded and re-evaluated. Also, in preparing this report for publication, some classified material may have been removed. Users are cautioned to avoid interpretations and conclusions based on unknown or incomplete data.

## ABSTRACT

In order to understand better the transmission and scattering of radiation in air, a series of measurements were made to determine the energy and angular distributions at large distances from the Oak Ridge National Laboratory Health Physics Research Reactor and an 800-curie  $^{60}\text{Co}$  source. Both sources were positioned at various elevations on a 1527-ft tower while data were acquired by detectors located in collimators at either 750 or 1000 yd from the base of the tower. Good measurements were obtained of neutron and gamma-ray doses from the HPRR and gamma doses from the  $^{60}\text{Co}$  source as a function of angle of incidence. Scintillation spectra of the gamma rays from the  $^{60}\text{Co}$  source were also obtained. No useful spectrum information was obtained from the HPRR.

## ACKNOWLEDGMENTS

The help of F. W. Sanders, W. H. Shinpaugh, and E. T. Loy during the course of the experimental measurements is gratefully acknowledged.

## CONTENTS

ABSTRACT . . . . .	5
ACKNOWLEDGMENTS . . . . .	6
CHAPTER 1 INTRODUCTION . . . . .	13
CHAPTER 2 APPARATUS . . . . .	14
2.1 Tower . . . . .	14
2.2 Radiation Sources . . . . .	14
2.2.1 HPRR. . . . .	14
2.2.2 Cobalt-60 Source. . . . .	16
2.3 Collimators. . . . .	16
2.4 Dosimetry . . . . .	24
2.4.1 Neutron Dosimeter . . . . .	24
2.4.2 HPRR Gamma Dosimeter. . . . .	24
2.4.3 Cobalt-60 Gamma Dosimeter . . . . .	29
2.5 Spectrometry . . . . .	29
2.5.1 Neutron Spectrometer. . . . .	29
2.5.2 HPRR Gamma Spectrometer . . . . .	32
2.5.3 Cobalt-60 Gamma Spectrometer. . . . .	37
2.6 Normalization of Radiation Field Variations. . . . .	37
2.6.1 HPRR. . . . .	37
2.6.2 Cobalt-60 . . . . .	39
CHAPTER 3 PROCEDURES . . . . .	42
3.1 Collimators. . . . .	42
3.2 Dose Measurements as a Function of Incident Angle . . . . .	43
3.2.1 Neutron Dose. . . . .	43
3.2.2 HPRR Gamma Dose . . . . .	44
3.2.3 Cobalt-60 Gamma Dose. . . . .	44
3.3 Spectrum Measurements . . . . .	45
3.3.1 HPRR Neutron Spectrum . . . . .	45
3.3.2 HPRR Gamma Spectrometry . . . . .	46
3.3.3 Cobalt-60 Gamma Spectrum. . . . .	46
3.4 Normalization . . . . .	47
3.4.1 HPRR. . . . .	47
3.4.2 Cobalt-60 . . . . .	47

## CONTENTS (Continued)

CHAPTER 4 DATA . . . . .	48
4.1 Dosimetry Data . . . . .	48
4.1.1 General Discussion of Presentation . . . . .	48
4.1.2 HPRR Neutron Dose as a Function of Incident Angle . . . . .	48
4.1.3 HPRR Gamma Dose as a Function of Incident Angle . . . . .	50
4.1.4 Cobalt-60 Gamma Dose as a Function of Incident Angle. . . . .	50
4.2 Spectrometry Data . . . . .	67
4.2.1 HPRR Neutron Spectrum . . . . .	67
4.2.2 HPRR Gamma Spectrum . . . . .	67
4.2.3 Cobalt-60 Gamma Spectrum. . . . .	67
CHAPTER 5 CONCLUSION . . . . .	91

## ILLUSTRATIONS

### CHAPTER 2 APPARATUS

2.1 BREN Tower and Source Hoist. . . . .	15
2.2 Health Physics Research Reactor. . . . .	17
2.3 Diagram of Gamma Source Shield and Exposure Mechanism . . . . .	18
2.4 Photograph of Gamma Source Shield and Exposure Mechanism . . . . .	19
2.5 Diagram of Collimators Used with Detectors . . . . .	20
2.6 Collimator Acceptance for a Gamma Ray . . . . .	21
2.7 Front View of Collimators in the Positioning Cradle. . . . .	22
2.8 Rear View of Collimators in the Position Cradle Showing Means of Positioning . . . . .	23
2.9 Inclinomometer Used to Set Collimator Angles . . . . .	25
2.10 Radsan Fast Neutron Dose Integrator with Remote Solenoid Supply . . . . .	26
2.11 Absolute Fast Neutron Dosimeter. . . . .	27
2.12 Phil Gamma-Ray Dosimeter . . . . .	28
2.13 Diagram of the Thick Radiator Proton Telescope Neutron Spectrometer . . . . .	30
2.14 Block Diagram of the Neutron Spectrometer Electronics . . . . .	31
2.15 Compton Gamma-Ray Spectrometer . . . . .	33
2.16 Compton Spectrometer Magnet Supply Diagram . . . . .	34
2.17 Front View of the Compton Spectrometer Shield and Collimator Showing 10° Opening . . . . .	35
2.18 Rear View of the Compton Spectrometer Shield Showing Stacked Transite . . . . .	36
2.19 Normalizing Channel Number 1 . . . . .	38
2.20 Normalizing Channel Number 2 . . . . .	40

### CHAPTER 4 DATA

4.1 Normalized Neutron Dose as a Function of Angle for a Reactor Height of 1125 Ft, Collimator Acceptance Angle = 30°, with $\theta$ Kept at 0°, and Collimator Located at 750 Yd from the Base of the Tower. . . . .	51
4.2 Normalized Neutron Dose as a Function of Angle for a Reactor Height of 1125 Ft, Collimator Acceptance Angle = 30°, with $\phi$ Kept at 0°, and Collimator Located at 750 Yd from the Base of the Tower. . . . .	52

## ILLUSTRATIONS (Continued)

4.3	Normalized Neutron Dose as a Function of Angle for a Reactor Height of 500 Ft, Collimator Acceptance Angle = $10^\circ$ , with $\theta$ Kept at $0^\circ$ , and Collimator Located at 750 Yd from the Base of the Tower . . . . .	53
4.4	Normalized Neutron Dose as a Function of Angle for a Reactor Height of 1125 Ft, Collimator Acceptance Angle = $10^\circ$ , with $\theta$ Kept at $0^\circ$ , and Collimator Located at 750 Yd from the Base of the Tower . . . . .	54
4.5	Normalized Neutron Dose as a Function of Angle for a Reactor Height of 1500 Ft, Collimator Acceptance Angle = $10^\circ$ , with $\theta$ Kept at $0^\circ$ , and Collimator Located at 750 Yd from the Base of the Tower . . . . .	55
4.6	Normalized Neutron Dose as a Function of Angle for a Reactor Height of 1500 Ft, Collimator Acceptance Angle = $30^\circ$ , with $\theta$ Kept at $0^\circ$ , and Collimator Located at 1000 Yd from the Base of the Tower . . . . .	56
4.7	Normalized Neutron Dose as a Function of Polar Angle . . . . .	57
4.8	Normalized Neutron Dose for Total Solid Angle as a Function of Polar Angle . . . . .	58
4.9	Normalized HPRR Gamma-Ray Dose as a Function of Angle for a Reactor Height of 1125 Ft, Collimator Acceptance Angle = $30^\circ$ , with $\theta$ Kept at $0^\circ$ , and Collimator Located at 750 Yd from the Base of the Tower . . . . .	59
4.10	Normalized HPRR Gamma-Ray Dose as a Function of Angle for a Reactor Height of 1125 Ft, Collimator Acceptance Angle = $30^\circ$ , with $\phi$ Kept at $0^\circ$ , and Collimator Located at 750 Yd from the Base of the Tower . . . . .	60
4.11	Normalized HPRR Gamma-Ray Dose as a Function of Angle for a Reactor Height of 500 Ft, Collimator Acceptance Angle = $10^\circ$ , with $\theta$ Kept at $0^\circ$ , and Collimator Located at 750 Yd from the Base of the Tower . . . . .	61
4.12	Normalized HPRR Gamma-Ray Dose as a Function of Angle for a Reactor Height of 1125 Ft, Collimator Acceptance Angle = $10^\circ$ , with $\theta$ Kept at $0^\circ$ , and Collimator Located at 750 Yd from the Base of the Tower . . . . .	62
4.13	Normalized HPRR Gamma-Ray Dose as a Function of Angle for a Reactor Height of 1500 Ft, Collimator Acceptance Angle = $10^\circ$ , with $\theta$ Kept at $0^\circ$ , and Collimator Located at 750 Yd from the Base of the Tower . . . . .	63
4.14	Normalized HPRR Gamma-Ray Dose as a Function of Angle for a Reactor Height of 1500 Ft, Collimator Acceptance Angle = $30^\circ$ , with $\theta$ Kept at $0^\circ$ , and Collimator Located at 1000 Yd from the Base of the Tower . . . . .	64
4.15	Normalized HPRR Gamma-Ray Dose as a Function of Polar Angle. . . . .	65
4.16	Normalized HPRR Gamma-Ray Dose for Total Solid Angle as a Function of Polar Angle . . . . .	66
4.17	Normalized $^{60}\text{Co}$ Gamma-Ray Dose for a Source Height of 1125 Ft, Collimator Acceptance Angle = $30^\circ$ , with $\theta$ Kept at $0^\circ$ , and Collimator Located at 750 Yd from the Base of the Tower . . . . .	68
4.18	Normalized $^{60}\text{Co}$ Gamma-Ray Dose as a Function of Polar Angle. . . . .	69
4.19	Normalized $^{60}\text{Co}$ Gamma-Ray Dose for Total Solid Angle as a Function of Polar Angle. . . . .	70
4.20	Neutron Spectrometer Response to Monoenergetic Neutrons. . . . .	71
4.21	Typical Measured BREN Neutron Spectrum . . . . .	72

## ILLUSTRATIONS (Continued)

4.22	Typical Background Neutron Spectrum. . . . .	73
4.23	Compton Spectrometer Results . . . . .	74
4.24	$^{60}\text{Co}$ Spectrum at a Distance to the Base of the Tower from the Detector of 750 Yd, Source Height of 1125 Ft, Collimator Acceptance Angle = $30^\circ$ , with $\theta$ Kept at $0^\circ$ and $\phi$ Kept at $270^\circ$ . . . . .	75
4.25	$^{60}\text{Co}$ Spectrum at a Distance to the Base of the Tower from the Detector of 750 Yd, Source Height of 1125 Ft, Collimator Acceptance Angle = $30^\circ$ , with $\theta$ Kept at $0^\circ$ and $\phi$ Kept at $300^\circ$ . . . . .	75
4.26	$^{60}\text{Co}$ Spectrum at a Distance to the Base of the Tower from the Detector of 750 Yd, Source Height of 1125 Ft, Collimator Acceptance Angle = $30^\circ$ , with $\theta$ Kept at $0^\circ$ and $\phi$ Kept at $330^\circ$ . . . . .	76
4.27	$^{60}\text{Co}$ Spectrum at a Distance to the Base of the Tower from the Detector of 750 Yd, Source Height of 1125 Ft, Collimator Acceptance Angle = $30^\circ$ , with $\theta$ Kept at $0^\circ$ and $\phi$ Kept at $0^\circ$ . . . . .	76
4.28	$^{60}\text{Co}$ Spectrum at a Distance to the Base of the Tower from the Detector of 750 Yd, Source Height of 1125 Ft, Collimator Acceptance Angle = $30^\circ$ , with $\theta$ Kept at $0^\circ$ and $\phi$ Kept at $30^\circ$ . . . . .	77
4.29	$^{60}\text{Co}$ Spectrum at a Distance to the Base of the Tower from the Detector of 750 Yd, Source Height of 1125 Ft, Collimator Acceptance Angle = $30^\circ$ , with $\theta$ Kept at $0^\circ$ and $\phi$ Kept at $60^\circ$ . . . . .	77
4.30	$^{60}\text{Co}$ Spectrum at a Distance to the Base of the Tower from the Detector of 750 Yd, Source Height of 1125 Ft, Collimator Acceptance Angle = $30^\circ$ , with $\theta$ Kept at $0^\circ$ and $\phi$ Kept at $90^\circ$ . . . . .	78
4.31	$^{60}\text{Co}$ Spectrum at a Distance to the Base of the Tower from the Detector of 750 Yd, Source Height of 1125 Ft, Collimator Acceptance Angle = $30^\circ$ , with $\theta$ Kept at $0^\circ$ and $\phi$ Kept at $120^\circ$ . . . . .	78
4.32	$^{60}\text{Co}$ Spectrum at a Distance to the Base of the Tower from the Detector of 750 Yd, Source Height of 1125 Ft, Collimator Acceptance Angle = $30^\circ$ , with $\theta$ Kept at $0^\circ$ and $\phi$ Kept at $150^\circ$ . . . . .	79
4.33	$^{60}\text{Co}$ Spectrum at a Distance to the Base of the Tower from the Detector of 750 Yd, Source Height of 1125 Ft, Collimator Acceptance Angle = $30^\circ$ , with $\theta$ Kept at $0^\circ$ and $\phi$ Kept at $180^\circ$ . . . . .	79
4.34	$^{60}\text{Co}$ Spectrum at a Distance to the Base of the Tower from the Detector of 750 Yd, Source Height of 1125 Ft, Collimator Acceptance Angle = $30^\circ$ , with $\phi$ Kept at $0^\circ$ and $\theta$ Kept at $330^\circ$ . . . . .	80
4.35	$^{60}\text{Co}$ Spectrum at a Distance to the Base of the Tower from the Detector of 750 Yd, Source Height of 1125 Ft, Collimator Acceptance Angle = $30^\circ$ , with $\phi$ Kept at $0^\circ$ and $\theta$ Kept at $30^\circ$ . . . . .	80
4.36	$^{60}\text{Co}$ Spectrum at a Distance to the Base of the Tower from the Detector of 750 Yd, Source Height of 1125 Ft, Collimator Acceptance Angle = $30^\circ$ , with $\phi$ Kept at $0^\circ$ and $\theta$ Kept at $60^\circ$ . . . . .	81

## ILLUSTRATIONS (Continued)

4.37	<sup>60</sup> Co Spectrum at a Distance to the Base of the Tower from the Detector of 750 Yd, Source Height of 1125 Ft, Collimator Acceptance Angle = 30°, with $\phi$ Kept at 0° and $\theta$ Kept at 90° . . .	81
4.38	<sup>60</sup> Co Spectrum at a Distance to the Base of the Tower from the Detector of 750 Yd, Source Height of 1125 Ft, Collimator Acceptance Angle = 30°, with $\phi$ Kept at 0° and $\theta$ Kept at 120° . . .	82
4.39	<sup>60</sup> Co Spectrum at a Distance to the Base of the Tower from the Detector of 750 Yd, Source Height of 1125 Ft, Collimator Acceptance Angle = 10°, with $\theta$ Kept at 0° and $\phi$ Kept at 340° . . .	82
4.40	<sup>60</sup> Co Spectrum at a Distance to the Base of the Tower from the Detector of 750 Yd, Source Height of 1125 Ft, Collimator Acceptance Angle = 10°, with $\theta$ Kept at 0° and $\phi$ Kept at 350° . . .	83
4.41	<sup>60</sup> Co Spectrum at a Distance to the Base of the Tower from the Detector of 750 Yd, Source Height of 1125 Ft, Collimator Acceptance Angle = 10°, with $\theta$ Kept at 0° and $\phi$ Kept at 0° . . .	83
4.42	<sup>60</sup> Co Spectrum at a Distance to the Base of the Tower from the Detector of 750 Yd, Source Height of 1125 Ft, Collimator Acceptance Angle = 10°, with $\theta$ Kept at 0° and $\phi$ Kept at 10° . . .	84
4.43	<sup>60</sup> Co Spectrum at a Distance to the Base of the Tower from the Detector of 750 Yd, Source Height of 1125 Ft, Collimator Acceptance Angle = 10°, with $\theta$ Kept at 0° and $\phi$ Kept at 20° . . .	84
4.44	<sup>60</sup> Co Spectrum at a Distance to the Base of the Tower from the Detector of 750 Yd, Source Height of 1125 Ft, Collimator Acceptance Angle = 10°, with $\theta$ Kept at 0° and $\phi$ Kept at 30° . . .	85
4.45	<sup>60</sup> Co Spectrum at a Distance to the Base of the Tower from the Detector of 1000 Yd, Source Height of 27 Ft, Collimator Acceptance Angle = 30°, with $\theta$ Kept at 0° and $\phi$ Kept at 0° . . .	85
4.46	<sup>60</sup> Co Spectrum at a Distance to the Base of the Tower from the Detector of 1000 Yd, Source Height of 27 Ft, Collimator Acceptance Angle = 30°, with $\theta$ Kept at 0° and $\phi$ Kept at 30° . . .	86
4.47	<sup>60</sup> Co Spectrum at a Distance to the Base of the Tower from the Detector of 1000 Yd, Source Height of 300 Ft, Collimator Acceptance Angle = 30°, with $\theta$ Kept at 0° and $\phi$ Kept at 0° . . .	86
4.48	<sup>60</sup> Co Spectrum at a Distance to the Base of the Tower from the Detector of 1000 Yd, Source Height of 300 Ft, Collimator Acceptance Angle = 30°, with $\theta$ Kept at 0° and $\phi$ Kept at 30° . . .	87
4.49	<sup>60</sup> Co Spectrum at a Distance to the Base of the Tower from the Detector of 1000 Yd, Source Height of 1500 Ft, Collimator Acceptance Angle = 30°, with $\theta$ Kept at 0° and $\phi$ Kept at 0° . . .	87
4.50	<sup>60</sup> Co Spectrum at a Distance to the Base of the Tower from the Detector of 1000 Yd, Source Height of 1500 Ft, Collimator Acceptance Angle = 30°, with $\theta$ Kept at 0° and $\phi$ Kept at 30° . . .	88
4.51	<sup>60</sup> Co Spectrum at a Distance to the Base of the Tower from the Detector of 1000 Yd, Source Height of 1500 Ft, Collimator Acceptance Angle = 30°, with $\theta$ Kept at 0° and $\phi$ Kept at 60° . . .	88
4.52	<sup>60</sup> Co Spectrum at a Distance to the Base of the Tower from the Detector of 1000 Yd, Source Height of 1500 Ft, Collimator Acceptance Angle = 30°, with $\theta$ Kept at 0° and $\phi$ Kept at 90° . . .	89

**TABLE**

CHAPTER 4 DATA

4.1 Solid Angle Corrections Summary. . . . . 49

## Chapter 1

### INTRODUCTION

As a part of the continuing refinement of the dose values assigned to Japanese survivors through the Ichiban Program, Operation BREN (Bare Reactor Experiment Nevada) was conducted at the Nevada Test Site in the first half of 1962. During Operation BREN, weapons radiation was simulated by operating the Oak Ridge National Laboratory Health Physics Research Reactor (HPRR) at various elevations on a 1527-ft tower. While a bare reactor, such as the HPRR, produces a neutron field similar to that of a fission weapon, it does not simulate the entire gamma field. To obtain more complete gamma information, measurements were made using 800 curies of  $^{60}\text{Co}$  as the radiation source. The complete operation was described in detail in previous reports.<sup>1,2</sup>

There were seven experiments covered by Project 1.2 of Operation BREN. One of these, dealing with the spectrum of the gamma rays as a function of time after a reactor burst, was reported separately.<sup>3</sup> The other six experiments dealt with the measurements of gamma and neutron dose and spectrum as a function of angle of incidence at the point of measurement.

While measurements were made using two sources of radiation, most data were taken using the mixed neutron and gamma-ray field produced by the HPRR. Neutron and gamma-dose distributions as a function of angle were measured for various source heights at distances of 750 and 1000 yd from the base of the tower. The measurements of the fast neutron spectrum were made as a function of angle of incidence, and an attempt was made to measure the gamma-ray spectrum, during HPRR operation at  $0^\circ$ . Using 800 curies of  $^{60}\text{Co}$  as the radiation source, the angular distribution of spectrum and dose were measured at distances of 750 and 1000 yd.

#### REFERENCES

1. F. W. Sanders, F. F. Haywood, M. I. Lundin, L. W. Gilley, J. S. Cheka, and D. R. Ward, Operations Plan and Hazards Report - Operation BREN, USAEC Report CEX-62.02, April 1962.
2. J. A. Auxier, F. F. Haywood, and L. W. Gilley, General Correlative Studies - Operation BREN, USAEC Report CEX-62.03, September 1963.
3. J. H. Thorngate and E. T. Loy, Post Pulse Gamma-Radiation Spectrum - Operation BREN, USAEC Report CEX-62.13, June 1966.

## Chapter 2

### APPARATUS

#### 2.1 TOWER

In order to make exposures with the radiation source at various heights above the air-ground interface, a tower 1527 ft high was built in area 4 of the Nevada Test Site (Fig. 2.1). The tower base had a uniform equilateral triangular cross section with 10 ft between the legs. A hoist car located on the side of the tower was designed to support the radiation source and allowed exposures at source heights from 27 ft to 1500 ft. The minimum height resulted from a device installed below the hoist car to handle the control cables for the radiation sources. At several heights of particular interest, such as 300, 500, 1125, and 1500 ft, portions of the hoist car "raceway" supports were removed to minimize radiation scattering near the source. A smaller elevator within the main tower structure provided for personnel access to all heights on the tower. Six sets of guy wires spaced at 120° intervals around the tower held the top of the tower to ±2-in. sway under operational wind conditions.

#### 2.2 RADIATION SOURCES

##### 2.2.1 HPRR

The Health Physics Research Reactor served as the radiation source during the major portion of Operation BREN. An alloy of 10% by weight molybdenum and 90% highly enriched (93.14%) uranium was used in an unmoderated cylindrical fuel assembly 8 in. in diameter by 9 in. high. The addition of molybdenum improved the high-temperature characteristics and dimensional stability of the core thus allowing continuous reactor operation at levels up to 3 kw, shorter runs to 10 kw and maximum pulses of  $10^{17}$  fissions. A 2-in.-dia. stainless steel rod formed the axis of the core and allowed higher power reactor operation by flattening the distribution of fissions and decreasing the "peak-to-average" power distribution near the center of the core. Around the stainless steel was an annular fuel element 3.375 in. in outer diameter by 6.5 in. long that formed the largest movable portion of the core, the "safety block." As this element contained \$20 of reactivity, its removal from the core was the major nuclear safety feature of the reactor. The remainder of the core was annular rings of fuel around the safety block. Three control rods traversed the full length of the outer section of the core: the (1) regulating rod, (2) mass adjust rod, and (3) burst rod.

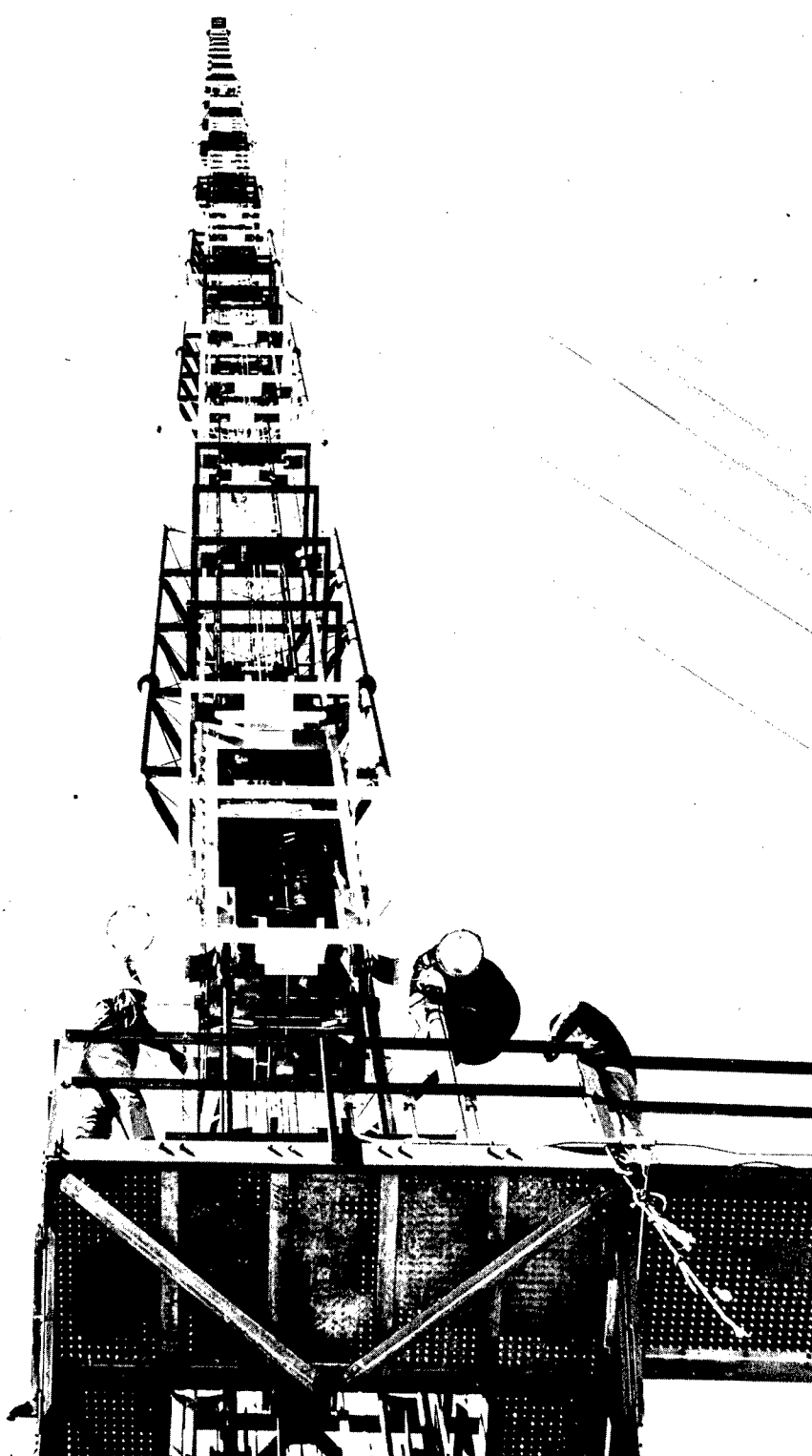


Fig. 2.1--BREN Tower and Source Hoist

Complete descriptions of the reactor and its operation are available in the literature.<sup>1,2</sup> A photograph of the reactor is shown as Fig. 2.2.

During BREN the reactor was enclosed in the hoist car on the tower. All control cables went from the car, down the tower, and into an underground bunker in which the reactor control console was located.

### 2.2.2 Cobalt-60 Source

An 800-curie  $^{60}\text{Co}$  source was used to improve the definition of the angular dose and spectrum distributions of gamma rays. The source was kept in a special lead shield that had a hoist mechanism attached to allow remote control of source exposure. Both the shield and source lifting-lowering mechanism were placed upon the hoist car that had held the HPRR during reactor operations. For this operation, the aluminum sides of the car were replaced with thin plastic sheets to reduce gamma-ray scattering. Figure 2.3 shows a diagram of the source-handling mechanism while Fig. 2.4 shows the device mounted on the tower.

### 2.3 COLLIMATORS

The collimators used during Operation BREN were modifications of those used during weapons tests and which are described in other reports.<sup>3,4</sup> Each consisted of a large cylindrical steel shell 54 in. long by 54 in. in diameter with a  $45^\circ$  conical opening in one end. The opening penetrated to a cylindrical cavity in the center of the device. As used, the shield was filled with water and a lead- or water-filled insert placed in the collimator for use with gamma detectors or neutron detectors, respectively. Figure 2.5 shows the cross-sectional diagrams of the collimator with the two basic inserts. The figure also indicates how the angle of the conical opening was decreased for more detailed measurements. For the BREN experiments, the total acceptance angles of the conical inserts used were  $10^\circ$  and  $30^\circ$ . The neutron spectrometer used a straight-walled water insert to provide collimation. When used with the neutron dosimeter, this insert provided an effective collimation angle of approximately  $10^\circ$ .

A 5-in.-dia. hole to the back of the collimator provided detector access and mounting space. During operation, this hole was plugged with lead wool for the gamma instruments and with polyethylene shot and borated soap for the neutron instruments.

A typical measurement of the angular acceptance of the collimator with a lead,  $30^\circ$  insert is shown in Fig. 2.6. The figure shows the detector response as a function of source location; a  $^{60}\text{Co}$  source was moved past the opening at a fixed distance from the detector. Leakage through the lead wool plug behind the detector was negligible. More detailed measurements on the acceptance angles of this type of collimator have been reported with respect to their use during weapons tests.<sup>5</sup>

These collimators were large devices, hence difficult to position. The method utilized during weapons tests involved placing the collimators on mounds of dirt in the correct attitudes. For Operation BREN, a cradle was devised that held two collimators for easy positioning. Figures 2.7 and 2.8 illustrate the device with the collimators in position. Azimuthal angle was adjusted by moving the collimators on a horizontal bearing until properly located and then

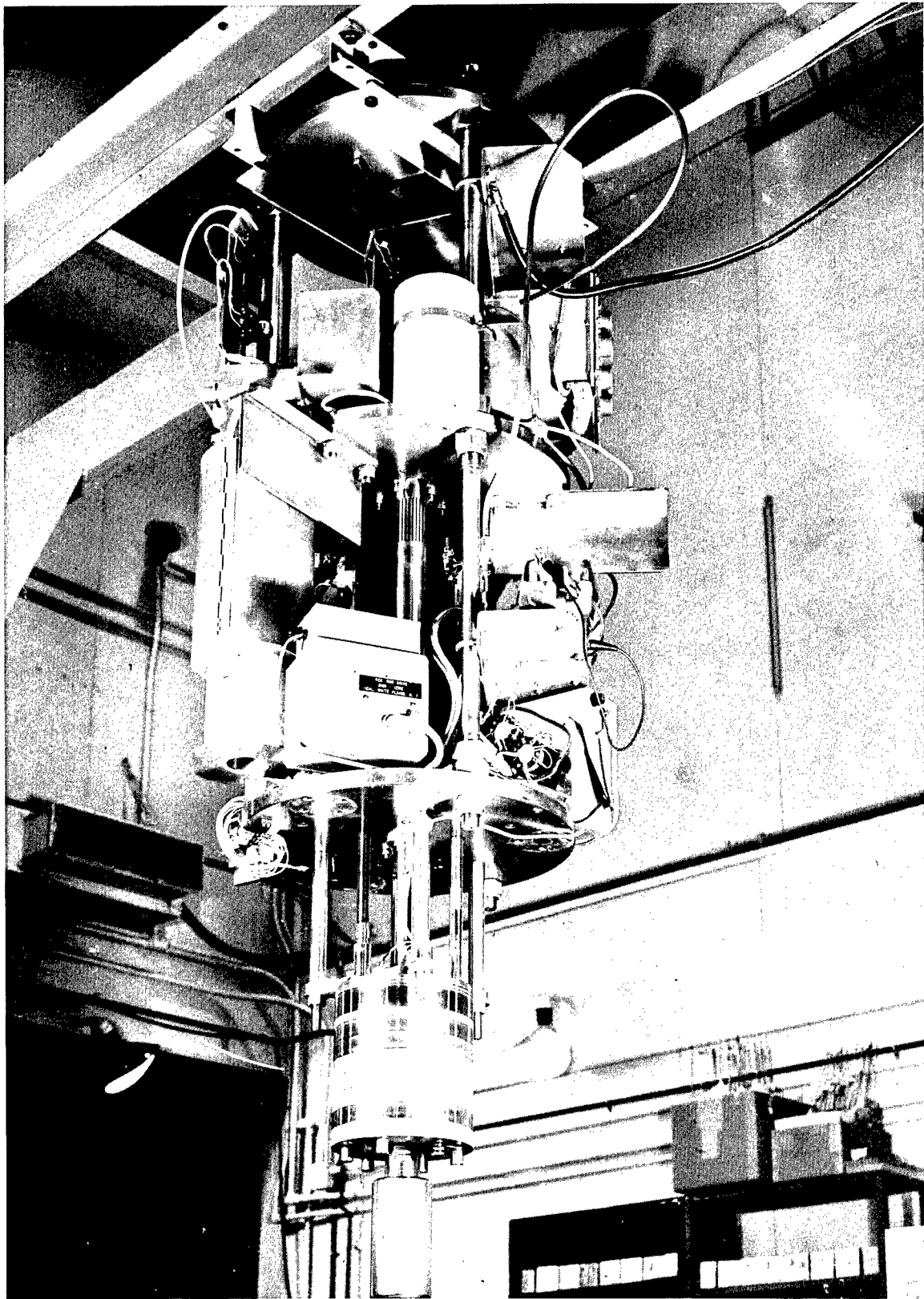


Fig. 2.2--Health Physics Research Reactor

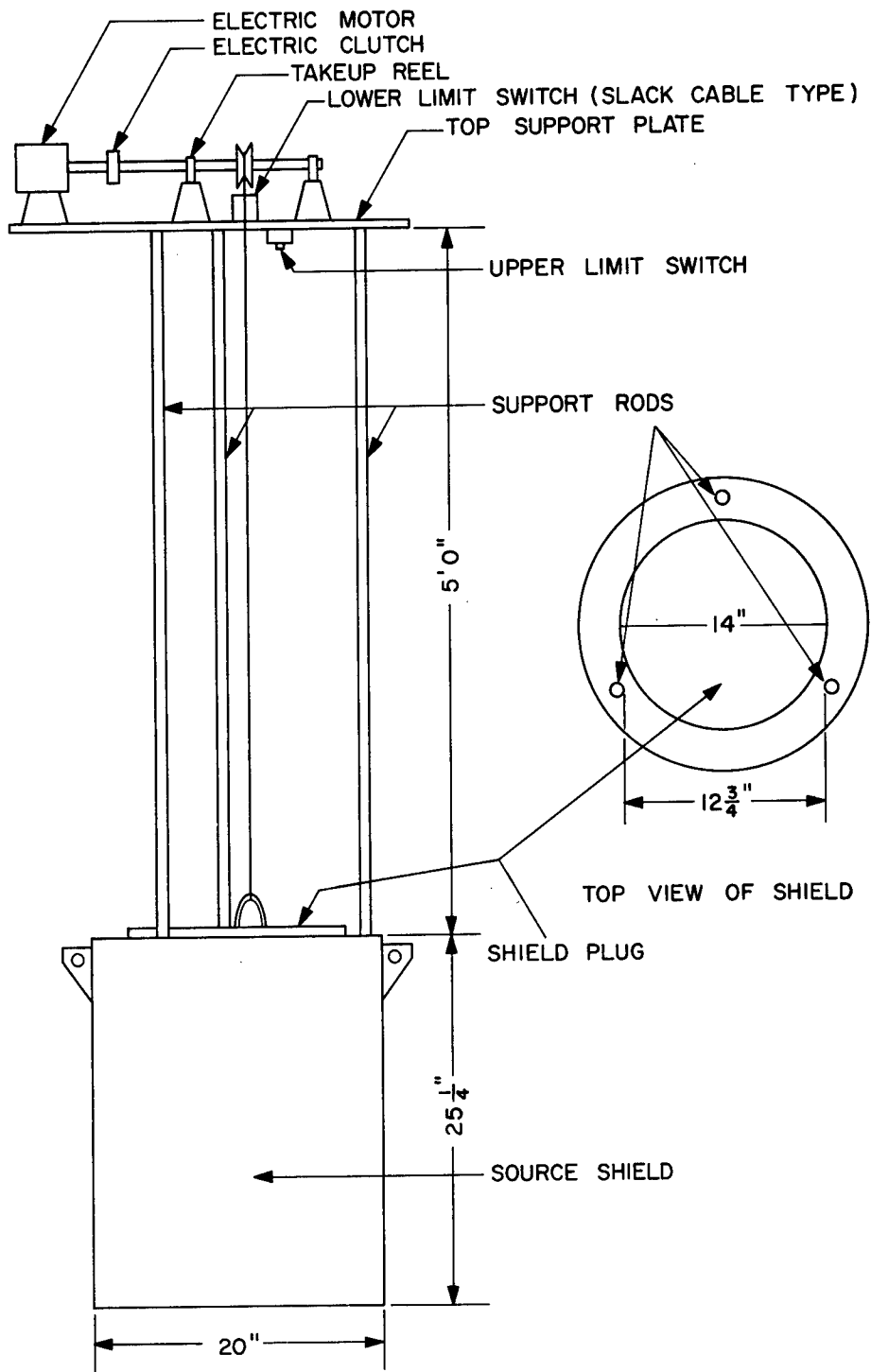


Fig. 2.3--Diagram of Gamma Source Shield and Exposure Mechanism

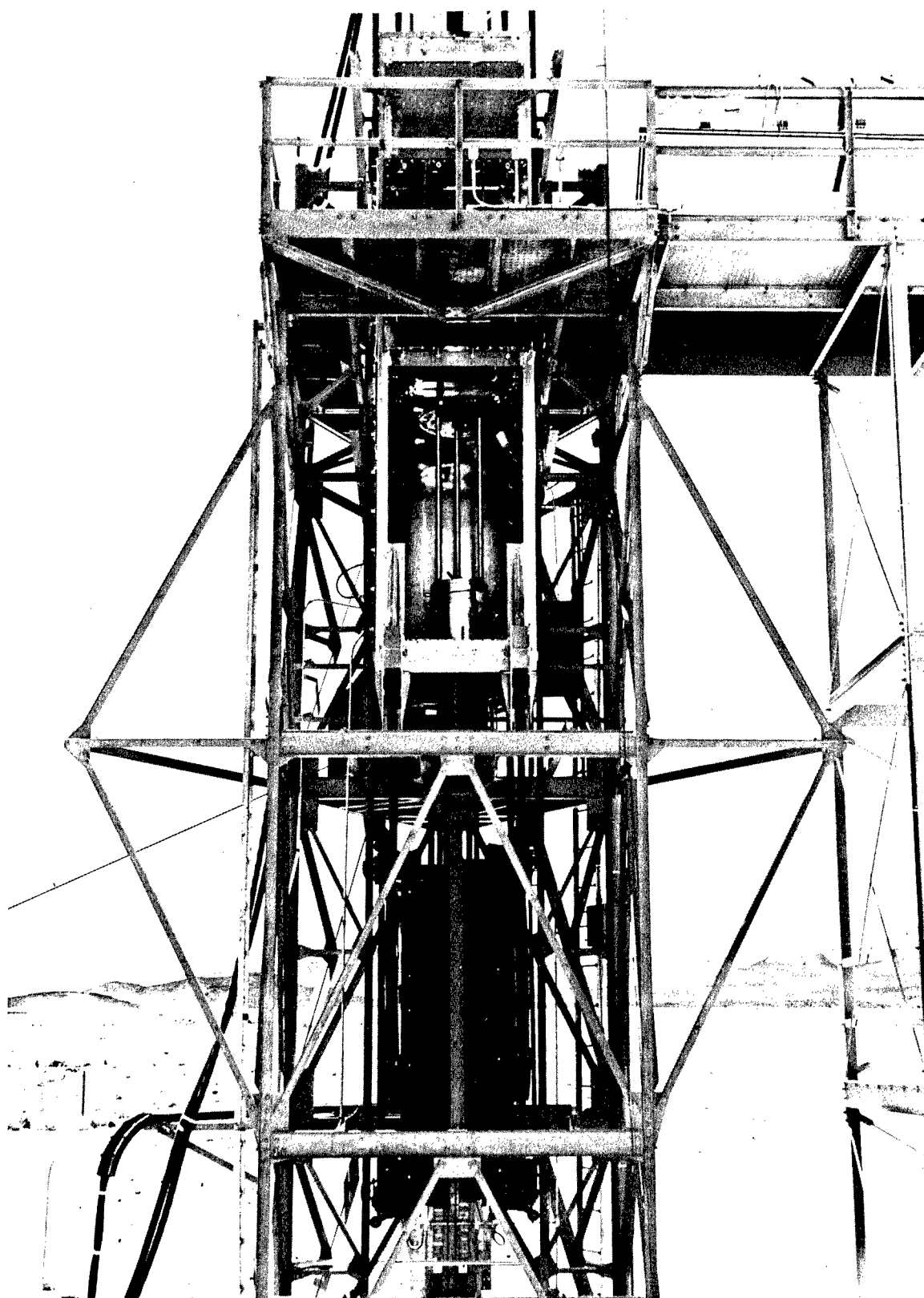


Fig. 2.4--Photograph of Gamma Source Shield and Exposure Mechanism

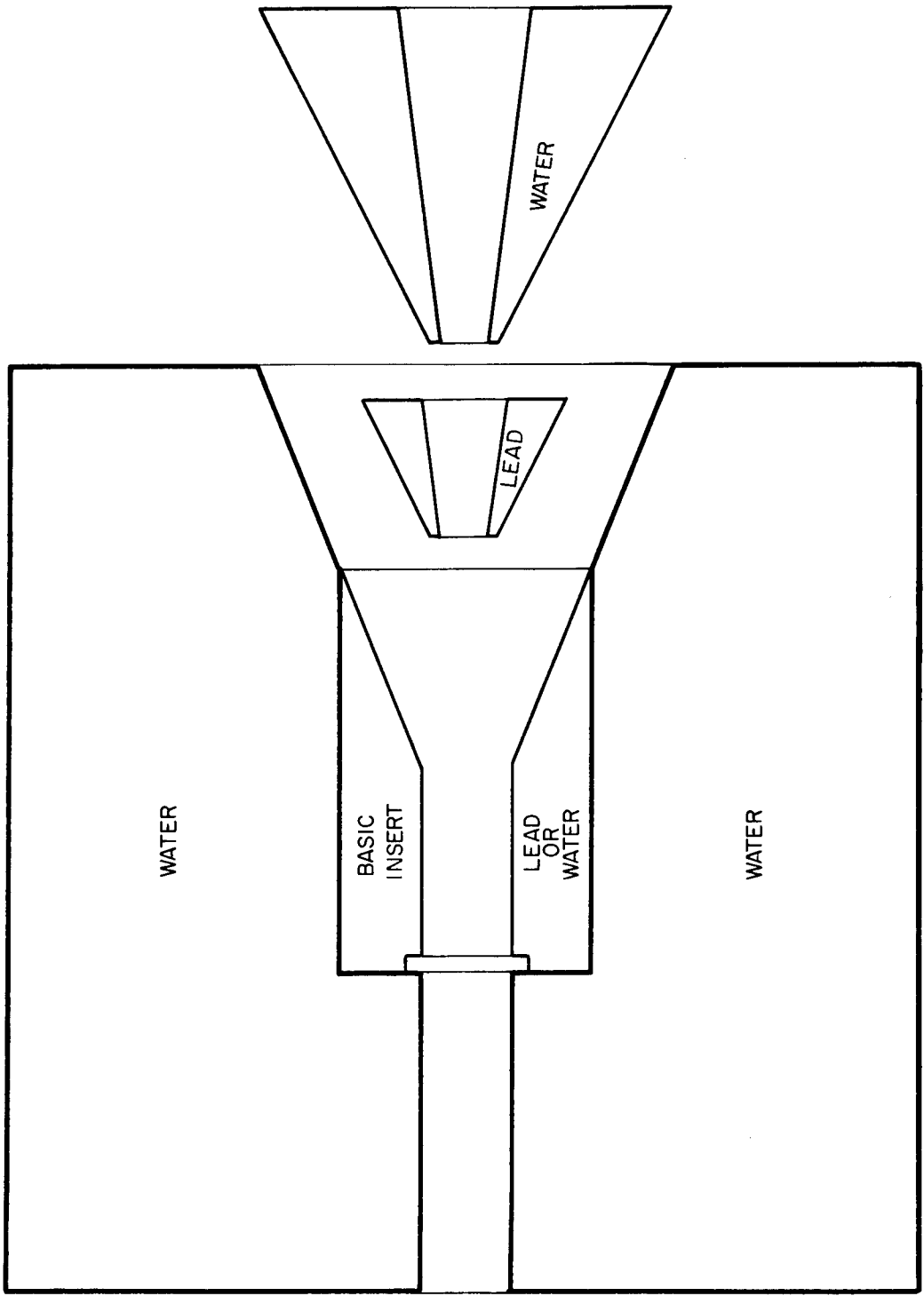


Fig. 2.5--Diagram of Collimators Used with Detectors

ANGULAR RESPONSE OF PHIL W/Li<sup>6</sup> SHIELD IN A  
COLLIMATOR W/30° INSERT

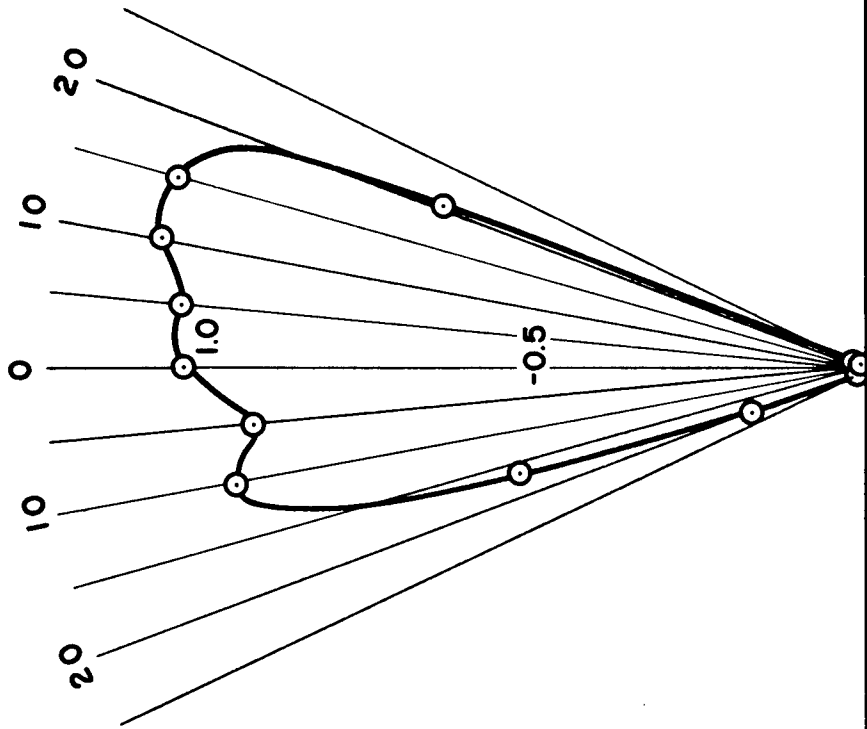


Fig. 2.6--Collimator Acceptance for a Gamma Ray

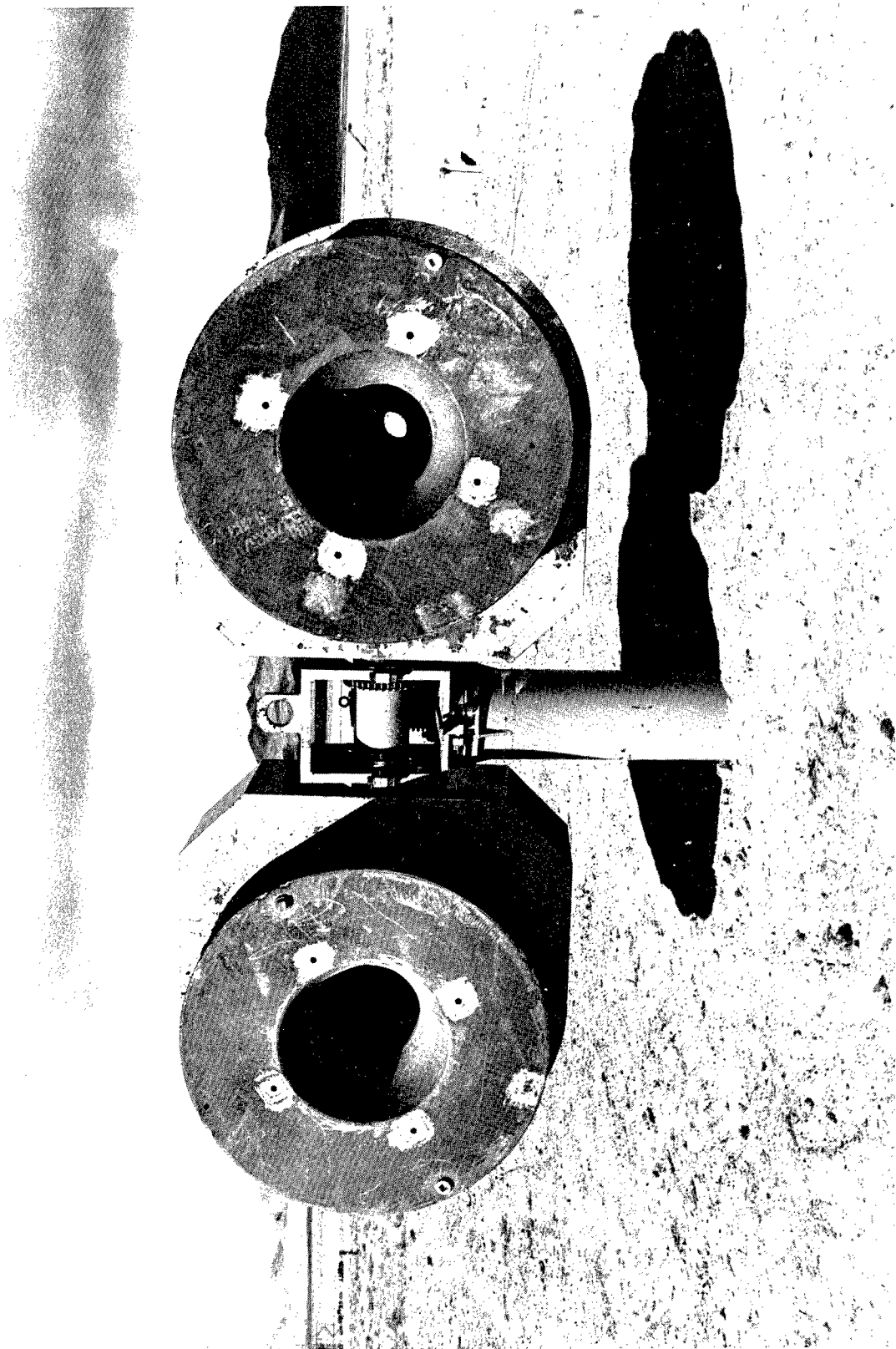


Fig. 2.7--Front View of Collimators in the Positioning Cradle

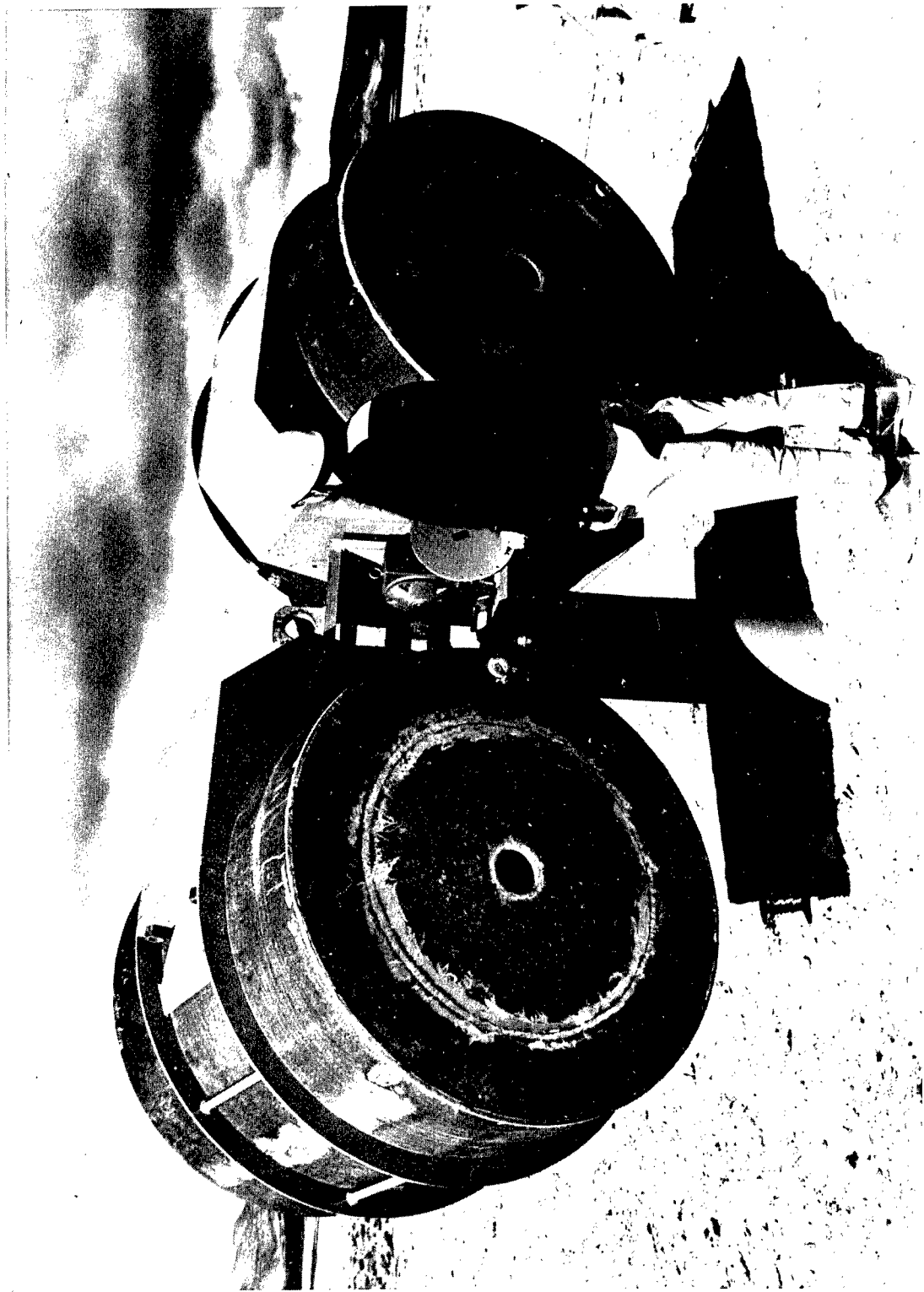


Fig. 2.8--Rear View of Collimators in the Position Cradle Showing Means of Positioning

tightening a locking collar to hold them in place. Vertical angles were set by turning a crank attached through a gear reduction box and a chain drive to the axle that held the collimators. Because a 35-tooth sprocket was used with the chain drive, the collimator vertical angle could be locked only in multiples of  $0.257^\circ$ .

Collimator positions were set using an inclinometer designed for weapons tests. This instrument included a protractor-mounted telescopic sight such that the azimuthal angle between a line to the tower and the axis of the collimator could be measured to within  $0.5^\circ$ . The angle of elevation was set with a similar protractor that had a spirit-level reference. A third spirit level on the base of the inclinometer assured that the device was placed reproducibly upon the collimator (Fig. 2.9).

## 2.4 DOSIMETRY

### 2.4.1 Neutron Dosimeter

A Radsan<sup>6</sup> integrator (Fig. 2.10) was used in conjunction with the standard fast-neutron dosimeter<sup>7</sup> to measure the fast-neutron dose. The neutron dosimeter is a cylindrical proportional counter lined with polyethylene and filled with cyclopropane gas to form a Bragg-Gray chamber (Fig. 2.11). Detector output went to a nuvistor-transistor preamplifier which transmitted the signal over a 250-ft low capacitance coaxial cable to the Radsan pulse integrator located in an instrument trailer.

The Radsan incorporated a linear pulse amplifier, a four-channel integral analog-to-digital converter, and a binary integrator. The binary integrator output, which was proportional to energy deposited in the detector, was registered by a decade scaler controlled by a timer adjusted so that the readout was approximately in mrad/hr. While the adjustment of the timer to produce a direct readout in mrad/hr was possible, it was felt unnecessary due to the relative nature of the angular distribution measurements.

A well-regulated, low noise, high-voltage supply, located in the instrument trailer, provided the high voltage for the proportional counter and the power for the operation of the preamplifier. The high voltage was transmitted to the counter over a 250-ft coaxial cable.

### 2.4.2 HPRR Gamma Dosimeter

A neutron-insensitive Geiger counter<sup>8,9</sup> (Fig. 2.12) was used for gamma dosimetry. The small Geiger tube was enclosed in a shield of lead and tin to decrease detector response at low gamma-ray energies. This instrument has a response to fast neutrons of less than 1% of that to gamma rays on the basis of absorbed dose in tissue. A <sup>6</sup>Li shield was used to reduce the dosimeter's thermal neutron response to a negligible level. High voltage for the Geiger tube and power for the preamplifier were supplied by power supplied located at the collimator site, and pulses were transmitted to the readout equipment over a 250-ft low capacitance coaxial cable. A glow transfer tube, decade, scaler-timer (ORNL type Q1743) registered the pulses. The scaler was modified for this operation with the timer input signal supplied by an external pulse generator<sup>10</sup> for timing in units of hours, minutes, seconds, or 60 cycles/sec.

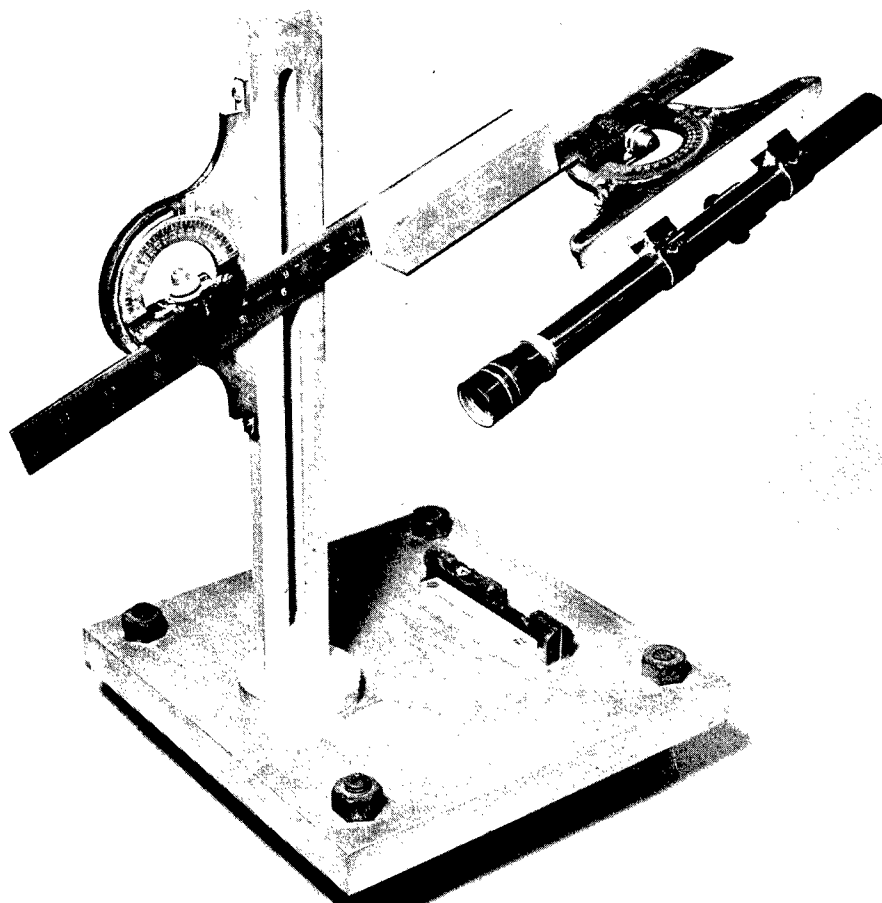


Fig. 2.9--Inclinometer Used to Set Collimator Angles

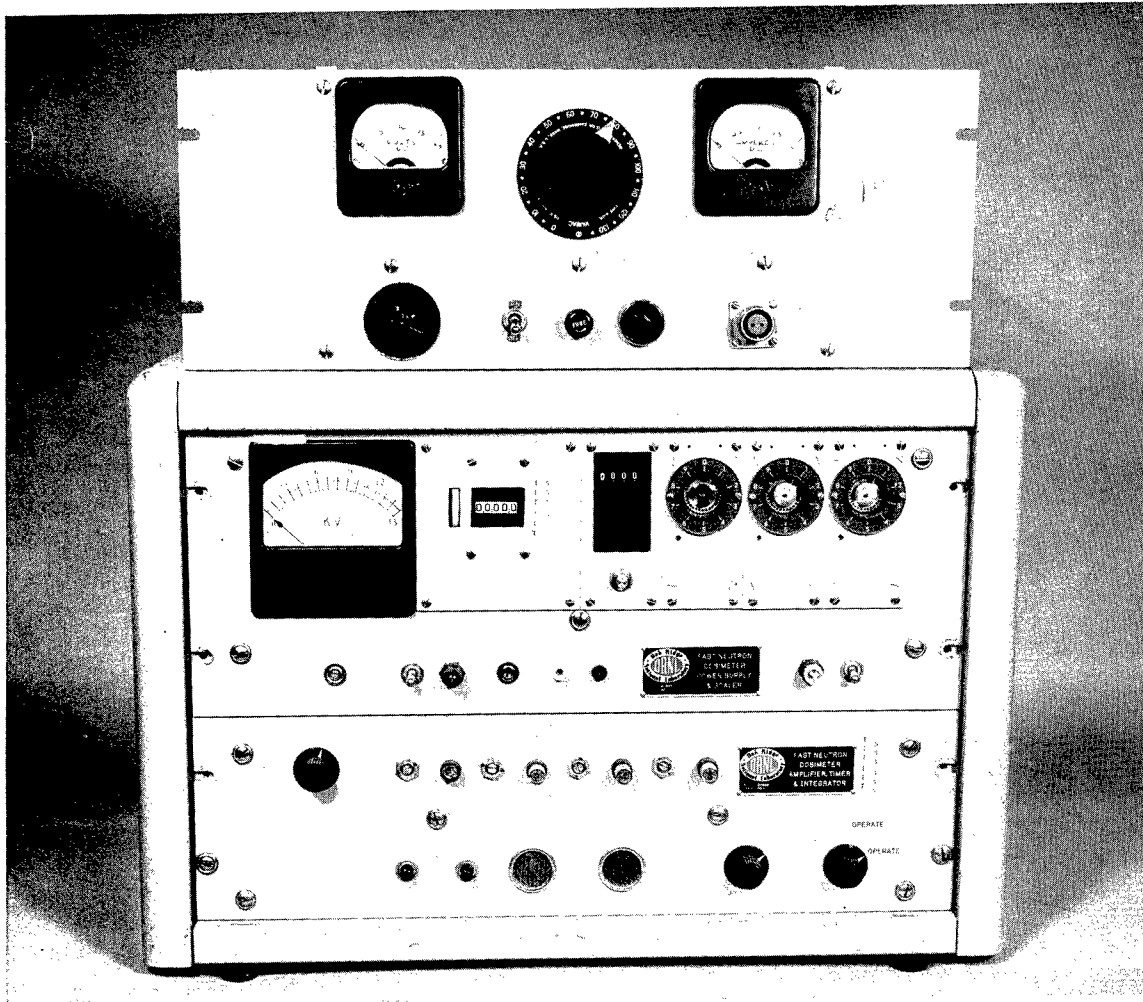


Fig. 2.10--Radsan Fast Neutron Dose Integrator with Remote Solenoid Supply

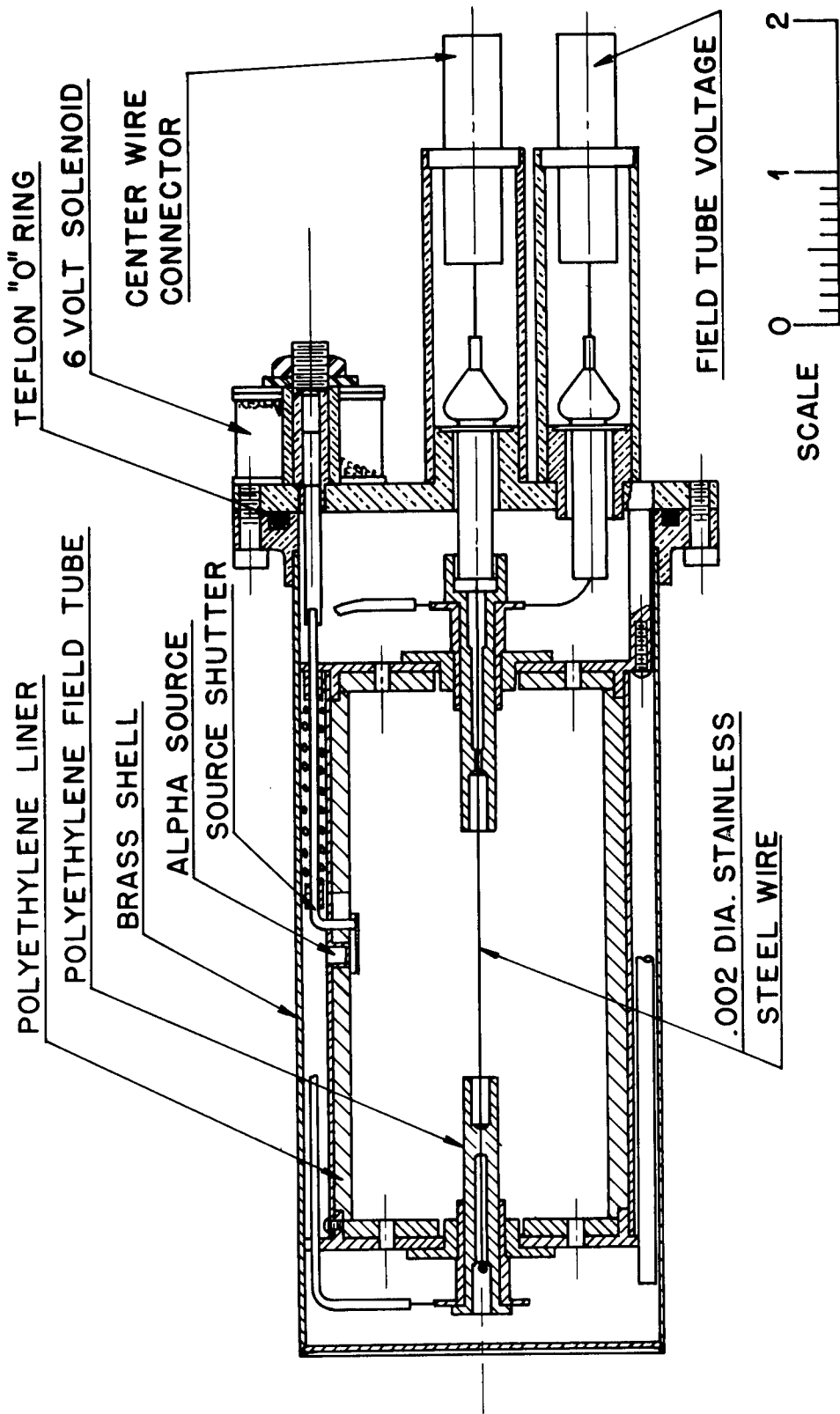
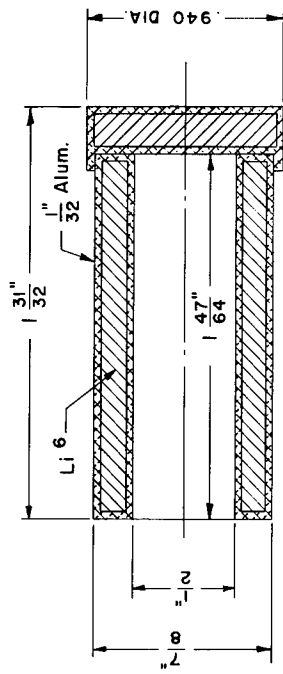
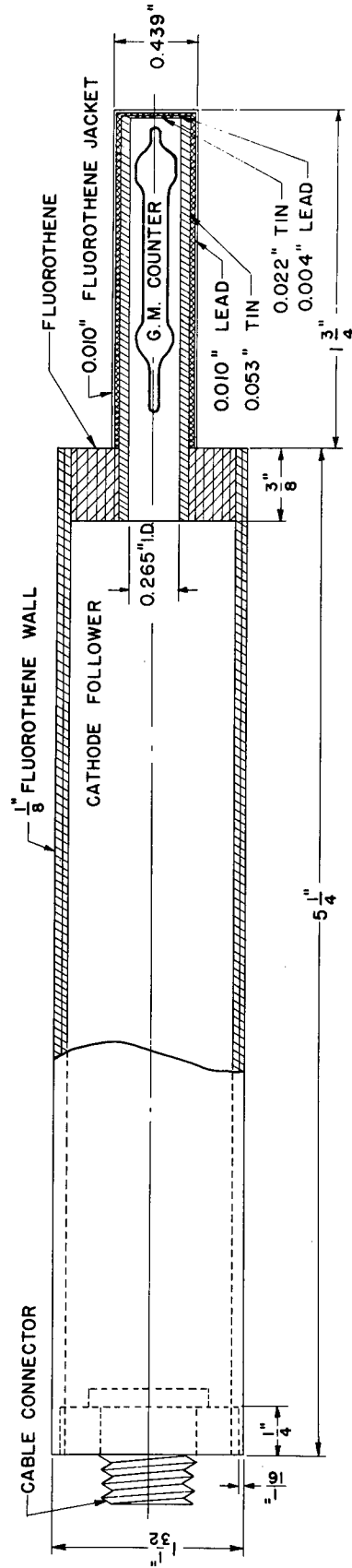


Fig. 2.11--Absolute Fast Neutron Dosimeter



THERMAL NEUTRON SHIELD



PROBE ASSEMBLY

Fig. 2.12--Phil Gamma-Ray Dosimeter

### 2.4.3 Cobalt-60 Gamma Dosimeter

Dose measurements as a function of angle were made with the  $^{60}\text{Co}$  source using a detector similar in operation to that used to measure reactor gamma rays, but which was larger and more sensitive.<sup>11</sup> The larger Geiger tube operated at a potential of 1100 volts, which was supplied by a high-voltage supply located in the trailer. A White cathode follower preamplifier at the collimator site was used to transmit the signal to the instrument trailer where it was recorded on the decade scaler.

## 2.5 SPECTROMETRY

### 2.5.1 Neutron Spectrometer

A sensitive neutron spectrometer was designed for use in Operation BREN. It followed the principles of a spectrometer developed by Mozley and Shoemaker.<sup>12</sup> The design which evolved for BREN (Fig. 2.13) was a cylinder 25 in. long and 4-1/2 in. in diameter. Inside this cylinder, two anthracene scintillation detectors, 3 in. in diameter by 2 mm thick, were set facing each other, separated by an evacuated chamber 10 in. long. The crystal thickness corresponded to the range of a 15 Mev proton in anthracene and set the upper energy limit of the device. Mounting the crystals on glass backings 3-1/2 in. in diameter and 1/8 in. thick made them easier to handle. The photomultiplier tubes used had nonhydrogenous bases and polytetrafluorethylene sockets to decrease neutron beam attenuation. The chamber walls were cut with a triangular thread to reduce proton scattering.

Collimated neutrons impinging upon the first anthracene crystal produced recoil protons. Those which deposited sufficient energy in the radiator crystal produced detectable light pulses. If the recoil proton emerged from the radiator at an angle near the forward direction, it traveled the evacuated chamber and entered the second crystal, which was sufficiently thick to stop any proton of less than 15 Mev.

The spectrometer electronic system is shown in a block diagram (Fig. 2.14). A regulated power supply located near the detector powered the preamplifiers which transmitted the detector pulses over two 250-ft-long, low capacitance coaxial cables (RG 62A/U) to the instrument trailer. Two ORNL-type DD-2 linear amplifiers<sup>13</sup> and crossover point discriminator circuits<sup>14</sup> were installed in the trailer. The discriminator outputs operated a solid state coincidence circuit.<sup>15</sup> Linear amplifier noise was rejected by the discriminator threshold settings used. Detector pulses coincident within 0.1  $\mu\text{sec}$  initiated an output pulse that operated the input gate of a multichannel analyzer which analyzed the sum of the two DD-2 linear amplifiers input pulses.

A regulated, low noise, power supply located in the instrument trailer, provided the 1000 volts to operate the photomultiplier tubes. The high-voltage output was coupled to a circuit designed to provide small voltage adjustments for each tube independently. From the control panel, the high voltage was transmitted to the detectors over a pair of 250-ft-long, high-voltage (RG 59A/U) coaxial cables.

The gains of the two detector systems were equalized with the aid of an internally mounted alpha source that irradiated both anthracene crystals. During neutron measurements, the alpha source was kept in a recess in the

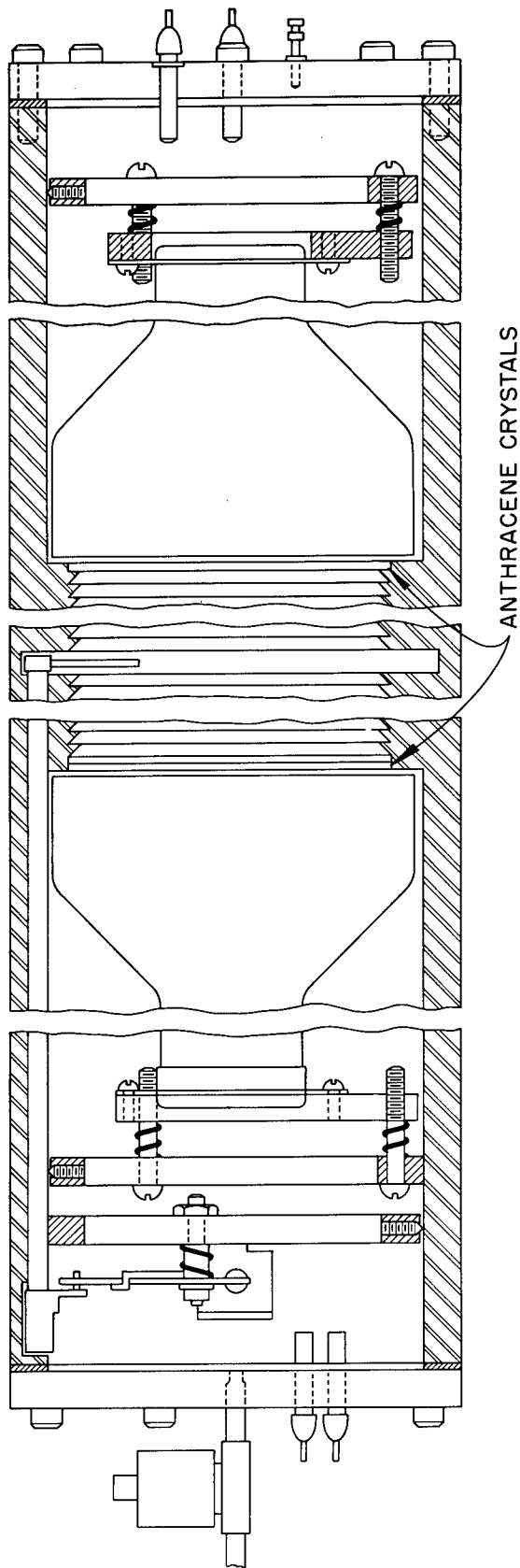


Fig. 2.13--Diagram of the Thick Radiator Proton Telescope Neutron Spectrometer

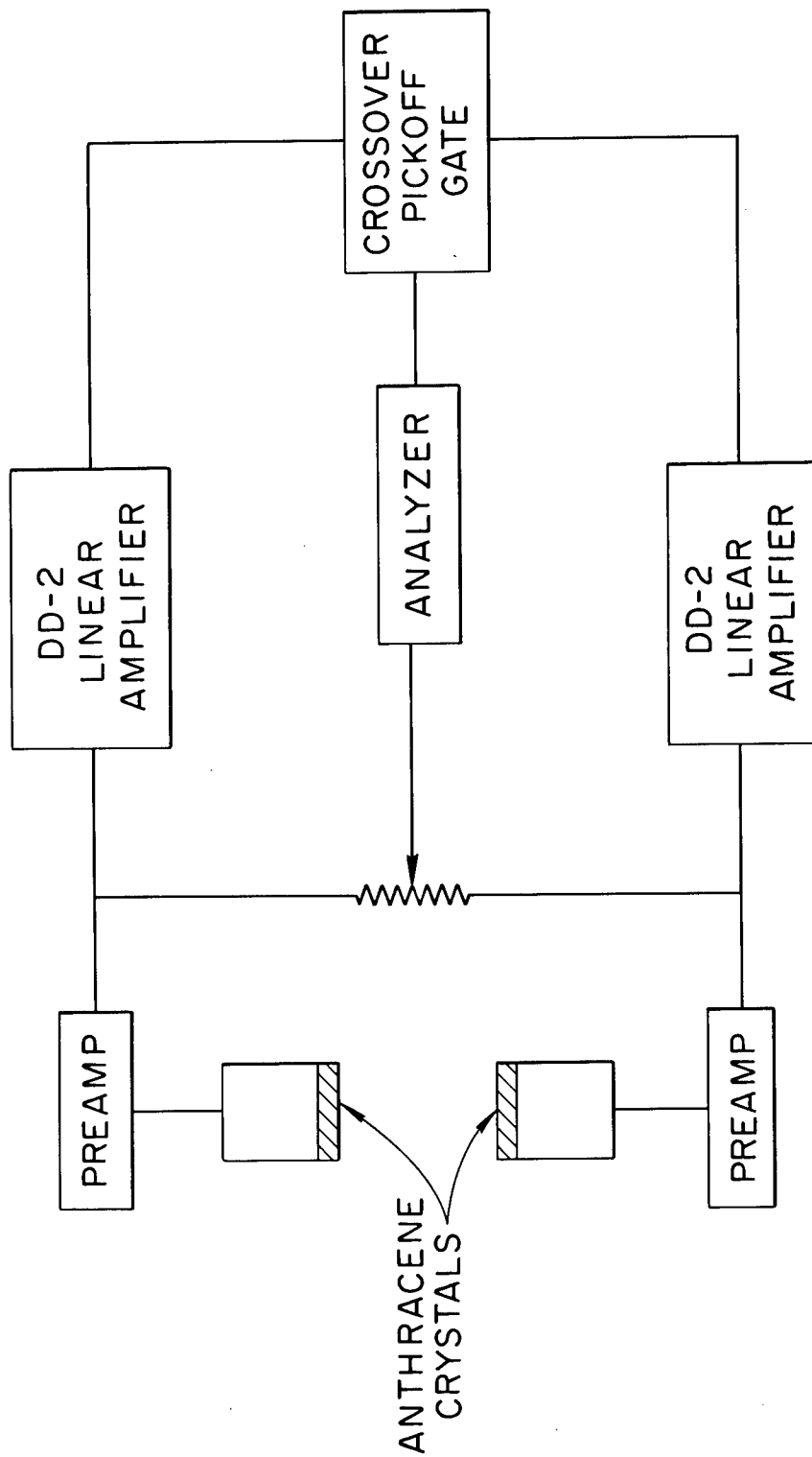


Fig. 2.14--Block Diagram of the Neutron Spectrometer Electronics

spectrometer wall. When a gain check was made, a solenoid mounted at one end of the spectrometer moved the source to the operating position. Gain adjustments were made by independently adjusting the photomultiplier high voltages until the alpha peaks, measured with a multichannel analyzer, coincided.

### 2.5.2 HPRR Gamma Spectrometer

A gamma spectrometer for use in a mixed neutron and gamma-ray radiation field was built for Operation BREN (Fig. 2.15). It used a  $13.5 \times 10^{-3}$ -in.-thick by 3/16-in.-dia. beryllium foil as a Compton electron radiator and a magnetic field for analysis of the momenta of the recoil electrons. Electrons were detected with a small end-window Geiger tube. The radius, through which an electron was bent to reach the detector, was fixed at 5 cm. Magnetic fields up to 10 kilogauss were used to study the electron momenta of interest. A solid state, Hall-effect, device was used with a servo system to measure and control the magnetic flux.

A special power supply (Fig. 2.16) operated the electromagnet. It had a mechanical arrangement that allowed vernier control of the magnet current. Two variable autotransformers were driven by a servo motor so that the smaller had to travel to its limit in either direction before the setting of the larger unit would change. The large autotransformer output was in series with the secondary of a 5-volt, 10-amp filament transformer, the primary of which was controlled by the small autotransformer. A full wave bridge rectified the resulting a-c voltage. The d-c output was filtered by a 1000  $\mu$ f capacitor and applied to the electromagnet. No further filtering was required due to the high inductance of the magnet coil.

The electron detector signal was applied to an impedance matching preamplifier and transmitted to a binary scaler over a 15-ft coaxial cable. Detector anode potential and preamplifier operating voltages were obtained from a single supply. To reduce the length of the transmission cables required, the binary scaler, power supply, and vacuum system were housed in a small trailer at the spectrometer site. An intercommunications system connected this auxiliary trailer with the main instrument trailer. The vacuum system consisted of a fore pump, dry ice and acetone cold trap, and a thermocouple vacuum gauge. A length of gum rubber hose made the vacuum connection to the spectrometer.

A large shield assembly was built to reduce detector background, hold the magnet and spectrometer and provide collimation of the input radiation (Figs. 2.17 and 2.18). The electromagnet was enclosed in a stainless steel box as small as the magnet size would allow. Stainless steel was chosen to decrease magnetic field aberration by the box. A steel plate 1/2 in. thick and about 4 ft square formed the bottom of the box and provided a base plate for the remainder of the shield. This base plate was reinforced with "I" beams welded on the bottom. Lead brick were stacked around and on top of the inner box to provide 8 in. of shielding in the front and on top and 4 in. to the sides and rear. A welded steel box with a removable top enclosed the lead. The lead directly in front of the radiator foil was machined from a single block to provide a  $10^\circ$  conical opening and a means of mounting the electron collimator tube and radiator holder of the spectrometer. Water tanks surrounded the lead in the front, sides, and rear. The tank directly in front of the spectrometer had a conical opening which was aligned with that in the lead behind it. This tank was welded to the base plate to ensure permanent, correct collimator alignment. The front tank and the two movable tanks which fitted on either

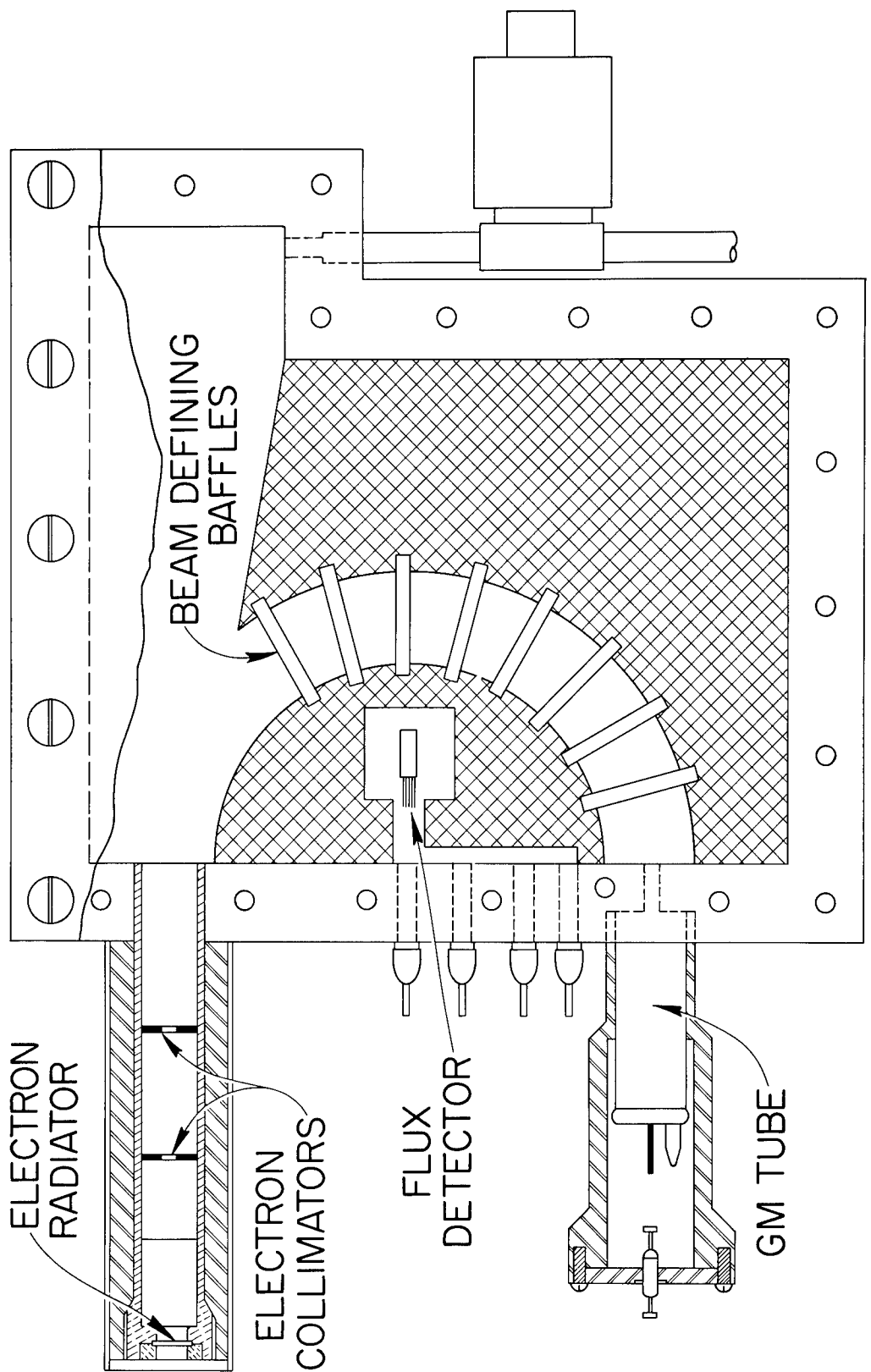
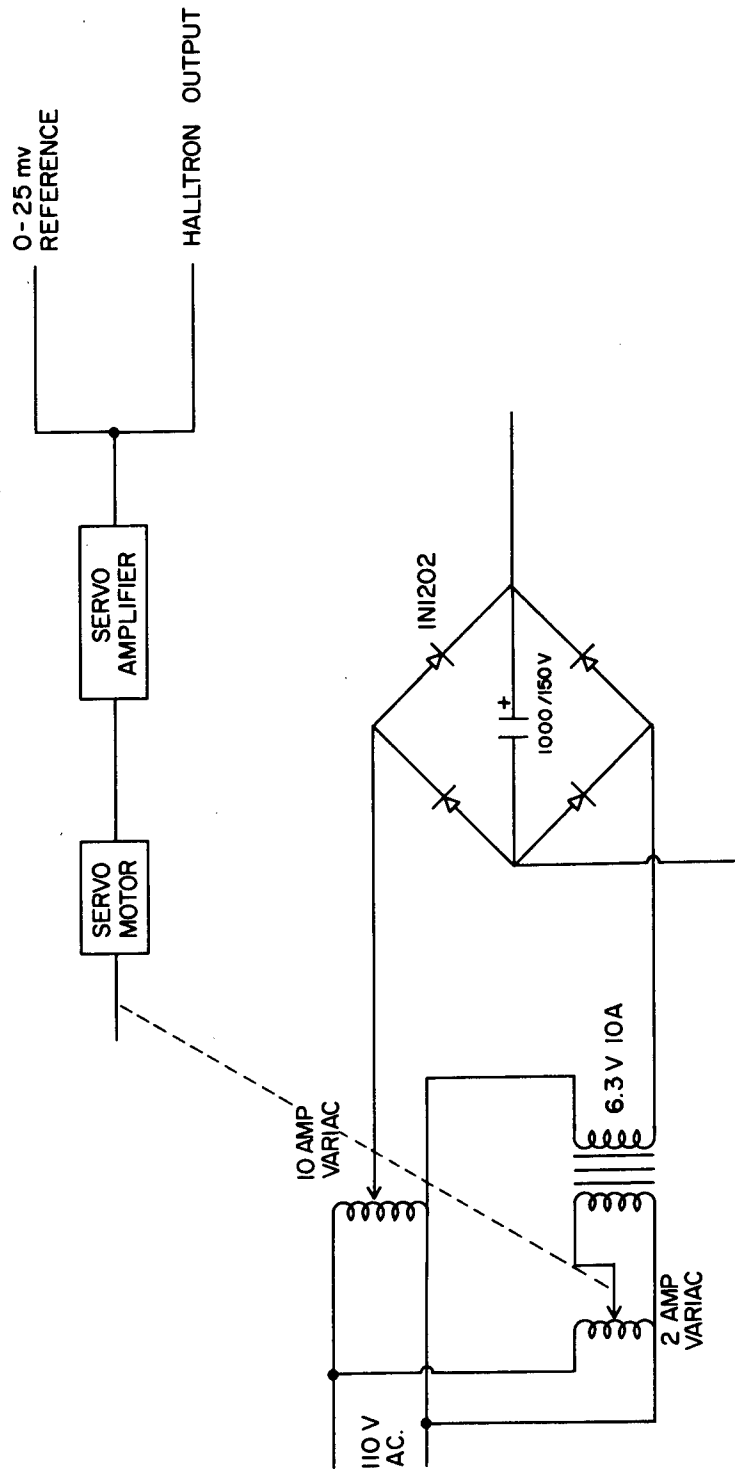


Fig. 2.15--Compton Gamma-Ray Spectrometer



### MAGNET POWER SUPPLY

Fig. 2.16--Compton Spectrometer Magnet Supply Diagram

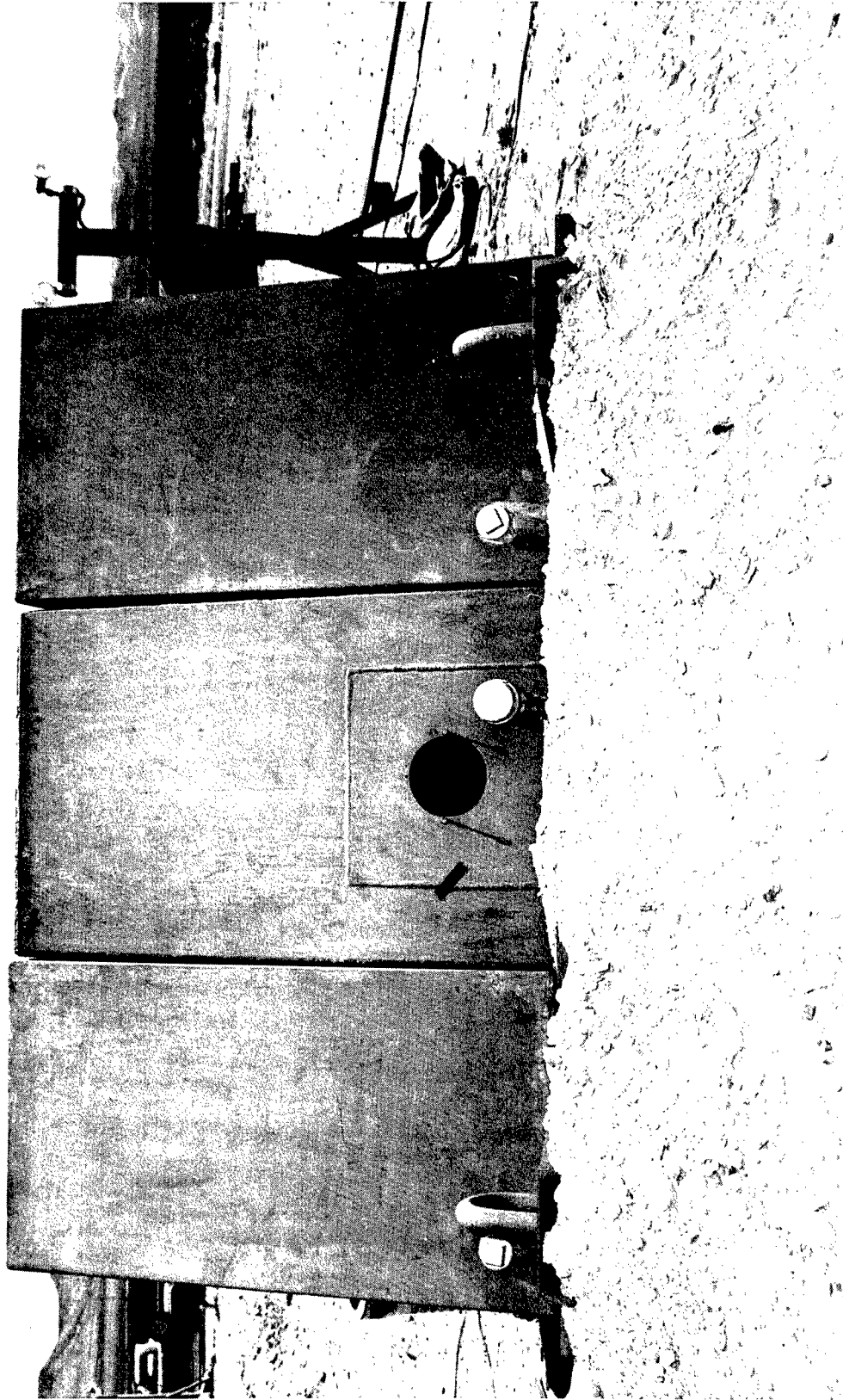


Fig. 2.17--Front View of the Compton Spectrometer Shield and Collimator Showing 10° Opening

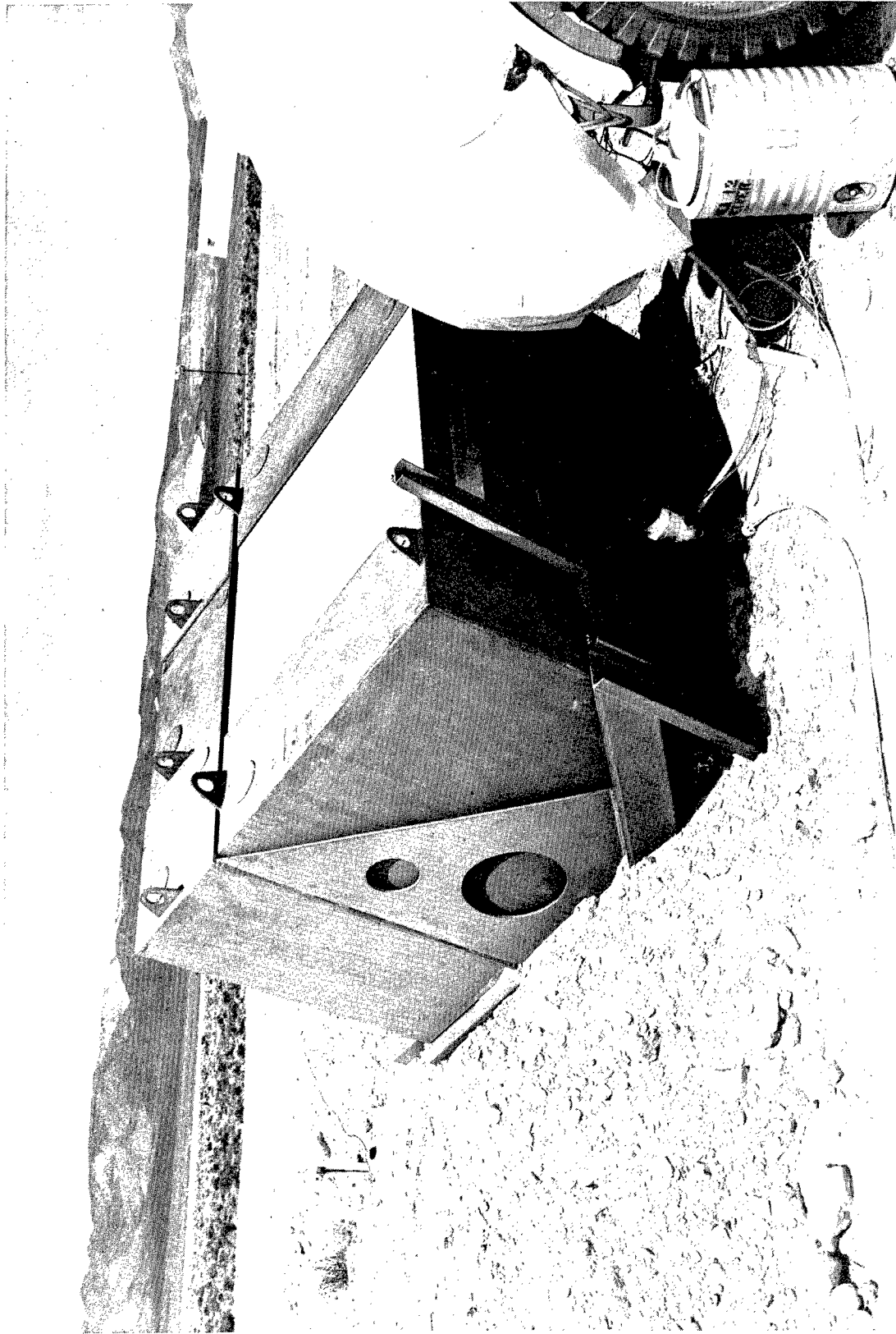


Fig. 2.18--Rear View of the Compton Spectrometer Shield Showing Stacked Transitite

side of the fixed tank were 20 in. thick. The two side tanks were 15 in. thick and went up as high as those in front while the rear tank, also 15 in. thick, went only as high as the top of the lead. Cement-asbestos board sheets 1/2 in. thick filled the indentation formed by the water tanks and simplified access to the spectrometer. The bottom was shielded by the ground upon which the collimator was set.

Access to the spectrometer for the magnet current and control wires, detector high voltage and signal cables, and the vacuum hose was provided by a pair of 2-in. conduits run along the top of the base plate through the back water and lead shields. The conduits served as a path for the magnet cooling air provided by a small exhaust fan located on one of the conduits.

A lead plug and a water plug closed the collimator opening for background measurements. From the front of the water plug a rod extended to hold a modified inclinometer used to set the collimator vertical angle. A transit was used, with the tower as a reference, to measure the azimuthal angle.

The adequacy of shield design was demonstrated when the same count rate was obtained for the natural background and the background during reactor operation. This background was due largely to the natural and fallout radioactivity present in the soil piled under the collimator shield.

### 2.5.3 Cobalt-60 Gamma Spectrometer

Gamma spectrum measurements were made of the  $^{60}\text{Co}$  source as a function of angle with a NaI(Tl) crystal in a collimator. The crystal was 3 in. long by 3 in. in diameter and was mounted as an integral unit with a 3-in. photomultiplier tube and magnetic shield. This unit was delivered from the manufacturer with a guaranteed resolution of 7.5% for the  $^{137}\text{Cs}$  gamma ray.

The 1100 volts necessary for the operation of the photomultiplier tube were transmitted over a 250-ft high-voltage coaxial cable from a regulated, low noise, high-voltage supply located in the instrument trailer. The photomultiplier tube output signal was transmitted to the instrument trailer over a 250-ft coaxial cable using a White cathode follower preamplifier, the power supply for which was located at the collimator site. Amplification was provided at the trailer by an ORNL-type DD-2 linear amplifier. Spectrum analysis was made with a multichannel analyzer.

## 2.6 NORMALIZATION OF RADIATION FIELD VARIATIONS

### 2.6.1 HPRR

In order to normalize variations in reactor power from run to run and between measurements during a single run, a neutron counting system was devised and operated at 750 yd and/or 1000 yd. Two channels were used simultaneously during the experiment. The primary channel used a  $^{10}\text{BF}_3$  proportional counter enclosed in a paraffin moderator enclosed in a 22.5-cm-dia. by 37-cm-long aluminum can. Figure 2.19 shows how this detector was mounted. A preamplifier having a gain of 20 and a special output stage for transmitting the signal over long cables was located near the detector. Power for the preamplifier was obtained from an ORNL A-1D amplifier located in the trailer with an auxiliary circuit to provide sufficient filament voltage to overcome losses in the cable.

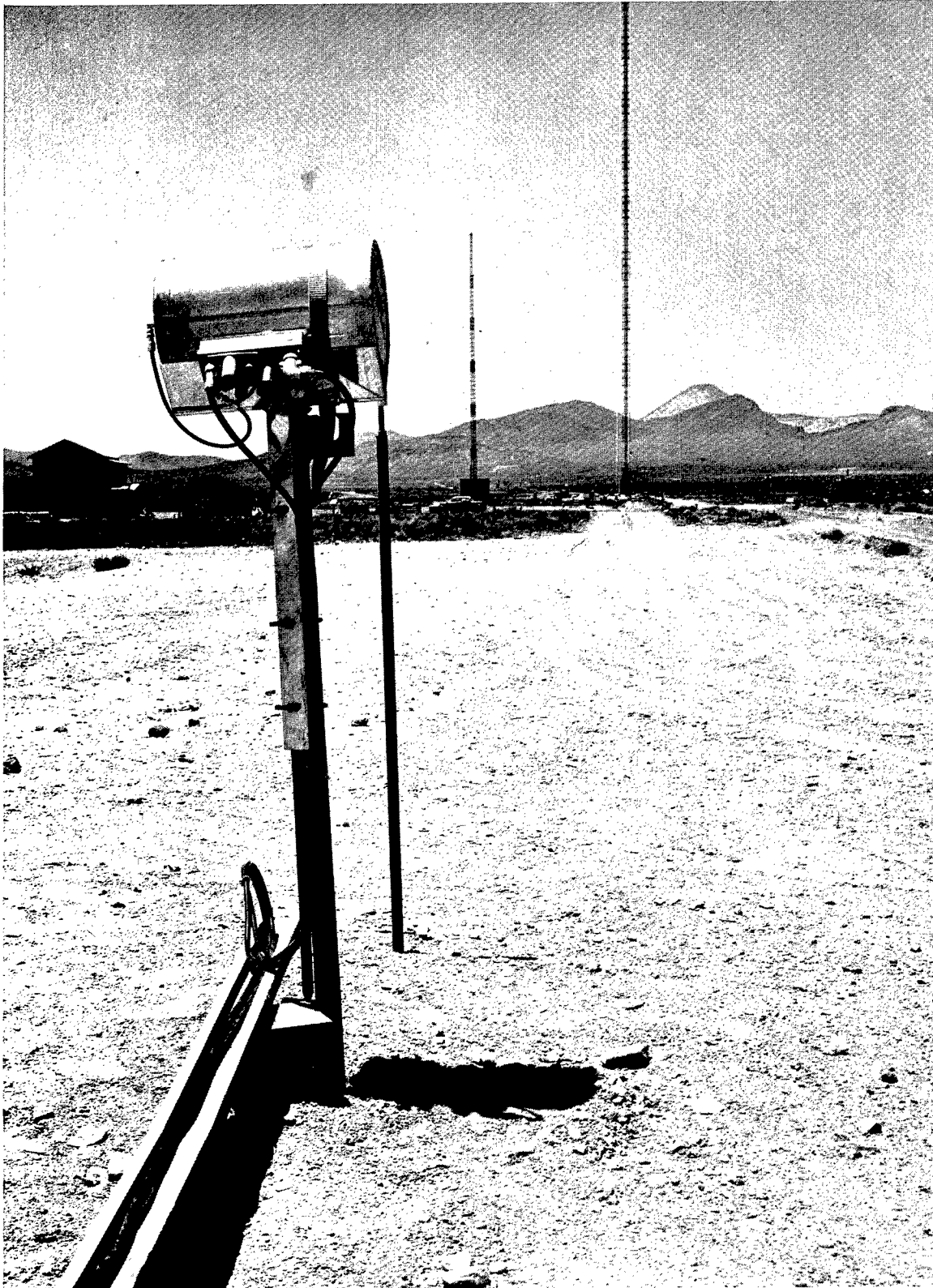


Fig. 2.19--Normalizing Channel Number 1

Preamplifier power and detector signals were carried over a multiconductor cable. Further amplification of the signal was provided by the A-1 amplifier operating in the 0.5 mc bandwidth position. The amplifier pulse-height selector output went to several scalers. A visual record was maintained by using a count-rate meter and strip chart recorder to record the normalizing channel pulse rate. Proportional counter anode potential was transmitted on RG 11A/U coaxial cable from a high-voltage supply located in the instrument trailer.

A back-up channel was similar in design. Identical electronic equipment was used, but the neutron moderator was made of wood in an approximately cylindrical shape (Fig. 2.20). When the instrument trailer was moved back for measurements at 1000 yd from the tower, the primary normalizing channel was moved back as well. The secondary channel remained at 750 yd to provide a means of correlating the two positions.

Additional normalization of reactor runs was made using sulfur pellets located in a reproducible position on the source hoist car. Data obtained from these pellets contained none of the effects of changes in air density which was reflected in the counts obtained from the other normalizing channels.

Further description of these normalizing systems and a summary of the data obtained from them have been published in CEX-62.03.<sup>16</sup>

#### 2.6.2 Cobalt-60

Two methods were used to normalize data taken when the <sup>60</sup>Co source was in use. Because source output decayed at a known rate, only air-density corrections were necessary to normalize data taken under different atmospheric conditions. However, a counting system was also used that had a sensitive Geiger-tube detector located at 750 yd. Detector output was displayed on scalers and was also plotted using a count-rate meter and strip chart recorder.

#### REFERENCES

1. M. I. Lundin, Health Physics Research Reactor Hazards Summary, USAEC Report ORNL-3248, Oak Ridge National Laboratory, August 1962.
2. J. A. Auxier, The Health Physics Research Reactor, Health Phys., 11: 89-93 (1965).
3. G. S. Hurst and R. H. Ritchie, Project 39.5, Operation Plumbbob Report, WT-1504, September 19, 1958. (Classified)
4. R. H. Ritchie and G. S. Hurst, Penetration of Weapons Radiation: Application to the Hiroshima-Nagasaki Studies, Health Phys., 1: 390-404 (1959).
5. J. A. Auxier and T. V. Blosser (Private communication).
6. E. B. Wagner and G. S. Hurst, Advances in the Standard Proportional Counter Method of Fast Neutron Dosimetry, Rev. Sci. Instr., 29: 153-158 (1958).
7. G. S. Hurst, An Absolute Tissue Dosemeter for Fast Neutrons, Brit. J. Radiol., 27: 353-357 (1954).
8. E. B. Wagner and G. S. Hurst, A Geiger-Mueller Gamma-Ray Dosimeter with Low Neutron Sensitivity, Health Phys., 5: 20-26 (1961).
9. J. H. Thorngate and D. R. Johnson, The Response of a Neutron Insensitive Gamma-Ray Dosimeter as a Function of Photon Energy, Health Phys., 11: 133-136 (1965).



Fig. 2.20--Normalizing Channel Number 2

10. J. H. Thorngate, A Versatile Frequency Divider, Health Phys., 10: 687-689 (1963).
11. E. B. Wagner, Health Physics Division Annual Progress Report for Period Ending July 31, 1962, USAEC Report ORNL-3347, p. 85, Oak Ridge National Laboratory, November 2, 1962.
12. R. F. Mozley and F. C. Shoemaker, A Fast Neutron Scintillation Spectrometer, Rev. Sci. Instr., 23: 569 (1952).
13. E. Fairstein, Nonblocking Double-Line Linear Pulse Amplifier, Rev. Sci. Instr., 27: 475-482 (1956).
14. E. Fairstein, A Pulse Crossover Pickoff Gate for Use with a Medium-Speed Coincidence Circuit, Instrument and Controls Division Annual Progress Report for Period Ending July 1, 1957, USAEC Report ORNL-2480, pp. 1-5, Oak Ridge National Laboratory, July 14, 1958.
15. J. H. Thorngate, Medium Speed Coincidence Circuit Using Tunnel Diodes, Health Phys., 10: 283-284 (1964).
16. J. A. Auxier, F. F. Haywood, and L. W. Gilley, General Correlative Studies - Operation BREN, USAEC Report CEX-62.03, September 1963.

## Chapter 3

### PROCEDURES

#### 3.1 COLLIMATORS

The two collimator acceptance angles used,  $10^\circ$  and  $30^\circ$ , were defined by the inserts placed in the basic  $45^\circ$  conical openings. Measurements were taken in two planes with the axis of the tower and the collimator station in the first plane while the second plane passed through the source and collimator and was perpendicular to the first. Zero angle was determined by the source-to-collimator line which was the intersection of the two planes described. The notation  $\phi$  represented angles in the first plane and  $\theta$  angles in the second plane. The value of  $\phi$  increased as the angle opened upward from the zero direction as viewed from the side and  $\theta$  increased as the angle opened to the right, or clockwise, from the zero direction as viewed from above. Measurements were made varying  $\phi$  from  $270^\circ$  through zero to  $180^\circ$  with the  $30^\circ$  acceptance cone and from  $330^\circ$  through zero to  $30^\circ$  when the  $10^\circ$  acceptance cone was used. The angle increments used in all cases were the same size as the acceptance cone. In the second plane,  $30^\circ$  measurements were made from  $\theta = 60^\circ$  through zero to  $\theta = 300^\circ$ .

The collimator was aimed with the inclinometer described in Chapter 2. In operation, this device was similar to a mortar sight. A spirit level was the vertical angle reference and a post, in this case the tower, was the horizontal angle reference. Because the zero angle as defined varied with the source height, vertical angles were set on the protractor with respect to the angle between the horizon and the reactor position. Additional corrections were required in setting the vertical angle because the ground sloped up from the collimator sites to the tower base.

To set the collimator the negative values of the angles required were set on the vertical and horizontal protractors of the inclinometer. Next the inclinometer was set on top of the right hand collimator in the turret as viewed from behind. After the inclinometer was accurately positioned, the turret was rotated to adjust the vertical angle until the spirit level on the vertical angle protractor was centered. The vertical angle adjusting crank was locked by inserting a pin. Finally the horizontal angle was set by rotating the turret until the tower was viewed at the cross hairs of the sight mounted on the horizontal protractor. Horizontal angles were locked by tightening a clamp around the turret bearing.

## 3.2 DOSE MEASUREMENTS AS A FUNCTION OF INCIDENT ANGLE

### 3.2.1 Neutron Dose

Neutron dose measurements were made as a function of angle at 750 yd and 1000 yd from the base of the tower. The Hurst proportional counter was used in conjunction with the Radsan pulse-height integrator. Collimator acceptance angles were  $30^\circ$  and  $10^\circ$  at 750 yd and  $30^\circ$  at 1000 yd. The  $10^\circ$  measurements were made using the straight-sided collimator originally designed for use with the neutron spectrometer. When used with the dosimeter properly placed, this gave an acceptance angle close to  $10^\circ$ .

Neutron dose measurements were made at reactor heights of 1500, 1125, and 500 ft when the collimator was located at 750 yd. A  $10^\circ$  collimator was used for measurements at a reactor height of 1500 ft with readings taken at  $10^\circ$  increments from  $310^\circ$  to  $360^\circ$ . With the reactor at 500 ft, the measurements ranged in  $10^\circ$  increments from  $340^\circ$  through  $0^\circ$  to  $30^\circ$ . Both  $10^\circ$  and  $30^\circ$  collimators were used for the measurements at 1125 ft with  $10^\circ$  cone readings made for angles from  $320^\circ$  through  $0^\circ$  to  $30^\circ$  with the  $30^\circ$  measurements made at 750 yd in one direction ( $\theta$ ) in  $30^\circ$  increments from  $240^\circ$  to  $0^\circ$  and in the other direction ( $\phi$ ) from  $270^\circ$  through  $0^\circ$  to  $180^\circ$ . At 1000 yd from the base of the tower the measurements were made with the  $30^\circ$  cone from  $0^\circ$  to  $90^\circ$ .

All measurements used the "medium" setting of running time ( $\sim 210$  sec) of the Radsan integrator. The total number of runs made at any collimator setting was determined by the statistical uncertainty observed. Measurements made near zero required fewer runs than those made at greater angles with as few as four made at some angles and as many as 16 made at others. In a nuclear counting device, the statistical uncertainty of a count may be predicted if the total number of counts recorded is known. In the Radsan integrator, this number does not have a constant relationship to the dose value recorded but depends upon the neutron spectrum. The total number of counts is equivalent to the number of times the lowest discriminator operates and by counting these events, the statistical fluctuations may be computed. Moreover, for a given spectrum, the ratio of recorded dose to total pulses remains the same so that if the ratio is known, the recorded values may be used directly to determine statistical uncertainty. Such a procedure was followed during BREN.

Preamplifier power was obtained from a power supply, located near the detector, operated from a 110-volt a-c service available at the collimator site. This arrangement tended to produce "noise" as the preamplifier and amplifier were operated with different electrical grounds yet were interconnected through the signal cable ground. Therefore, the detector was insulated from the collimator in order to minimize the noise. Because the amplification of the preamplifier-main amplifier system was somewhat low, higher detector anode potentials were required for adequate overall gain. An increase in high voltage generally produced a concomitant noise increase due to high-voltage leakage at the detector. Adequate cleanliness of the insulators to prevent this noise was difficult in the dusty conditions prevalent in the desert.

To minimize noise, several detectors were used during the experiment. Routine calibration used a 1-curie PuBe neutron source located on the collimator axis 1 m from the detector center. Such calibrations were performed to detect any shift in detector response. Gain standardizations were made numerous times during the course of operation using an alpha source mounted inside the proportional counter. Operating gain was established using this alpha source as a

reference. To achieve a correct gain setting, the dose integrator discriminators were set using a calibrated oscilloscope and pulse source. The discriminators were calibrated in this manner each day before the start of reactor operations and during the course of the operation if there were some reason to suspect a change in discriminator setting had occurred.

### 3.2.2 HPRR Gamma Dose

No noise problems were encountered in the gamma dose measurements due to the simplicity of the detector used. The relatively low sensitivity of the detector required lengthy runs at some angles in order to obtain sufficient accuracy. Measurements ranged in length from 15 to 30 min each with from two to ten readings taken at a given collimator setting. Careful background runs were made before and after each run. The background was low, quite consistent, and had essentially no dependence upon the collimator angle. Calibration was obtained using a  $^{60}\text{Co}$  source of known output located at  $0^\circ$  1 m from the detector.

Gamma dose was measured as a function of angle at 750 yd from the base of the tower with the reactor at 500, 1125, and 1500 ft and at 1000 yd with the reactor at 1500 ft. At 750 yd  $10^\circ$  collimator measurements were made in  $10^\circ$  increments from  $310^\circ$  to  $0^\circ$ , with the reactor 1500 ft high, from  $320^\circ$  through  $0^\circ$  to  $30^\circ$ , with the reactor 1125 ft high, and from  $340^\circ$  through  $0^\circ$  with the reactor 500 ft high. Measurements were made in two directions at 750 yd using the  $30^\circ$  collimator with the reactor at 1125 ft. In the vertical direction ( $\phi$ ) measurements were made in  $30^\circ$  increments from  $270^\circ$  through  $0^\circ$  to  $180^\circ$  while in the lateral direction ( $\theta$ ) the measurements ranged from  $240^\circ$  through  $0^\circ$  to  $60^\circ$ . Measurements at 1000 yd from the base of the tower were limited to four measurements in  $30^\circ$  increments from  $0^\circ$  to  $90^\circ$ .

A separate experiment performed at the ORNL DOSAR Facility was necessary to determine the background due to neutron interaction with collimator materials. The correction, as a function of neutron normalization count, was determined and subtracted in the proper amount from each reading.

### 3.2.3 Cobalt-60 Gamma Dose

A larger Geiger tube detector was used to measure the angular gamma-ray dose distribution from the  $^{60}\text{Co}$  source. It was operated in essentially the same manner as the smaller detector used during reactor measurements. To calibrate the detector, a  $^{60}\text{Co}$  source was placed 1 m from the center of the detector on the  $0^\circ$  axis of the collimator. Due to the larger size of this detector, the angular resolution of the collimator was not quite as good as when the small gamma detector was used.

With the source at an 1125-ft elevation, measurements made at 750 yd using the  $30^\circ$  collimator were limited to  $330^\circ$ ,  $0^\circ$ , and  $30^\circ$  by the low dose. Measurements were made with the  $10^\circ$  collimator in  $10^\circ$  increments from  $330^\circ$  through  $0^\circ$  to  $30^\circ$ . At 1000 yd from the base of the tower measurements were attempted only with the  $30^\circ$  collimator. At reactor heights of 27 ft and at 300 ft measurements were made at  $0^\circ$  and  $30^\circ$ . With the reactor at 1500 ft the points were at  $0^\circ$ ,  $30^\circ$ ,  $60^\circ$ , and  $90^\circ$ . None of the data taken at 1000 yd proved useful because of poor statistical accuracy.

### 3.3 SPECTRUM MEASUREMENTS

#### 3.3.1 HPRR Neutron Spectrum

Each day before reactor operations, the neutron telescope was thoroughly checked. First, the cold trap was charged with dry ice and acetone and the vacuum pump started. A pulse generator was connected to the two preamplifiers at the collimator site to balance the gain of the two electronic channels. Balancing was performed by alternately removing the first or second input from the summing circuit and recording the signals produced by the pulser in alternate halves of a multichannel analyzer memory. The display of the memory halves was overlapped and the balance control in the summing circuit adjusted until the pulses produced by each channel could be superimposed. When the balance was correct the pulser was disconnected from the preamplifiers and the 20-ft cables to the photomultiplier tube anodes in the spectrometer were reconnected. The long cables provided sufficient input capacitance to integrate the anode pulse so the linear amplifiers would properly amplify them. To check gain settings and coincidence circuit operation, the pulser was connected directly to the linear amplifier inputs. Gain was checked by setting the pulser at a predetermined output and adjusting the analyzer linear amplifier gain so that the pulse was analyzed in channel 1. This setting was reduced by a factor of 2 to check the operation and triggering level of the discriminators in the pulse cross-over detecting circuits. An oscilloscope was used to set the discriminator hysteresis so the output pulse was occurring at the linear amplifier pulse cross-over point. When the settings were correct a check with the oscilloscope determined whether the coincidence circuit was operating. The correct time relationship between the analyzer gate pulse generated by the coincidence circuit and the analog pulse was determined by analyzing the analog pulse with and without the coincidence circuit functioning and setting the delay required in the gate signal circuit to put the analyzed pulse in the same channel in either case. A delay of 0.5  $\mu$ sec was typical.

Next, the pulser was removed from the inputs and the signal cables put in place. At this point, sufficient time had generally elapsed that the pressure in the spectrometer was below 100 microns and the photomultiplier high voltages were turned on. Turning the voltage on at pressures greater than 100 $\mu$  resulted in gas discharges in the residual air. After the photomultiplier tubes had stabilized for a few minutes, the solenoid was activated to expose the internal alpha source. Detector outputs were analyzed one at a time and photomultiplier tube high voltage independently adjusted until the alpha peaks recorded were in the same channel. When the solenoid was deenergized, the spectrometer was ready for measurements. Overall amplifier gain was set, originally, using a PuBe source located 1 m from the front, or radiator, crystal at the collimator 0° direction. Subsequent gain checks were made using a calibrated pulse generator. Midway through the operation solenoid sticking and outgassing became troublesome and necessitated frequent maintenance.

Numerous measurements were made with the collimator at 750 yd from the base of the tower with the reactor at an 1125-ft elevation. In all cases a straight-walled collimator 5 in. in diameter was used. Collimator angles were  $\phi = 330^\circ, 0^\circ, 30^\circ, 60^\circ, \text{ and } 180^\circ$  and  $\theta = 270^\circ, 300^\circ, 330^\circ, 30^\circ, \text{ and } 60^\circ$ . At 1000 yd from the tower with the reactor at 1500 ft, two runs were made, one at 0° and the other at 90°.

### 3.3.2 HPRR Gamma Spectrometry

Due to the low sensitivity of the Compton gamma spectrometer, it was operated in a fixed position 500 yd from the base of the tower and was permanently aimed at the 1125-ft elevation.

On suitable operational days, the vacuum system was activated as soon as possible. Typical operating pressures of 30 microns were achieved within a short time. This pressure was adequate for operation.

When the magnet supply was activated, the servo control system was set to produce a zero magnetic field. In order to cancel the residual magnetism of the pole pieces and the earth's magnetic field, magnet current polarity and the flux sensing device were reversed. A background count was made with the collimator opening plugged and the magnetic field at 0 Gauss. A similar background was measured after reactor operations had commenced. After making suitable background counts, the magnet servo control was set to produce the desired flux, the collimator plug was removed and a count made. Two or three 15-min counts were made for each magnet setting. Readings were made at even flux intervals up to a setting sufficient to analyze the electrons produced by a 10.3 Mev gamma ray. To prevent damage to the magnet power supply, the magnet current was reduced to zero before turning the power off or reversing the magnetic field.

Due to the safety regulations established to prevent irradiation in case of a reactor accident, the operator could go in to stop, read, and restart the scaler for only short periods. The intercom system between the collimator site and the instrument trailer enabled the operator to transmit the data verbally and allowed the detector scaler and a normalization scaler to be operated simultaneously.

A check of spectrometer operation was made using a  $^{60}\text{Co}$  source placed in the collimator throat.

### 3.3.3 Cobalt-60 Gamma Spectrum

Gamma spectrum measurements were made as a function of angle using the  $^{60}\text{Co}$  source and a 3-in. by 3-in. NaI(Tl) scintillation crystal. The detector was operated in a collimator located in the collimator turret, with  $10^\circ$  and  $30^\circ$  acceptance cones. All measurements at 1000 yd from the base of the tower used  $30^\circ$  cones. Ten-minute runs were made at  $\phi = 0^\circ$  and  $30^\circ$  with the source at elevations of 27 ft and 300 ft. When the source was raised to 1500 ft, 10-min runs were made at  $\phi = 0^\circ, 30^\circ, 60^\circ,$  and  $90^\circ$ . The measurements at 750 yd were made with the  $30^\circ$  collimator in  $30^\circ$  increments from  $\phi = 270^\circ$  through  $0^\circ$  to  $\phi = 180^\circ$  and for  $\phi = 330^\circ, 30^\circ, 60^\circ, 90^\circ,$  and  $120^\circ$ . These runs lasted from 40 min to 120 min, depending upon the angle. With the  $10^\circ$  acceptance angle measurements were made in  $10^\circ$  increments from  $\phi = 330^\circ$  through  $0^\circ$  to  $\phi = 30^\circ$ . One-hundred-minute intervals were used for all of these measurements. Backgrounds were run each day for periods comparable in length to the runs made.

A  $^{60}\text{Co}$  source set 3 m away from the crystal on the collimator  $0^\circ$  direction was used to establish the operating gain while a smaller  $^{137}\text{Cs}$  source placed in the collimator throat was used for day-to-day gain checks. Analyzer gain was set to give 1.6 Mev full scale.

To reduce the number of gamma rays leaking into the collimator, the 5-in.-dia. hole behind the detector was plugged with as much lead wool as possible. Aluminum foil 1 mil thick was placed over the collimator opening to reduce crystal heating due to exposure to the sun.

### 3.4 NORMALIZATION

#### 3.4.1 HPRR

Normalization of all runs made with the HPRR as the radiation source was necessary to compensate for changes in reactor power, source-detector separation, and air density, both from run to run and during the course of a single run. Two  $^{10}\text{BF}_3$  proportional counters enclosed in hydrogenous neutron moderators provided the necessary normalization information for the neutron measurements. One detector was located permanently at 750 yd from the tower, while the second was located at 750 yd when measurements were made at that distance or at 1000 yd for measurements there.

A separate gamma detector was not used for gamma measurement normalization during HPRR operation and as a result, considerable calculations were necessary to use the normalizing channel data correctly due to the different relaxation lengths of neutrons and gamma rays in air. Calculations were also required when the normalizing channel and the detectors were at different distances from the reactor, e.g., the Compton spectrometer was at 500 yd from the tower.

Both channels were installed carefully to assure correct counter and amplifier operation. A day-to-day check of the operation was achieved using a standard neutron source located at a reproducible distance from the detector.

To provide comparisons between reactor runs, a sulfur pellet was placed in a reproducible position on the hoist car for every run. The  $^{32}\text{P}$  beta activity of the pellets was measured after a suitable period to allow for decay of contaminant activation.

#### 3.4.2 Cobalt-60

Normalization between and during runs that used the  $^{60}\text{Co}$  source was easier than for the reactor because the source had an essentially unvarying output. Although corrections for radioactive decay were unnecessary because the experiment was short compared to the half-life of  $^{60}\text{Co}$ , corrections were required for changes in air density and changes in the source-ground geometry. Because data were available which permitted calculating these corrections, this approach was taken in analyzing the  $^{60}\text{Co}$  data.

Experimental normalization was also available utilizing the pulses produced by a sensitive Geiger counter and recorded on scalars operated simultaneously with the dosimeter and spectrometer. The detector was kept at a fixed position 750 yd from the tower. A small  $^{60}\text{Co}$  source set at a fixed distance was used to check the operation of this channel. Little of this information was used for reducing other data because the low count rate encountered produced normalizing data that had a statistical variation as great or greater than the other sources of error. The normalizing channel did provide a means of checking the calculations for air density and source-ground geometry corrections.

## Chapter 4

### DATA

#### 4.1 DOSIMETRY DATA

##### 4.1.1 General Discussion of Presentation

All angular dose measurements are presented graphically. The data have been normalized to a uniform air density, and the distance and interface corrections have been made. Corrections were applied to the normalizing channel data such that each reading in the collimator is compared to the total neutron or gamma-ray dose or fluence at the collimator site during the reading. For the  $^{60}\text{Co}$  source similar corrections were applied assuming a constant source output. Input data for the corrections were obtained from CEX-62.03.<sup>1</sup>

For these data presentations, the conical collimator opening used was chosen as the unit solid angle. For data presentation as a function of polar angle, all acceptable data were averaged. Corrections made to the polar angle data produced results for total solid angle as a function of polar angle. These corrections are the ratio of "unit" to total solid angle in the polar angle interval subtended by the collimator at a given setting. Numerical integration of the solid angle was made in  $1^\circ$  increments from the zero angle. The corrections, shown in Table 4.1, do not take the air-ground interface into consideration as its position varies with the inclination between the collimator zero angle and the horizon.

All data are shown graphically with the normalized dosimeter reading plotted vs. the vertical angle  $\phi$  or the lateral angle  $\theta$ . Angular limits shown with each point represent the opening of the collimator involved while the dose limits represent one standard deviation in the measured values. The vertical line, marked air-ground interface, represents the position of the horizon; this depended upon reactor height and distance from the tower.

##### 4.1.2 HPRR Neutron Dose as a Function of Incident Angle

This section presents the angular distribution of the fast-neutron dose as measured with the Radsan dosimeter system. Values plotted are proportional to dose but do not represent exact dose values. The angular definition shown is that of the collimator opening and is smaller than the effective size of the collimator opening which occurs due to the size of the detector. In this regard, it should be noted that the data marked  $10^\circ$  collimator were taken with a straight-throated collimator with the dosimeter placed in the proper position

TABLE 4.1--SOLID ANGLE CORRECTIONS  
SUMMARY

Polar Angle $\phi$	Acceptance Angle $\alpha$	Correction
0	10	1.000
10	10	8.812
20	10	17.364
30	10	25.384
0	30	1.000
30	30	8.784
60	30	15.215
90	30	17.571
116	30	15.790
120	30	15.215

to obtain essentially  $10^\circ$  collimation. No corrections have been included for the dose not measured due to the low energy cut-off of this system. The error caused by this factor was somewhat sensitive to the direction at which the collimator was aimed due to the change in neutron spectrum.

Deviations presented with the data were calculated from the average deviation of the large number of readings made at each setting. An advantage of this technique was the rejection of data which fell beyond  $2.5 \sigma$  from the average (Figs. 4.1 to 4.8).

#### 4.1.3 HPRR Gamma Dose as a Function of Incident Angle

Data recorded with the Phil dosimeter during reactor operations are presented here. While the numbers are all proportional to gamma-ray dose, they are not dose values. Due to the relative nature of the information, no correction to actual dose values was necessary. Each point displayed was leakage and natural background. In a few cases an additional correction was necessary due to a temporary loss of the  $^6\text{Li}$  shield used to reduce the detector's thermal neutron response.

Because this dosimeter has a low energy cut-off near 150 keV, no gamma dose from photons below this energy were recorded. It is difficult to estimate the amount of the dose produced by these low energy photons, however, it was assumed to be negligible due to the low dose delivered per photon. Only good spectral data would permit an accurate correction to be made, and no such information is available. Subsequent to BREN the dosimeter high energy response was checked up to 8 MeV and found uniform.

Statistical uncertainties shown with the data represent one standard deviation as calculated from the average deviation of the readings made. In general, the deviations obtained in this manner are greater than those obtained by considering only counting statistics and were used to indicate the overall errors involved (Figs. 4.9 to 4.16).

#### 4.1.4 Cobalt-60 Gamma Dose as a Function of Incident Angle

The gamma dosimeter used for these measurements was larger and more sensitive than that used with the reactor. Even so, substantially less data were taken because the source produced lower dose levels. Those points which were obtained are given graphically. The values are normalized to a constant source output with suitable corrections for source-detector geometry and air density. This approach resulted in a smaller statistical uncertainty than if the normalizing counter results were used.

The response of this detector was essentially uniform from the  $^{60}\text{Co}$  energies down to 55 keV. This is a lower energy than with the standard Phil, and was an advantage for measuring the field from the  $^{60}\text{Co}$  source. This lower energy response still leaves an uncertainty in data interpretation, but because of the relative nature of the measurements and the small range of angles over which they were made, the error is assumed to be negligible.

Additional angular dose response for angles not measured by the dosimeter might be deduced from spectrum measurements made as a function of angle using a NaI(Tl) scintillation detector, but for the purposes of this study, it was not feasible.

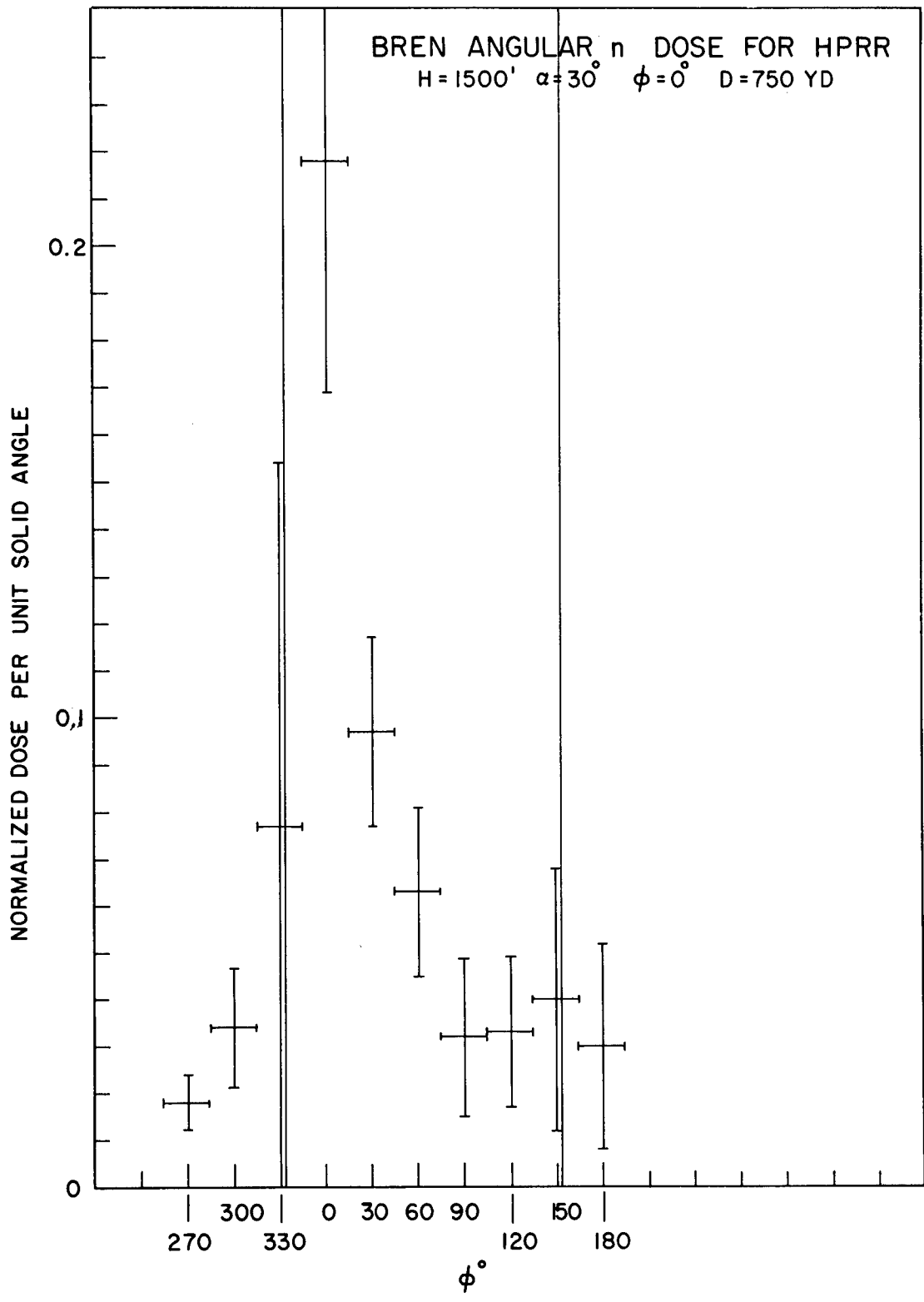


Fig. 4.1--Normalized Neutron Dose as a Function of Angle for a Reactor Height of 1125 Ft, Collimator Acceptance Angle =  $30^\circ$ , with  $\theta$  Kept at  $0^\circ$ , and Collimator Located at 750 Yd from the Base of the Tower

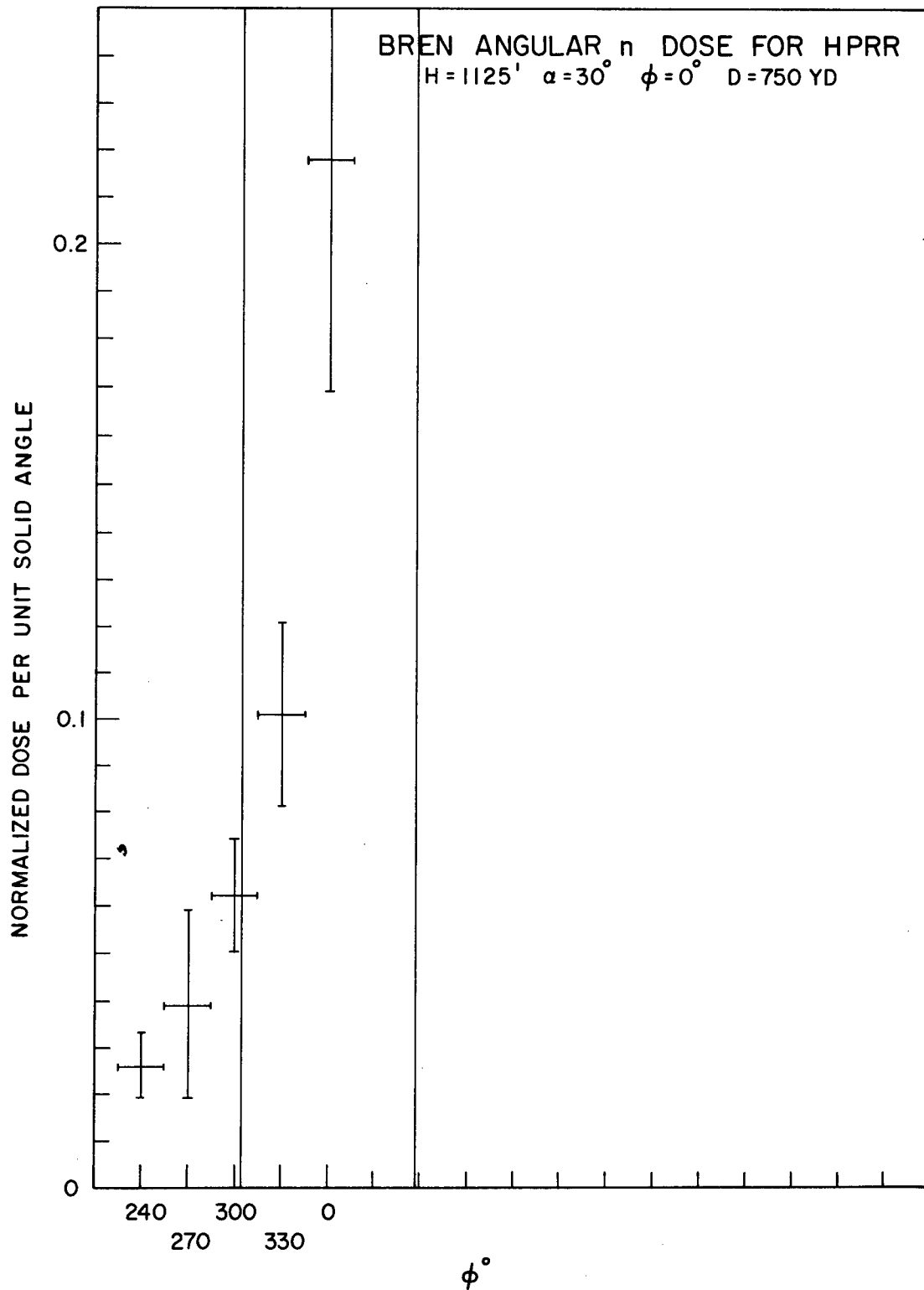


Fig. 4.2--Normalized Neutron Dose as a Function of Angle for a Reactor Height of 1125 Ft, Collimator Acceptance Angle =  $30^\circ$ , with  $\phi$  Kept at  $0^\circ$ , and Collimator Located at 750 Yd from the Base of the Tower

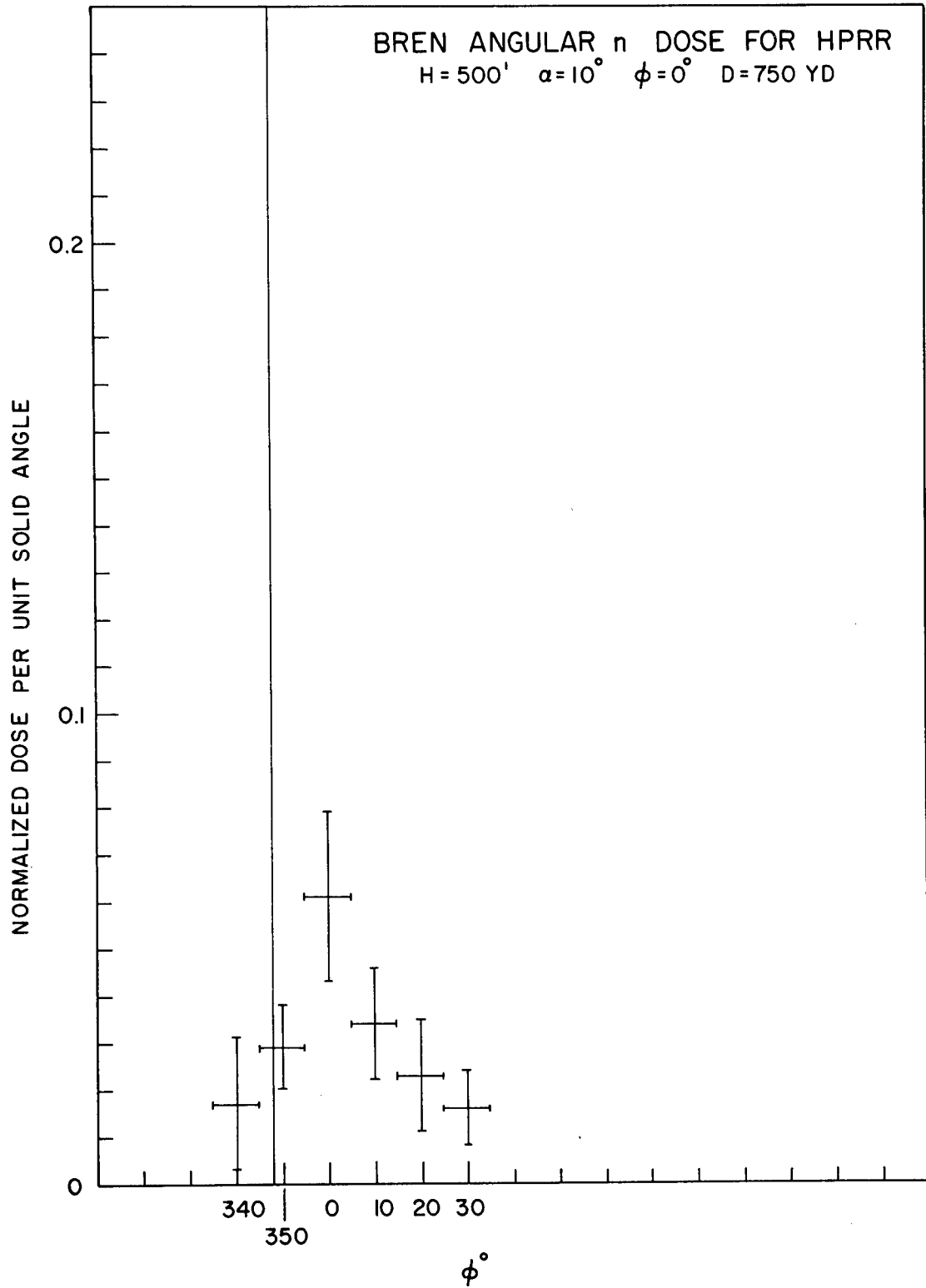


Fig. 4.3--Normalized Neutron Dose as a Function of Angle for a Reactor Height of 500 Ft, Collimator Acceptance Angle =  $10^\circ$ , with  $\theta$  Kept at  $0^\circ$ , and Collimator Located at 750 Yd from the Base of the Tower

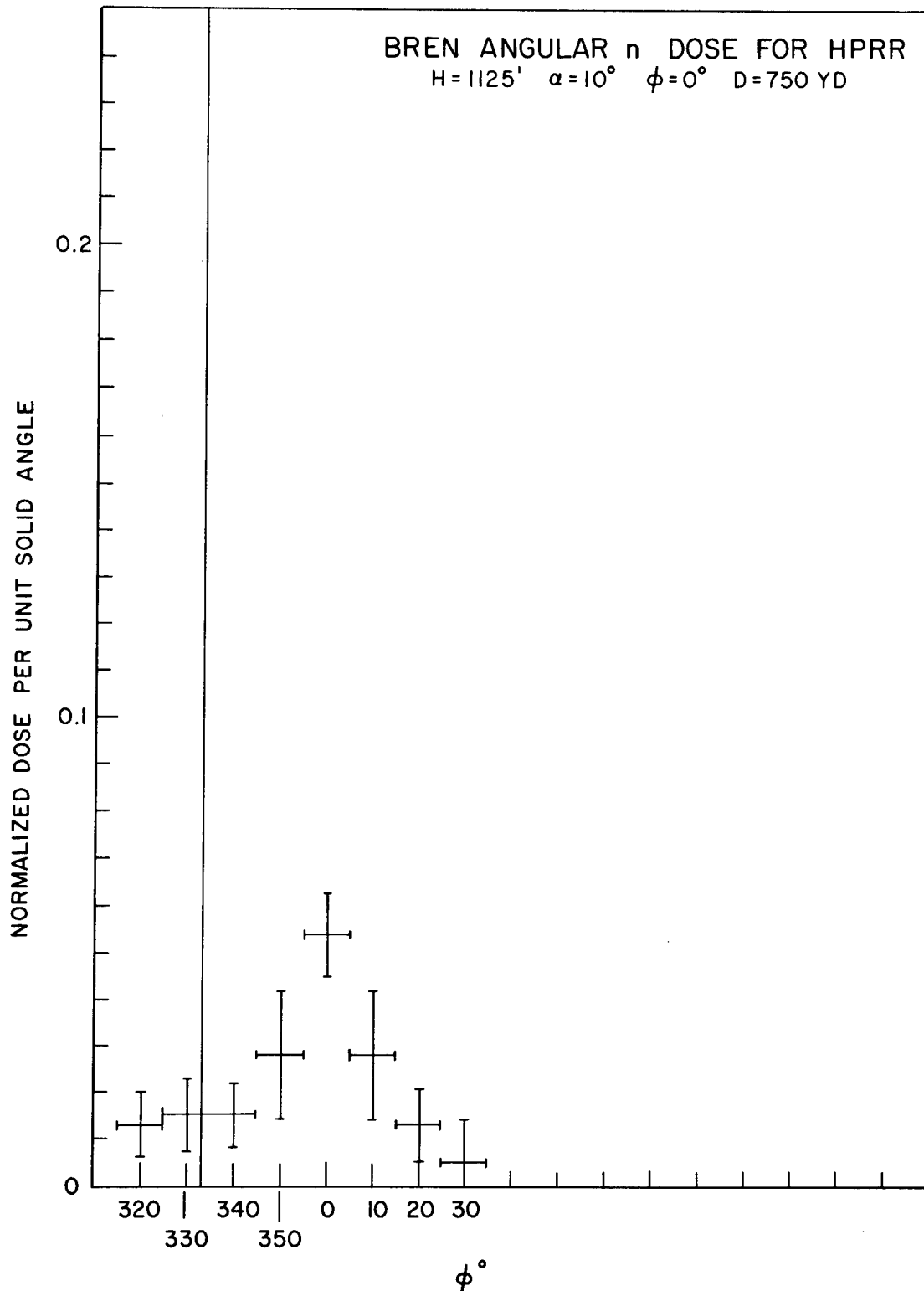


Fig. 4.4--Normalized Neutron Dose as a Function of Angle for a Reactor Height of 1125 Ft, Collimator Acceptance Angle =  $10^\circ$ , with  $\theta$  Kept at  $0^\circ$ , and Collimator Located at 750 Yd from the Base of the Tower

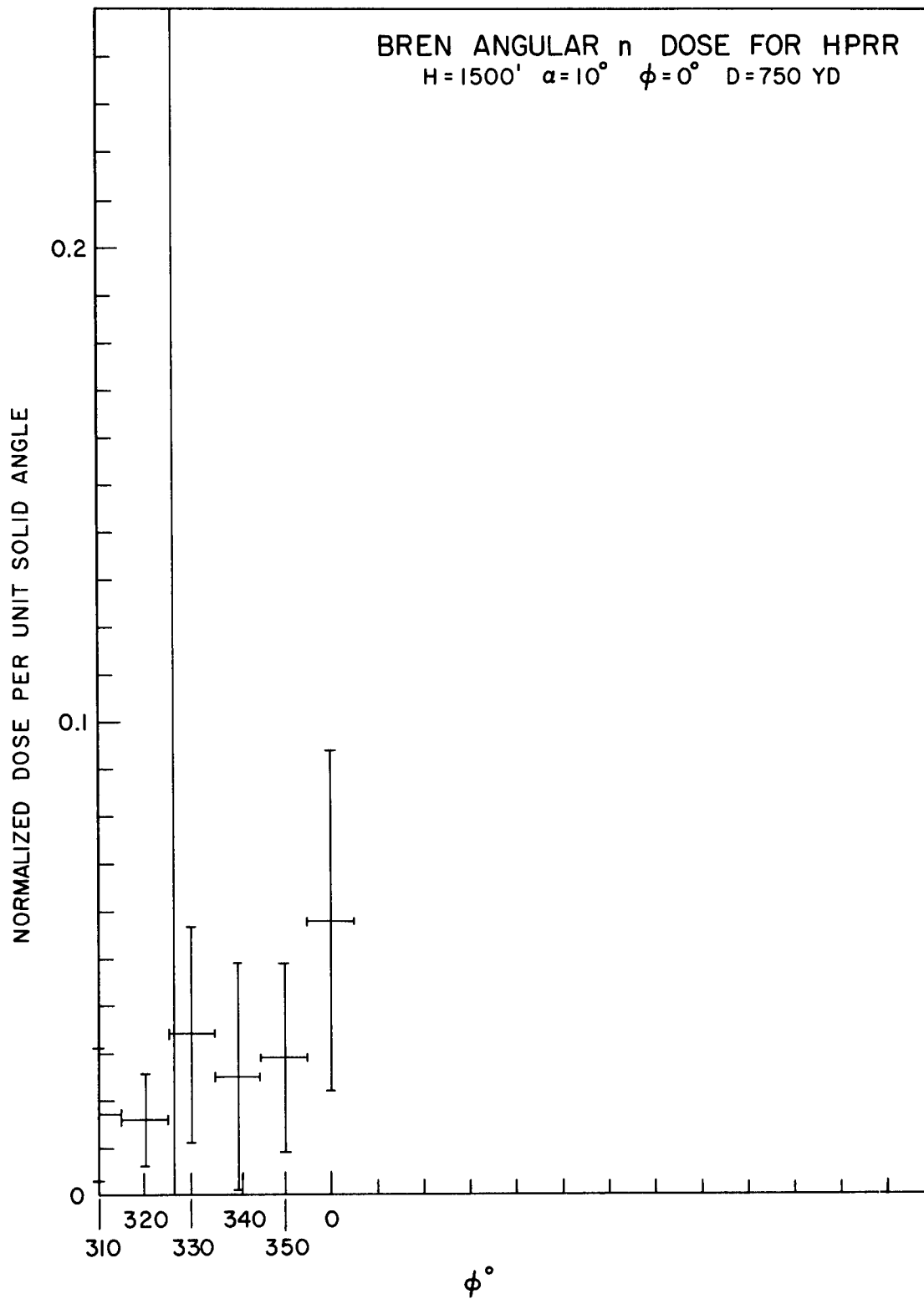


Fig. 4.5--Normalized Neutron Dose as a Function of Angle for a Reactor Height of 1500 Ft, Collimator Acceptance Angle =  $10^\circ$ , with  $\theta$  Kept at  $0^\circ$ , and Collimator Located at 750 Yd from the Base of the Tower

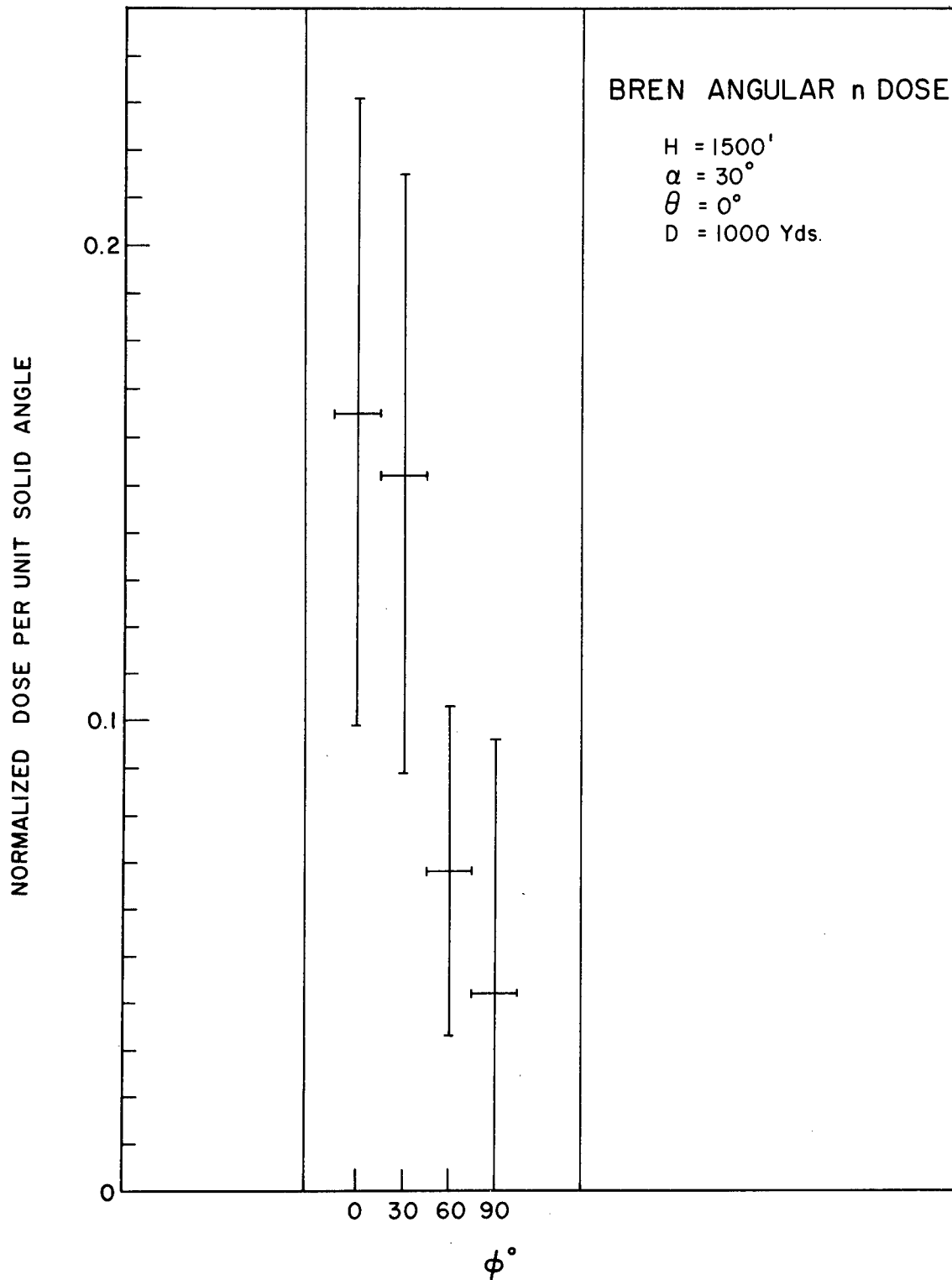


Fig. 4.6--Normalized Neutron Dose as a Function of Angle for a Reactor Height of 1500 Ft, Collimator Acceptance Angle =  $30^\circ$ , with  $\theta$  Kept at  $0^\circ$ , and Collimator Located at 1000 Yd from the Base of the Tower

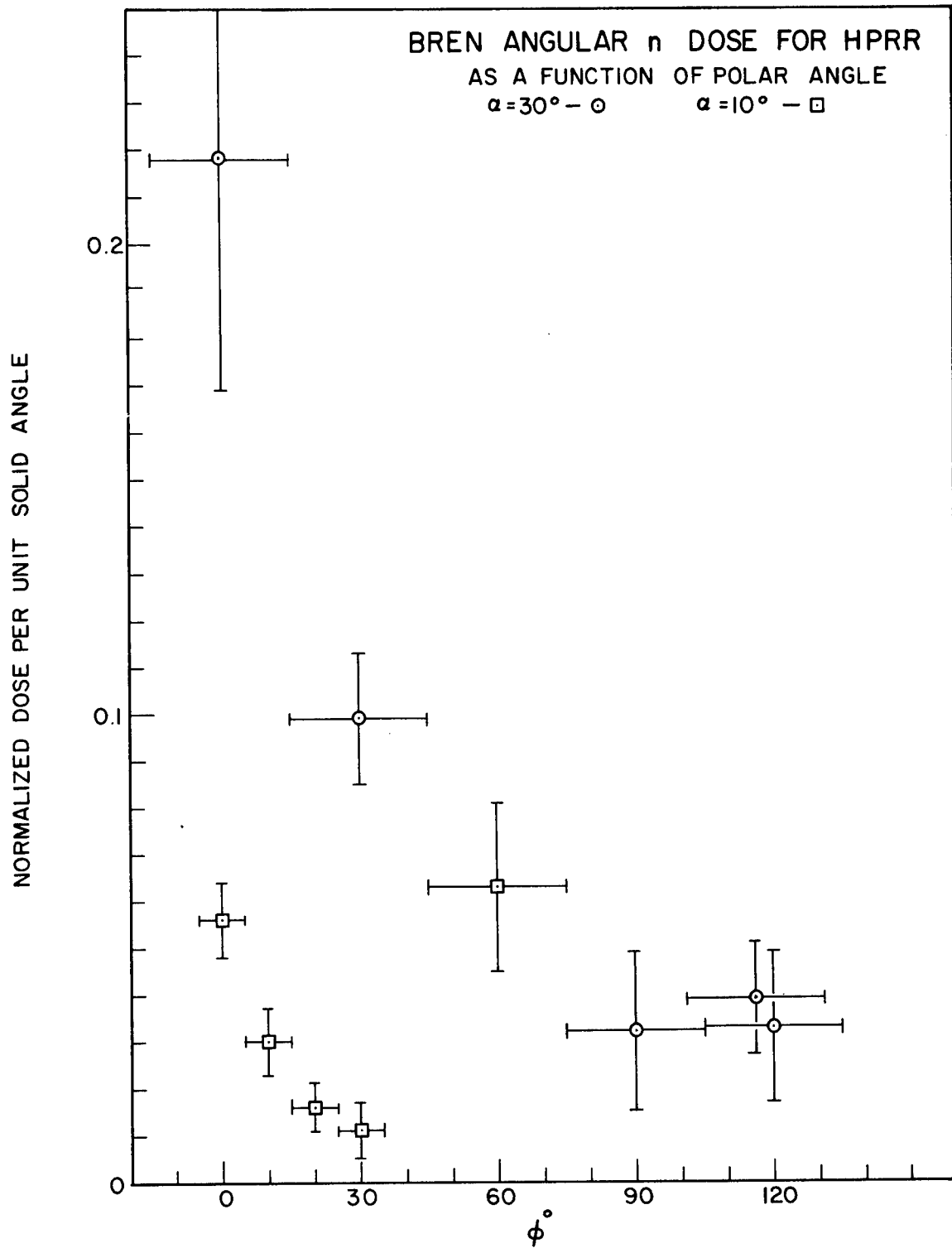


Fig. 4.7--Normalized Neutron Dose as a Function of Polar Angle

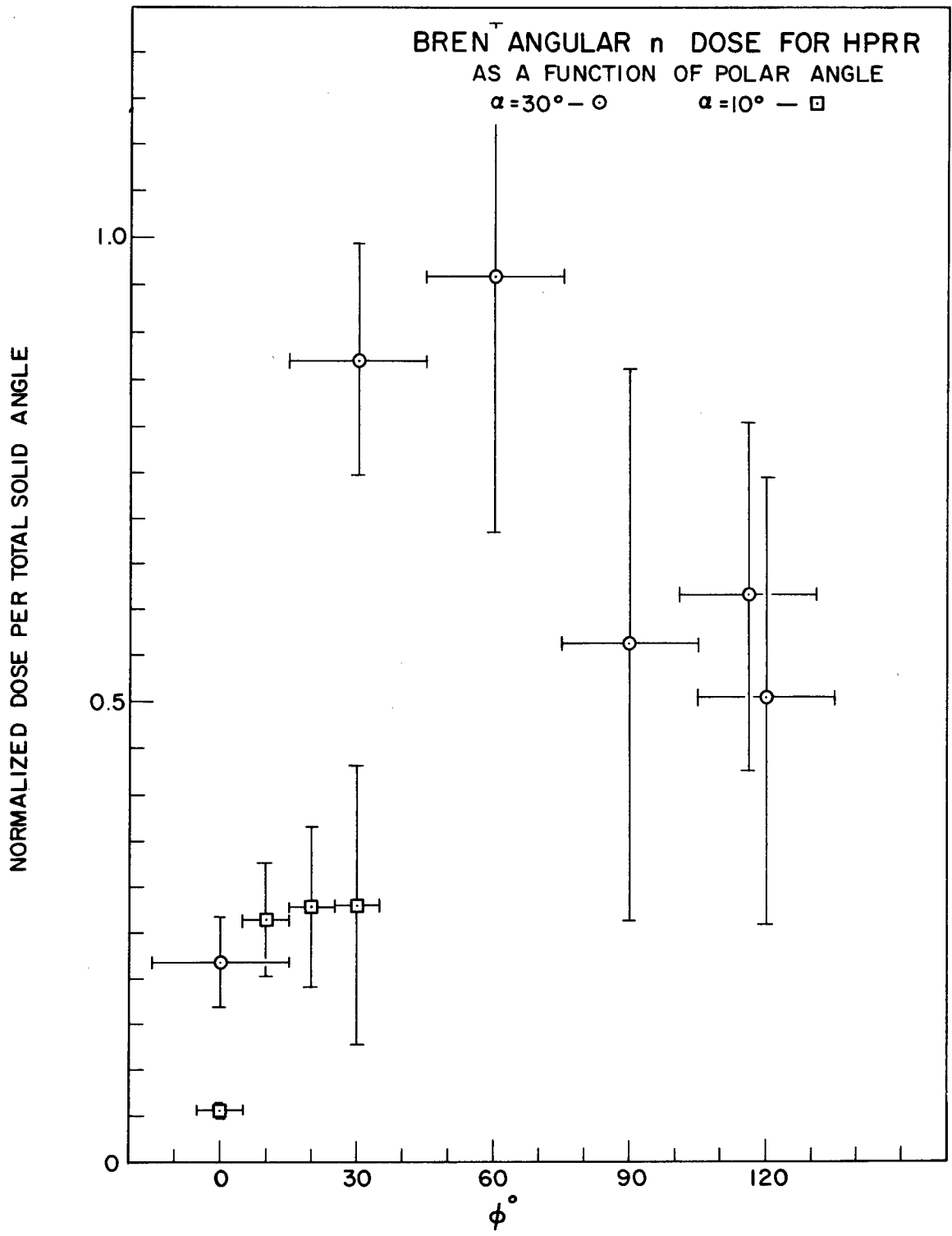


Fig. 4.8--Normalized Neutron Dose for Total Solid Angle as a Function of Polar Angle

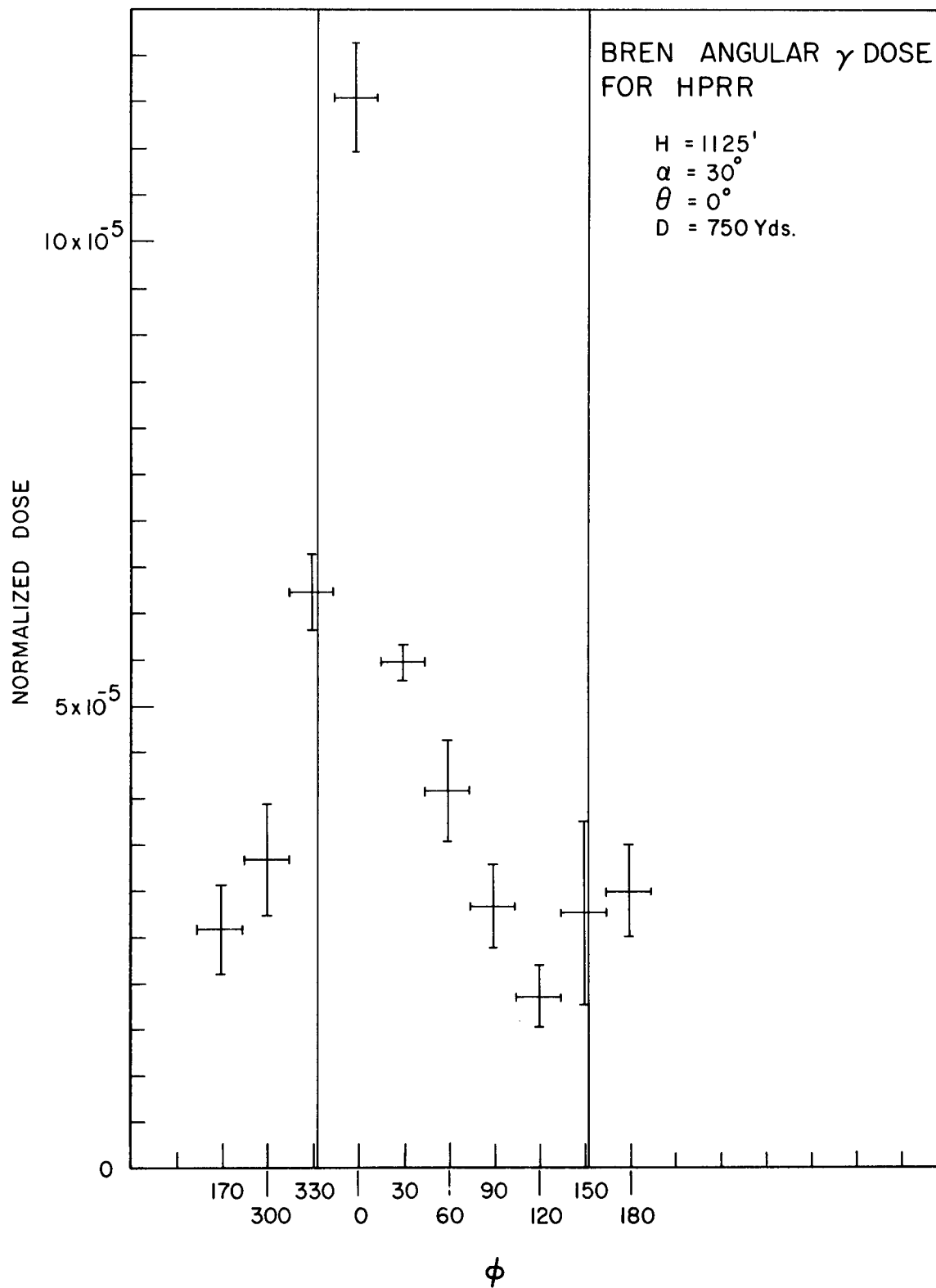


Fig. 4.9--Normalized HPRR Gamma-Ray Dose as a Function of Angle for a Reactor Height of 1125 Ft, Collimator Acceptance Angle =  $30^\circ$ , with  $\theta$  Kept at  $0^\circ$ , and Collimator Located at 750 Yd from the Base of the Tower

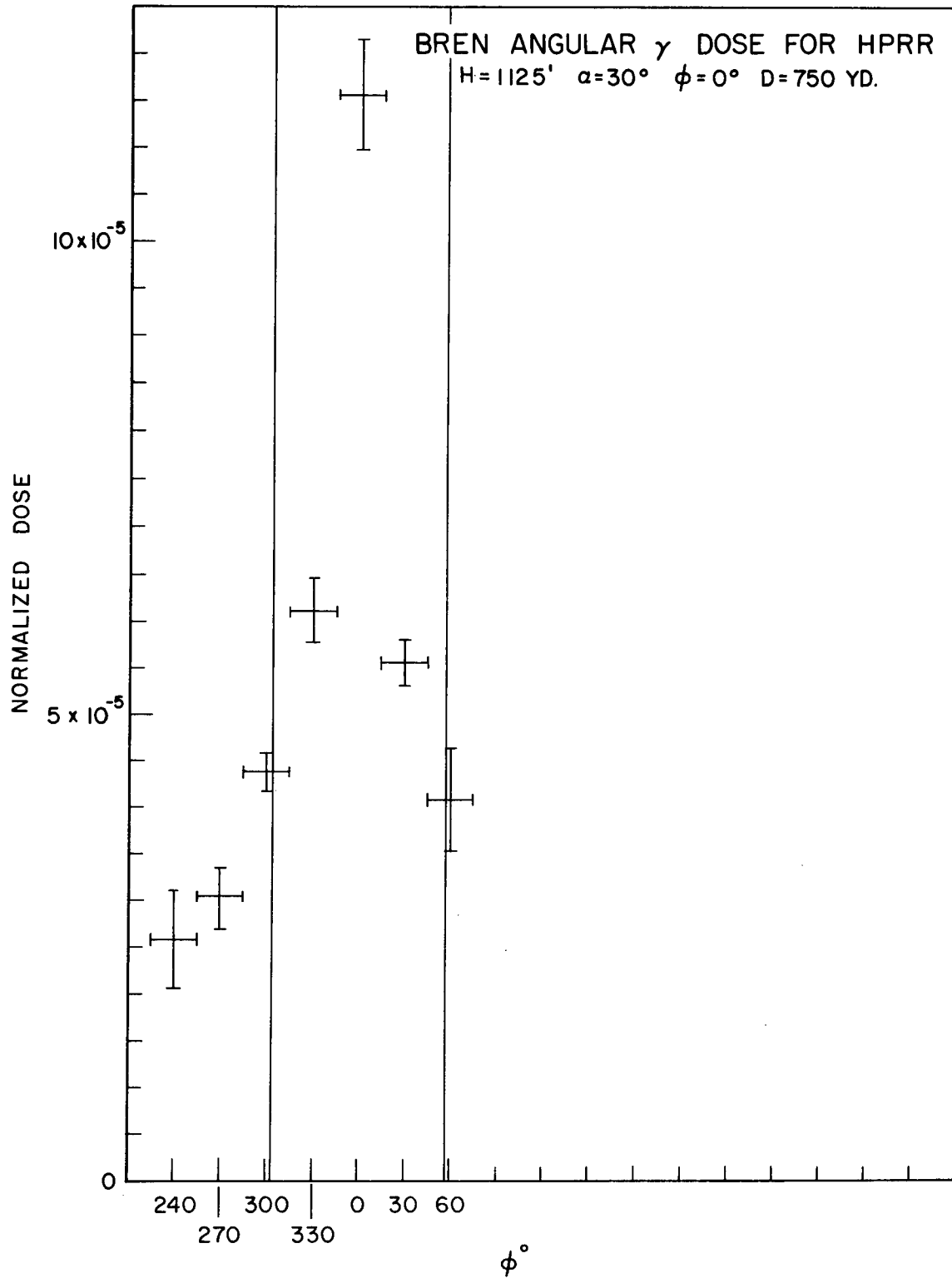


Fig. 4.10--Normalized HPRR Gamma-Ray Dose as a Function of Angle for a Reactor Height of 1125 Ft, Collimator Acceptance Angle =  $30^\circ$ , with  $\phi$  Kept at  $0^\circ$ , and Collimator Located at 750 Yd from the Base of the Tower

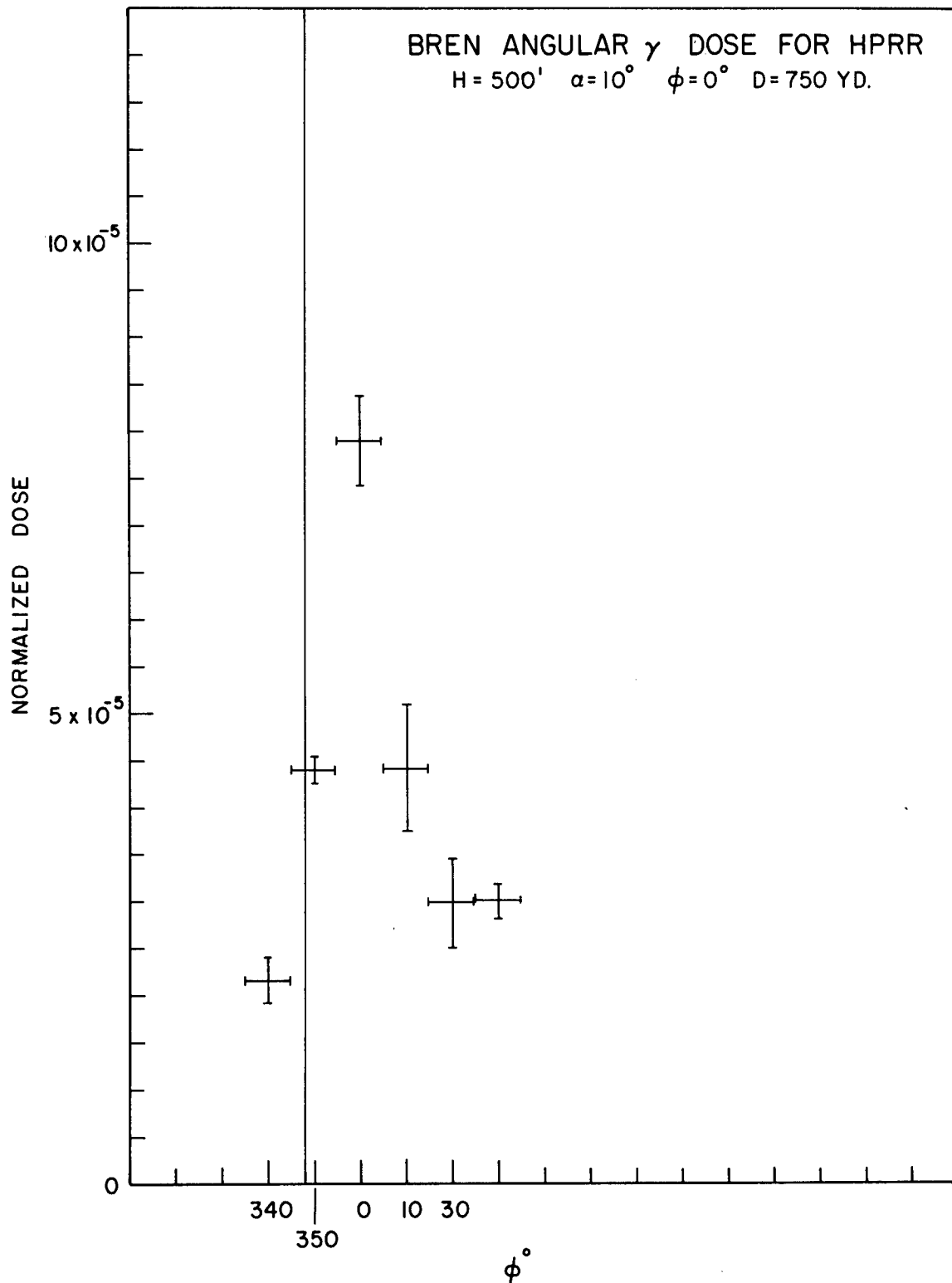


Fig. 4.11--Normalized HPRR Gamma-Ray Dose as a Function of Angle for a Reactor Height of 500 Ft, Collimator Acceptance Angle =  $10^\circ$ , with  $\theta$  Kept at  $0^\circ$ , and Collimator Located at 750 Yd from the Base of the Tower

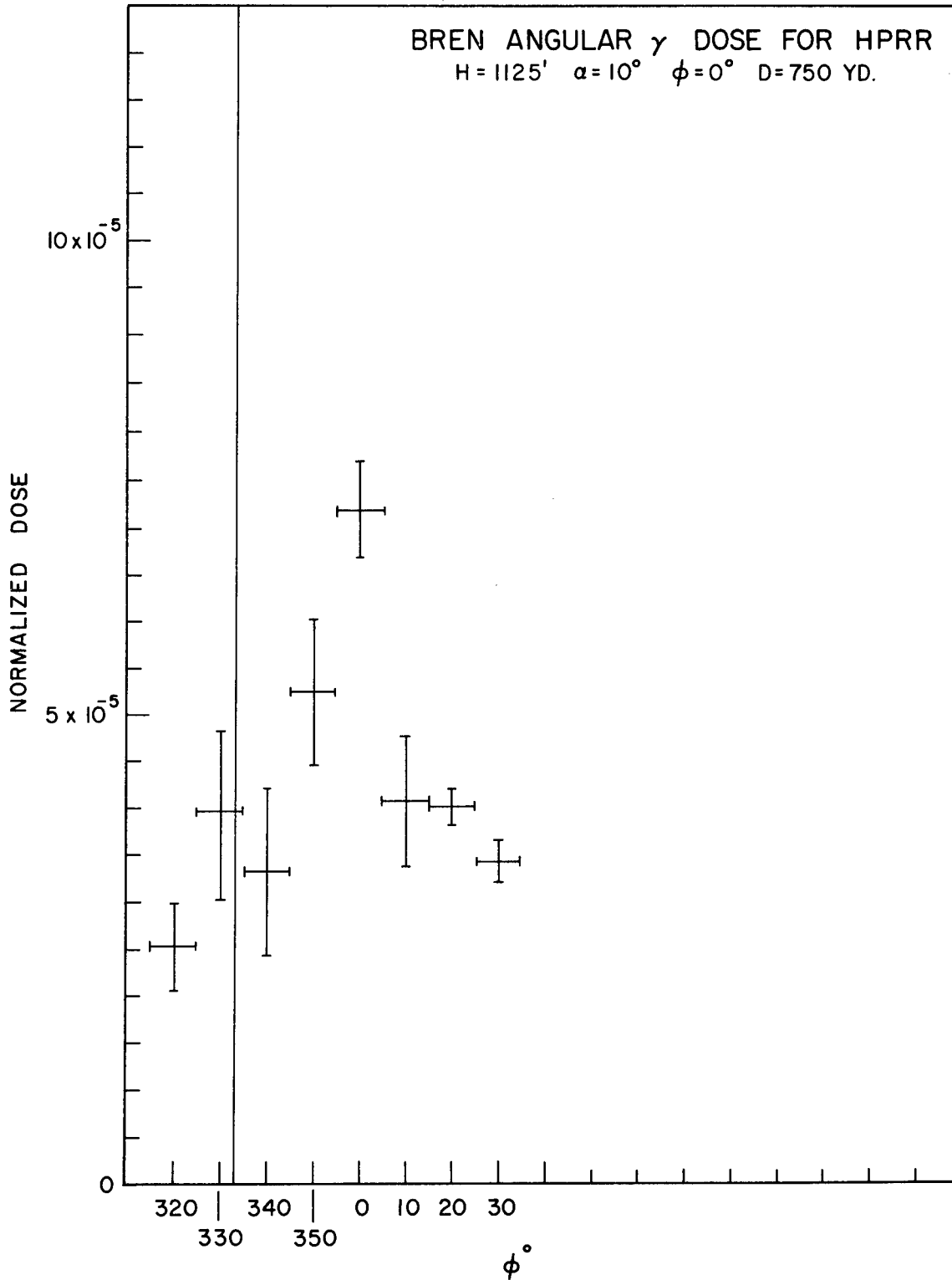


Fig. 4.12--Normalized HPRR Gamma-Ray Dose as a Function of Angle for a Reactor Height of 1125 Ft, Collimator Acceptance Angle =  $10^\circ$ , with  $\theta$  Kept at  $0^\circ$ , and Collimator Located at 750 Yd from the Base of the Tower

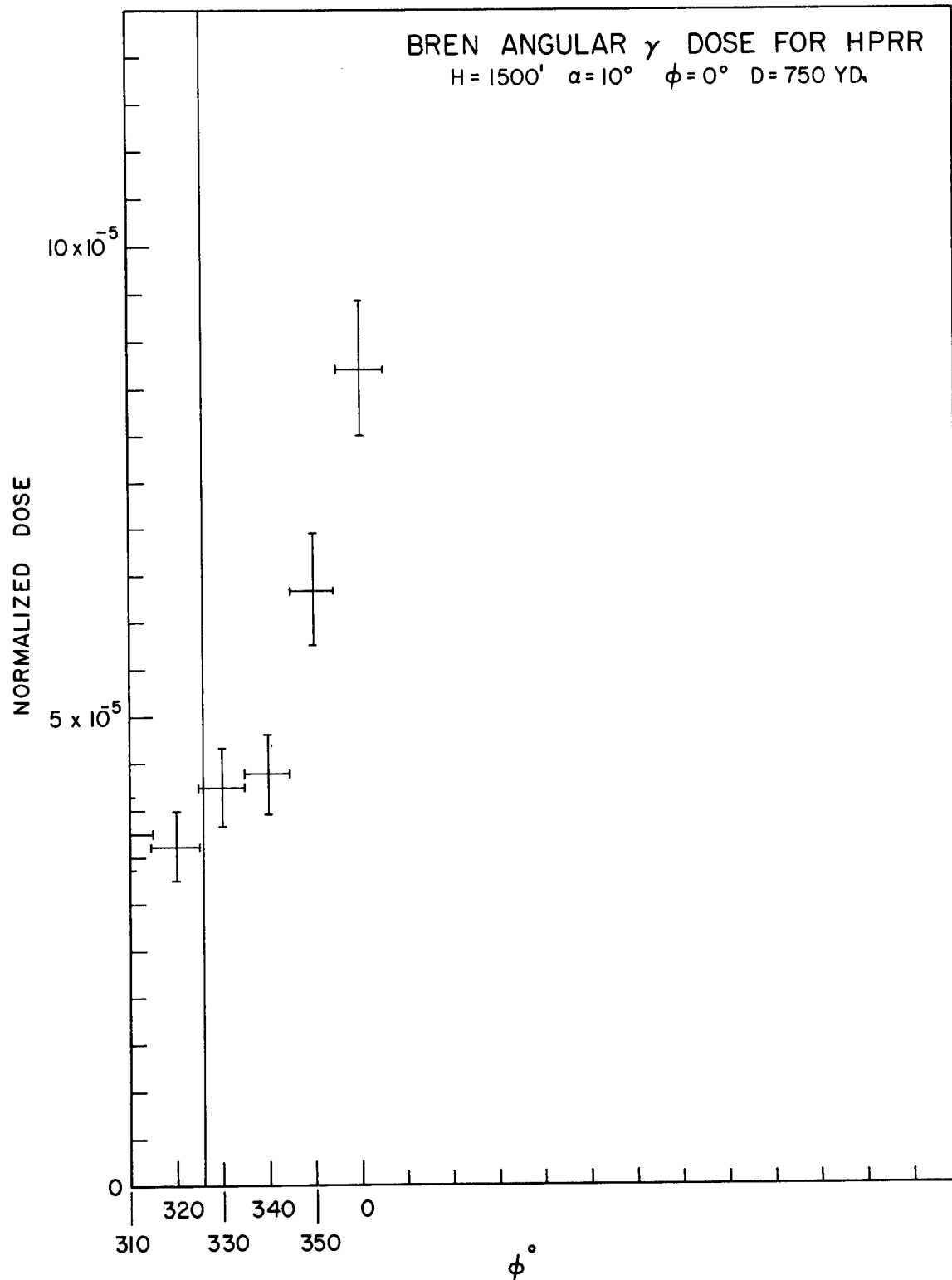


Fig. 4.13--Normalized HPRR Gamma-Ray Dose as a Function of Angle for a Reactor Height of 1500 Ft, Collimator Acceptance Angle =  $10^\circ$ , with  $\theta$  Kept at  $0^\circ$ , and Collimator Located at 750 Yd from the Base of the Tower

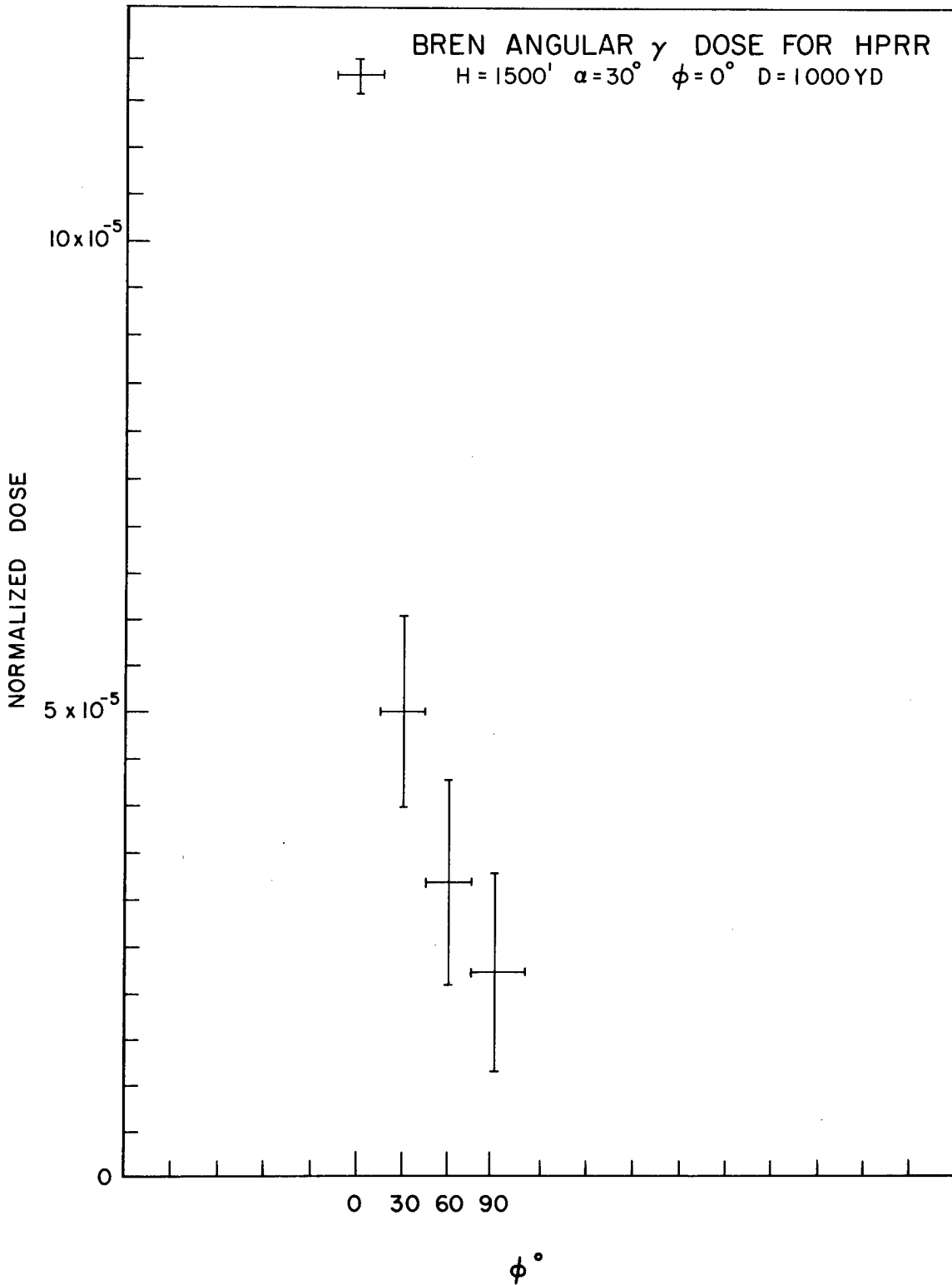


Fig. 4.14--Normalized HPRR Gamma-Ray Dose as a Function of Angle for a Reactor Height of 1500 Ft, Collimator Acceptance Angle =  $30^\circ$ , with  $\theta$  Kept at  $0^\circ$ , and Collimator Located at 1000 Yd from the Base of the Tower

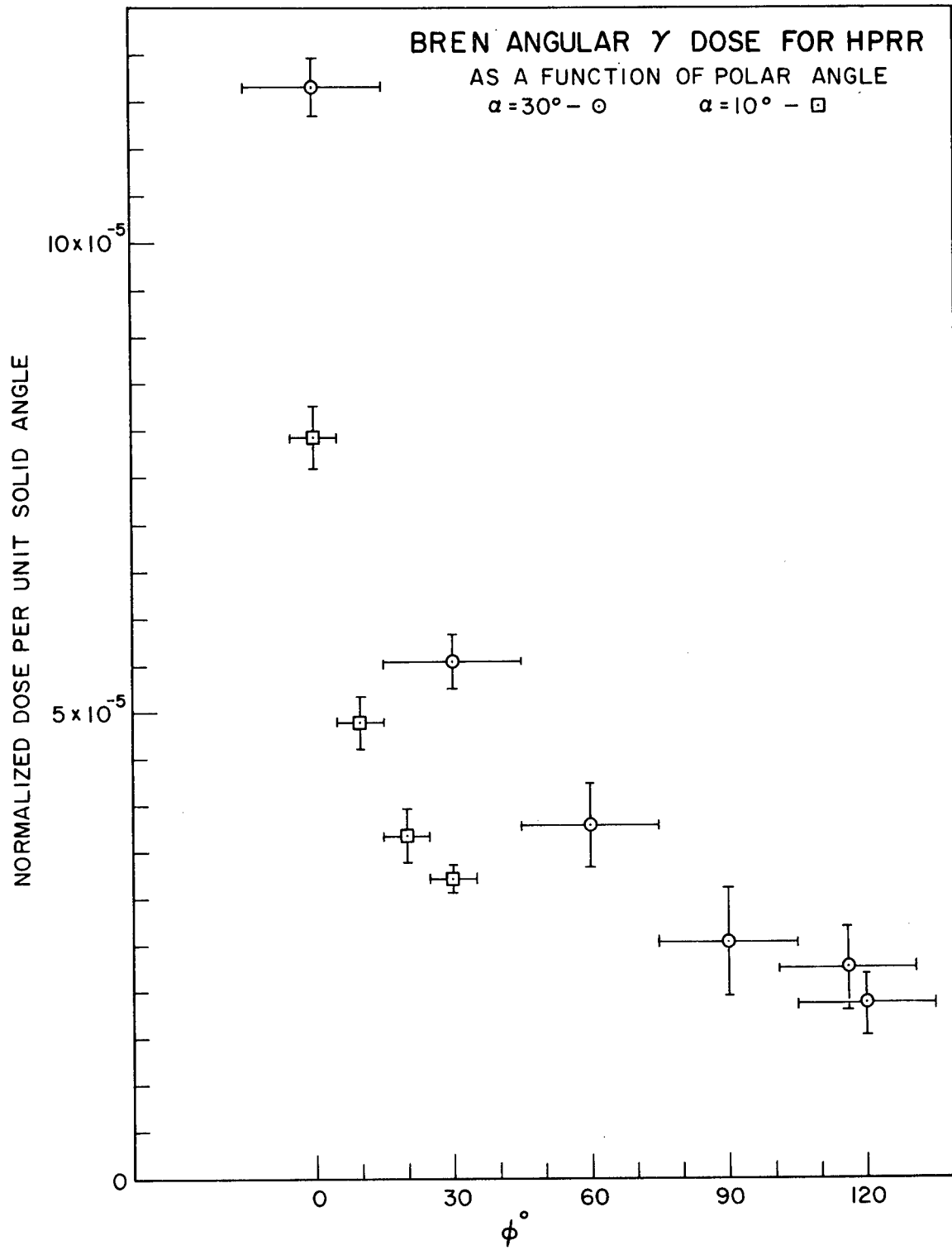


Fig. 4.15--Normalized HPRR Gamma-Ray Dose as a Function of Polar Angle

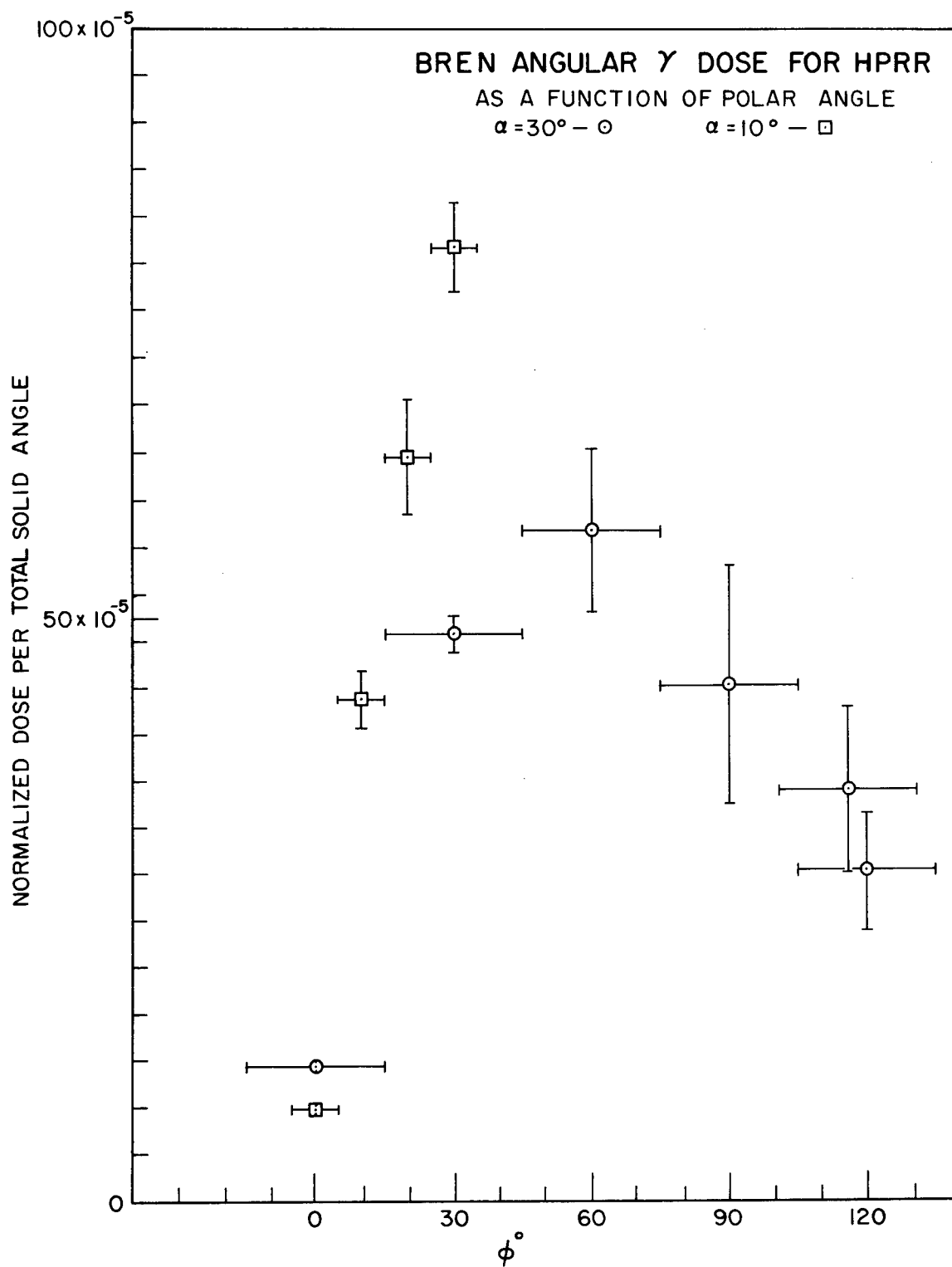


Fig. 4.16--Normalized HPRR Gamma-Ray Dose for Total Solid Angle as a Function of Polar Angle

Statistical variations on the data presented represent one standard deviation as determined from the average deviation of the readings made at each point (Figs. 4.17 to 4.19).

## 4.2 SPECTROMETRY DATA

### 4.2.1 HP RR Neutron Spectrum

Data that describe the response of the neutron spectrometer to monoenergetic neutrons are shown in Fig. 4.20. A typical measurement made at 750 yd and at  $\phi = 0^\circ$  is shown in Fig. 4.21. Because of the limited electronic equipment used with this spectrometer during BREN, it had considerable response to gamma rays. The spectrometer appears to have been sensitive to gamma rays incident from any direction. A background run made with the forward direction shielded with a 30-cm-long paraffin cone is shown in Fig. 4.22. Because direct reduction of the data proved impractical, three computer programs were written in an effort to use the monoenergetic neutron response data to reduce the BREN data. The approaches used were multiple regression analysis, linear programming, and finally, a trial-and-error program to force fit the data. None of the programs were successful so that little information is obtainable from the spectrometer data.

### 4.2.2 HP RR Gamma Spectrum

Compton gamma spectrometer data are presented with corrections for air density, background, and cross sections, and include the conversion of the momentum distribution to an energy distribution.

Poor statistical results were obtained due to the low signal-to-noise ratio encountered during the experiment. As a result, the smallest statistical uncertainty for the data shown is 600%. Therefore, these data are presented solely for information and completeness in presentation and cannot be said to represent truly the gamma spectrum produced (Fig. 4.23).

### 4.2.3 Cobalt-60 Gamma Spectrum

Spectral response as a function of angle for the  $^{60}\text{Co}$  source, as measured by the NaI crystal, are shown in Figs. 4.24 through 4.33. The full-scale energy on these graphs is 1.6 Mev; the ordinate is a logarithmic scale. The data presented have been normalized to allow direct comparison. Normalization was made to the total number of gamma rays present at the collimator site during the 750-yd, 1125-ft,  $0^\circ$  run. Data from the normalizing counter were used where possible because it corrected for all variables encountered. When insufficient normalization data was available, air-density corrections were used. No attempt has been made to strip the detector response from the data. Figures 4.24 through 4.33 show the data for  $\alpha = 30^\circ$ ,  $\theta = 0$ , 1125-ft elevation, 750-yd distance. For the points at  $\phi = 270^\circ$ ,  $300^\circ$ ,  $330^\circ$ ,  $150^\circ$ , and  $180^\circ$ , the collimator intercepts were below the air-ground interface. Data obtained at 750 yd for  $\alpha = 30^\circ$ ,  $\phi = 0$ , 1125-ft elevation are given in Figs. 4.34 through 4.38. The interface was intercepted for  $\theta = 60^\circ$ ,  $90^\circ$ ,  $120^\circ$ . Figures 4.39 through 4.44 show the 750-yd results using an  $\alpha$  of  $10^\circ$ . Data taken with the detector 1000 yd from the base of the tower are shown in Figs. 4.45 through 4.52. All measurements

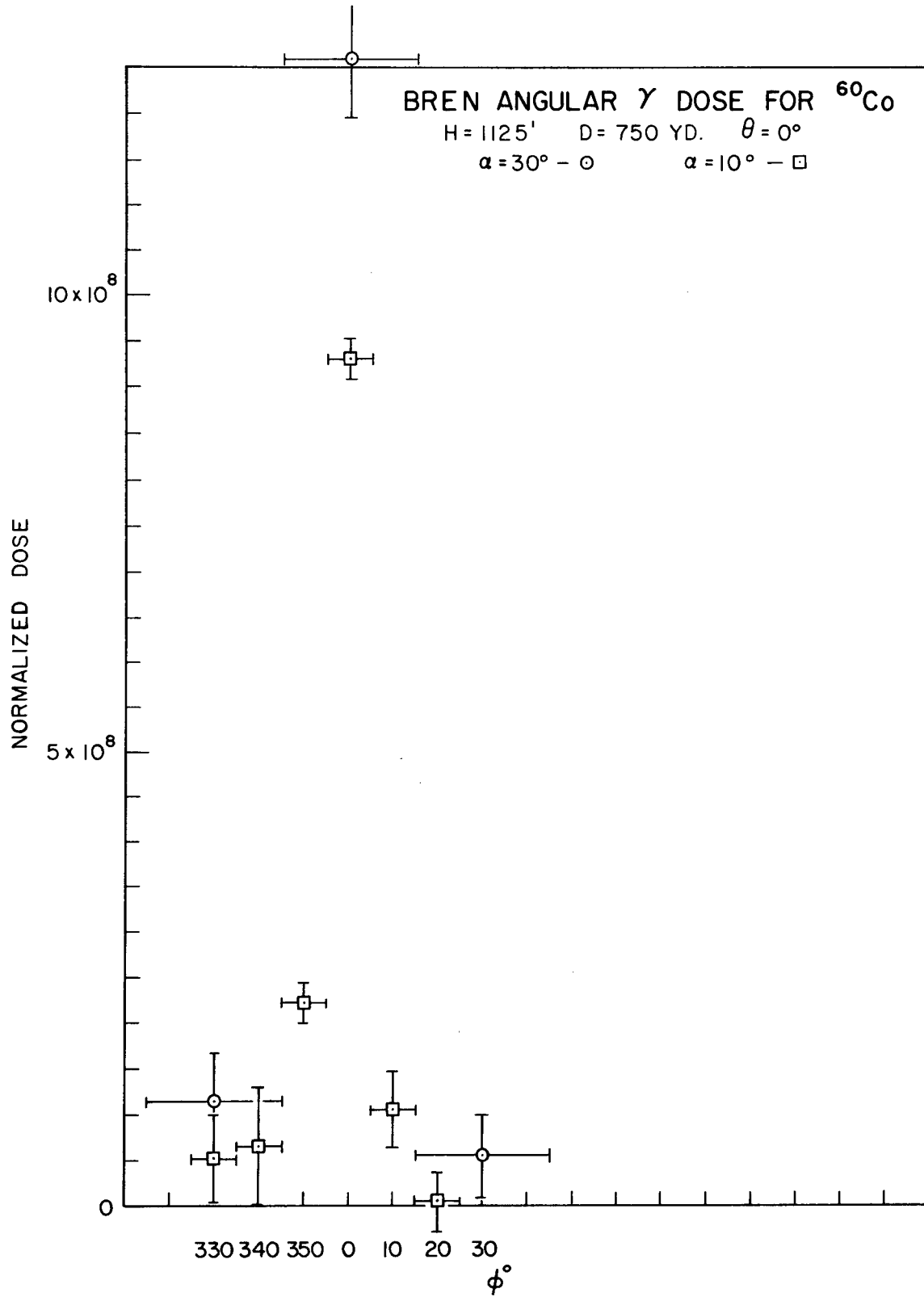


Fig. 4.17--Normalized  $^{60}\text{Co}$  Gamma-Ray Dose for a Source Height of 1125 Ft,  
 Collimator Acceptance Angle =  $30^\circ$ , with  $\theta$  Kept at  $0^\circ$ , and Collimator  
 Located at 750 Yd from the Base of the Tower

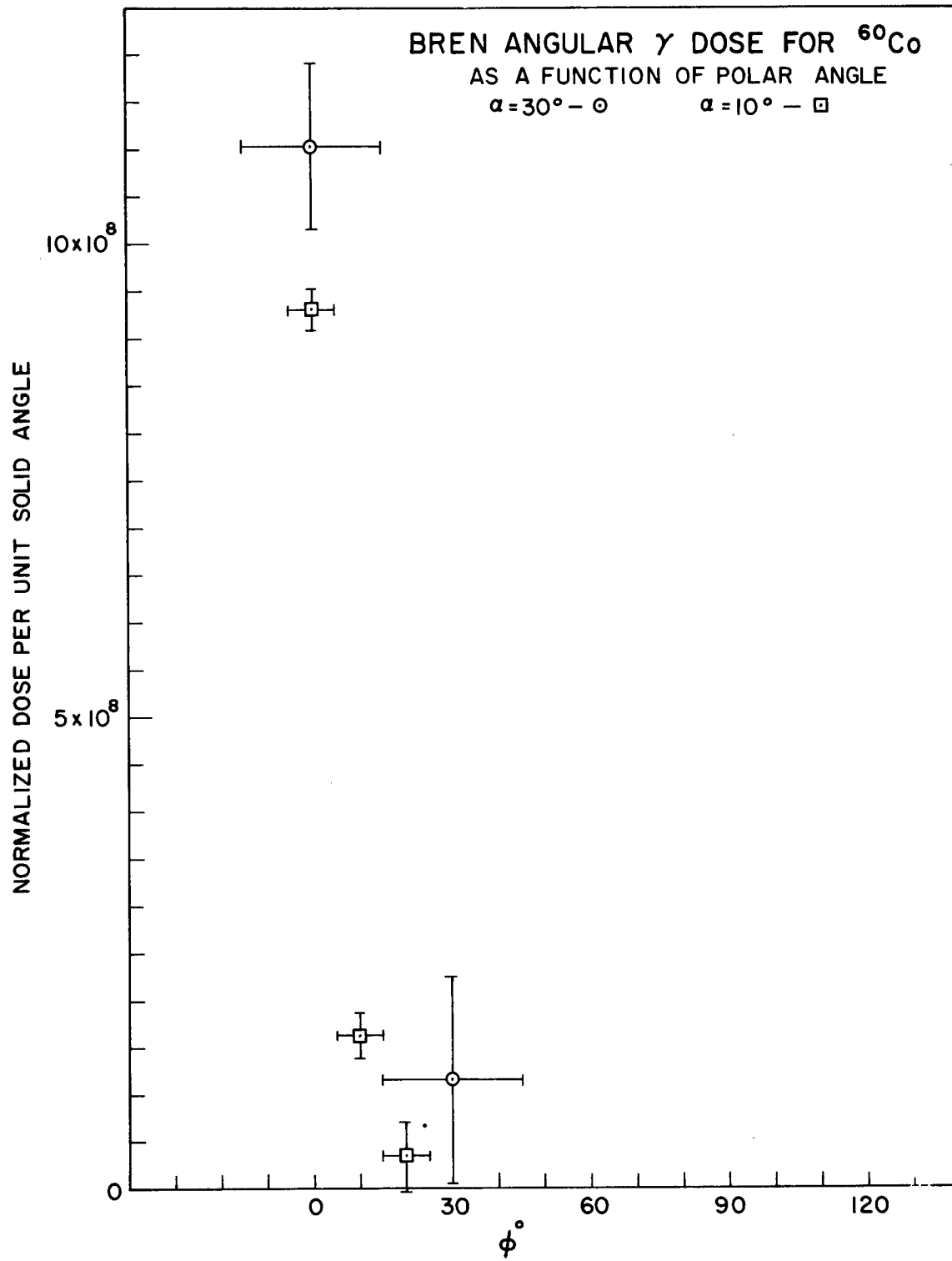


Fig. 4.18--Normalized  $^{60}\text{Co}$  Gamma-Ray Dose as a Function of Polar Angle

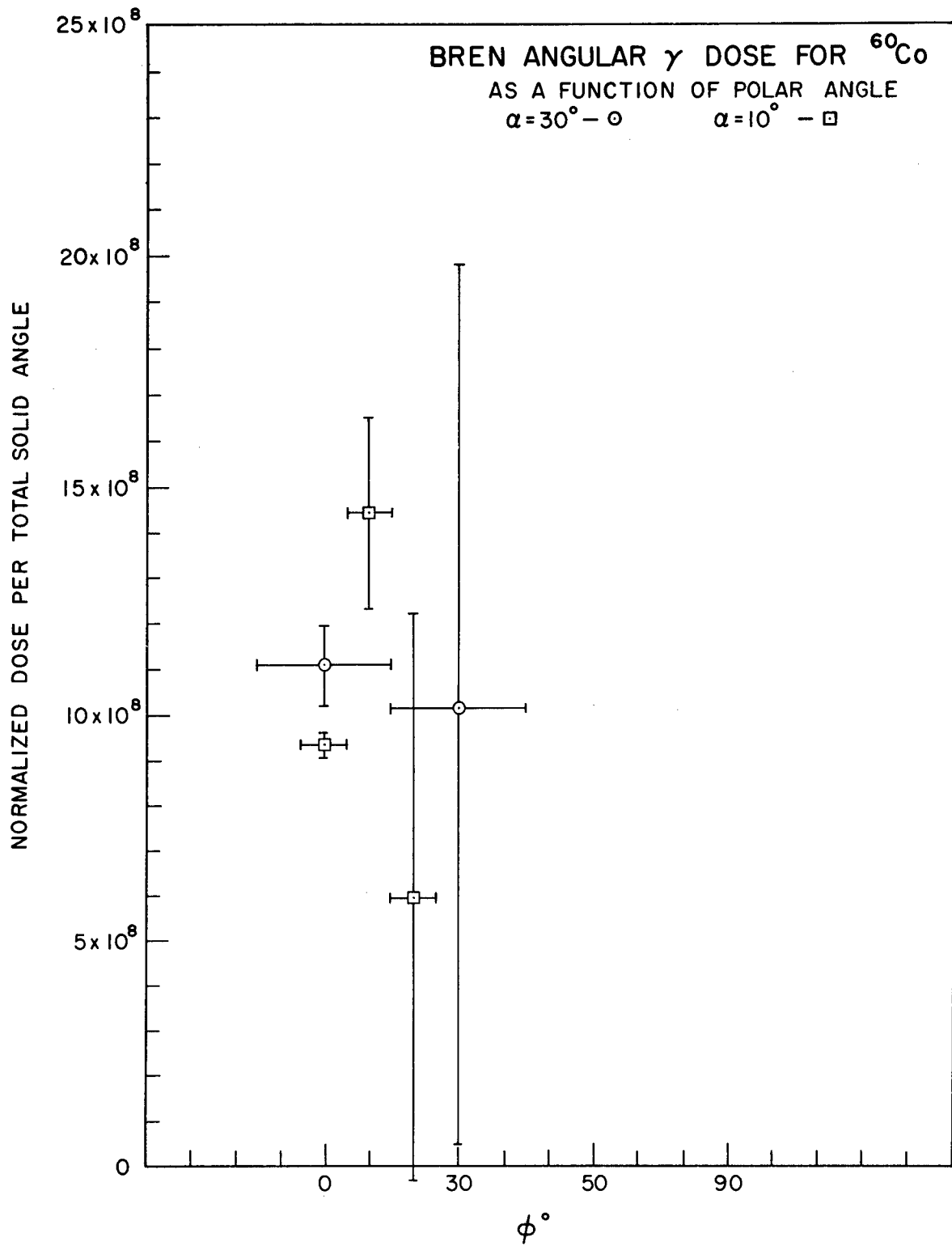


Fig. 4.19--Normalized  $^{60}\text{Co}$  Gamma-Ray Dose for Total Solid Angle as a Function of Polar Angle

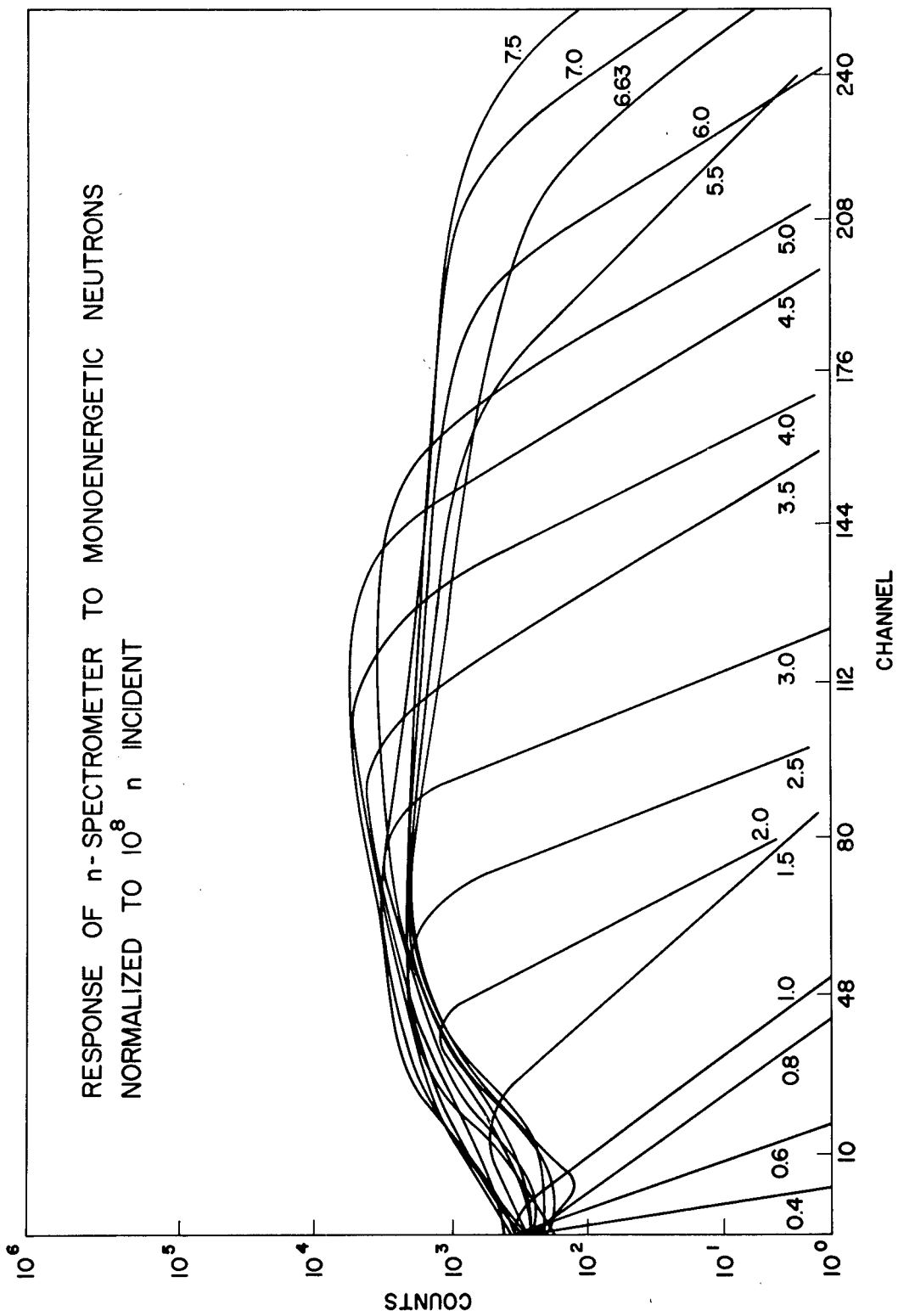
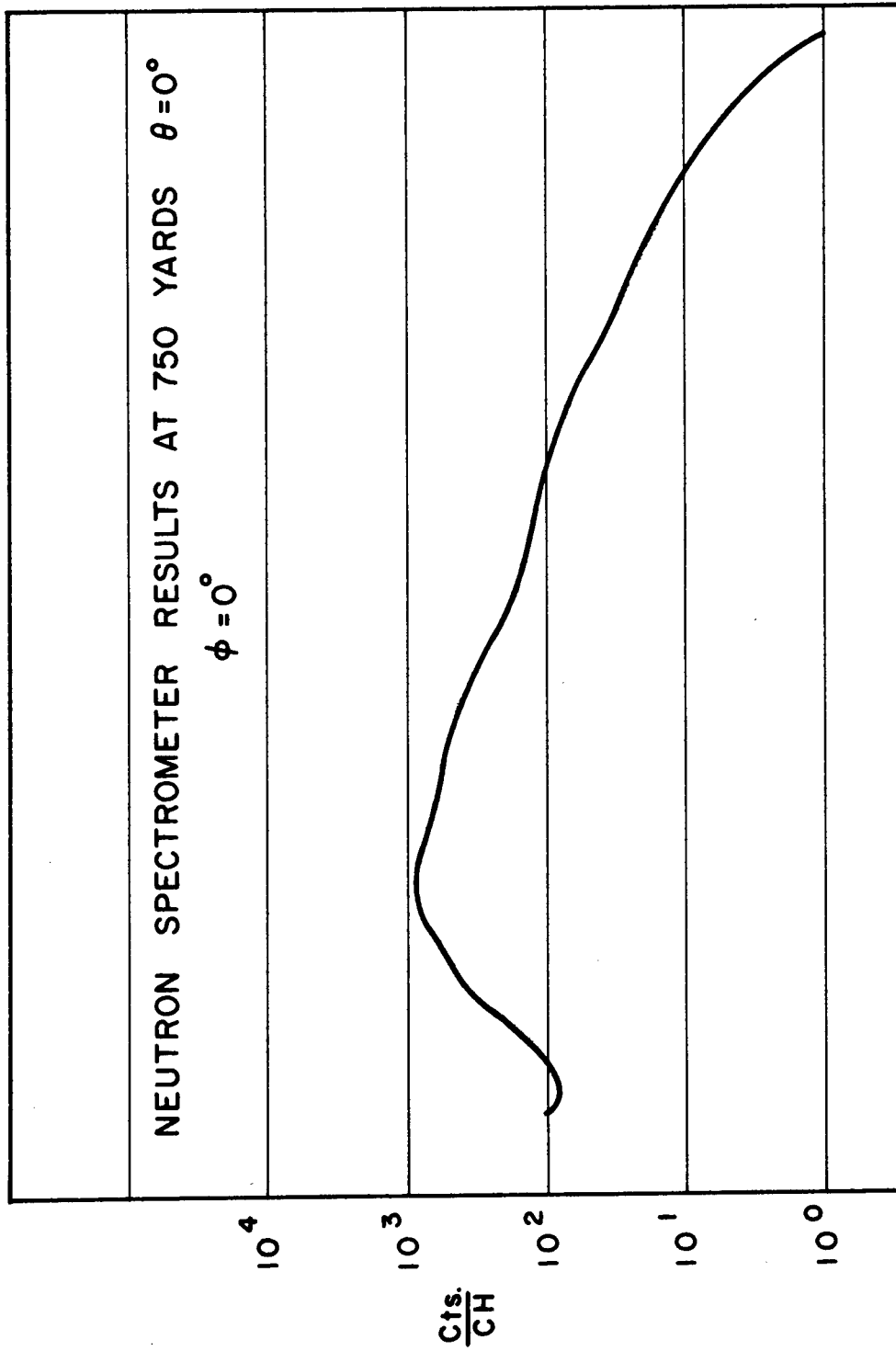


Fig. 4.20--Neutron Spectrometer Response to Monoenergetic Neutrons



CH

Fig. 4.21--Typical Measured BREN Neutron Spectrum

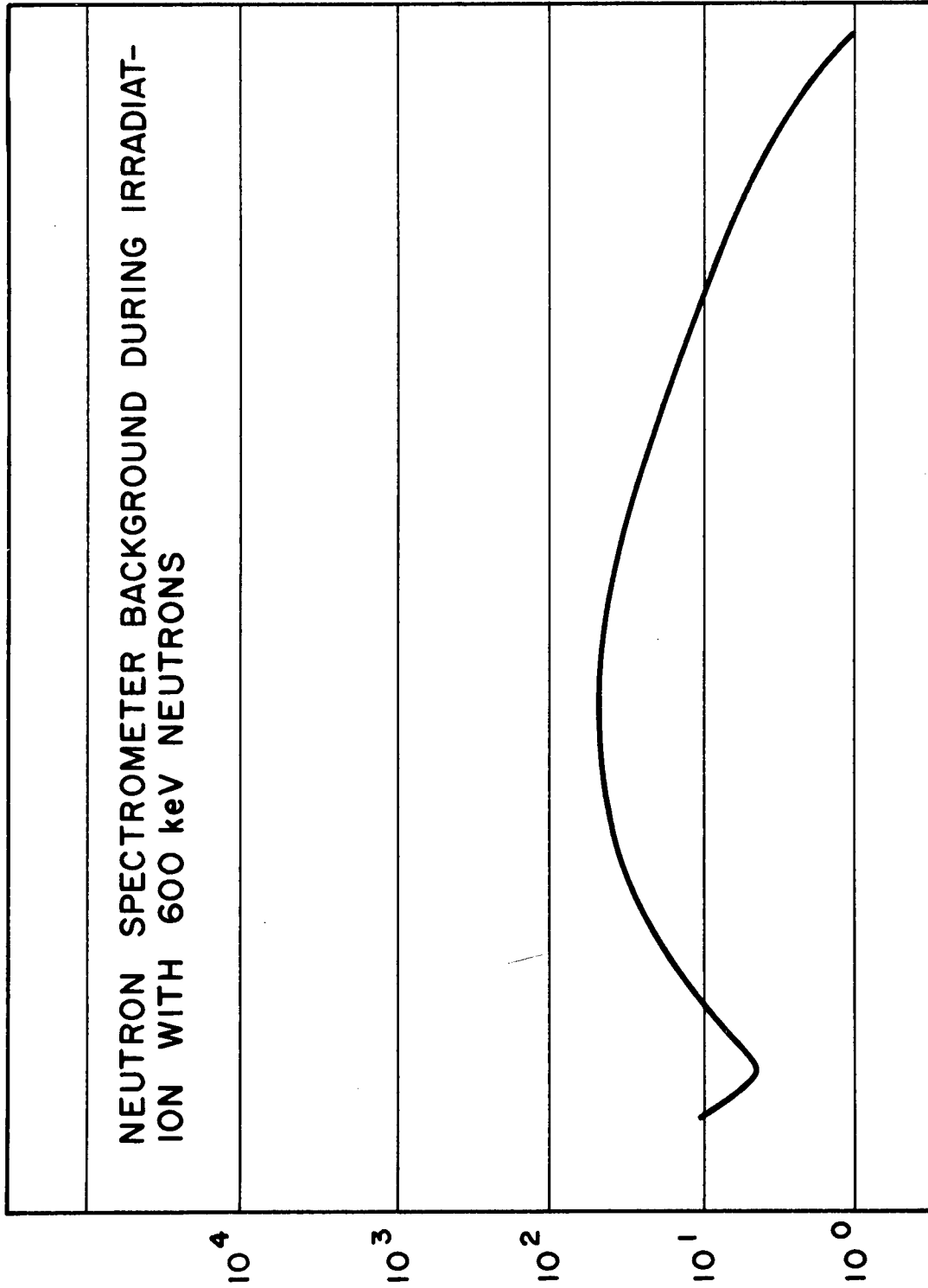


Fig. 4.22--Typical Background Neutron Spectrum

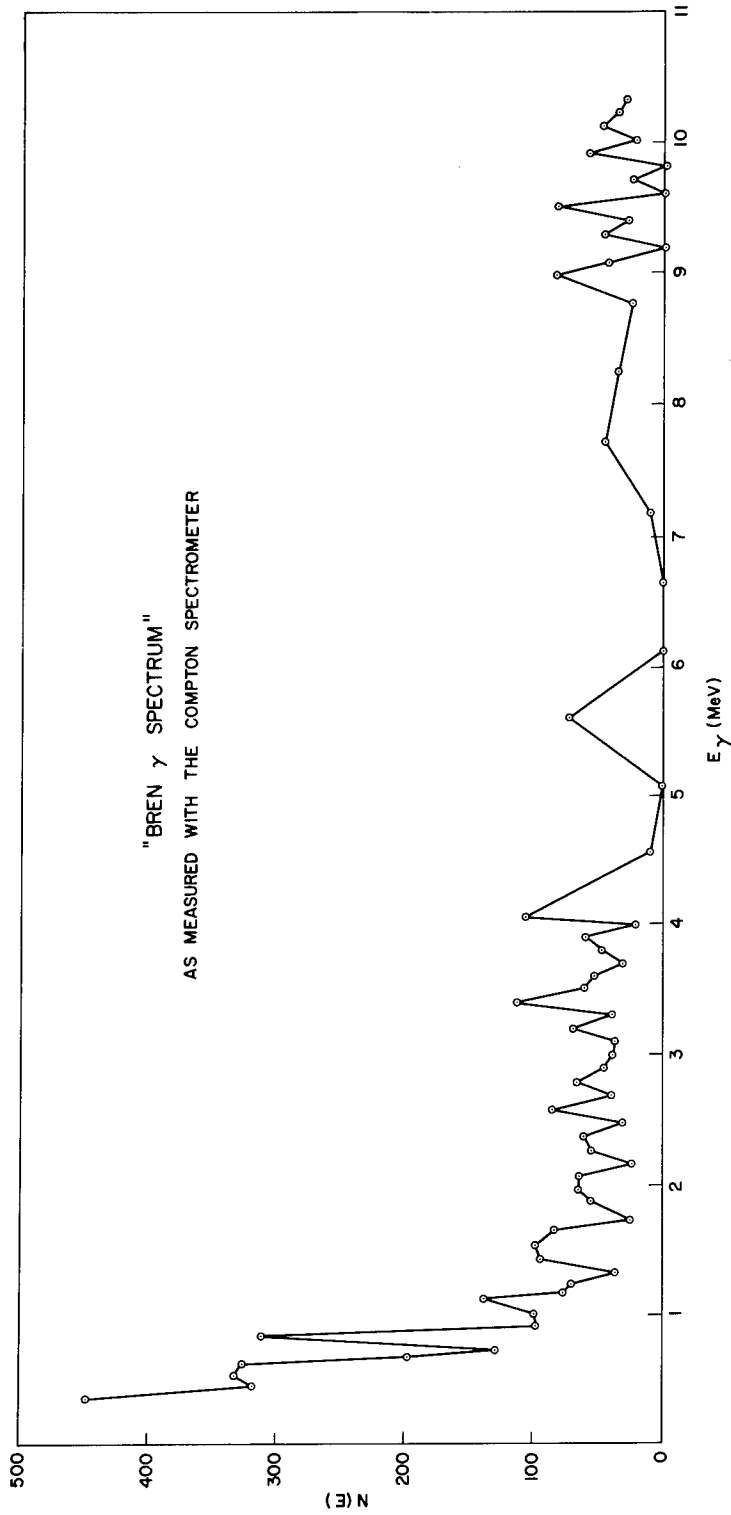


Fig. 4.23--Compton Spectrometer Results

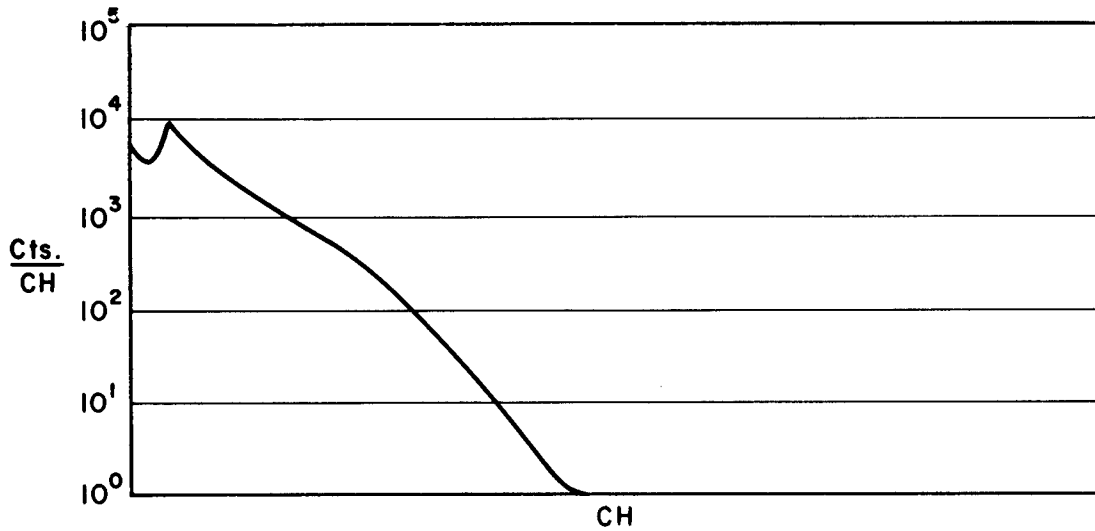


Fig. 4.24-- $^{60}\text{Co}$  Spectrum at a Distance to the Base of the Tower from the Detector of 750 Yd, Source Height of 1125 Ft, Collimator Acceptance Angle =  $30^\circ$ , with  $\theta$  Kept at  $0^\circ$  and  $\phi$  Kept at  $270^\circ$

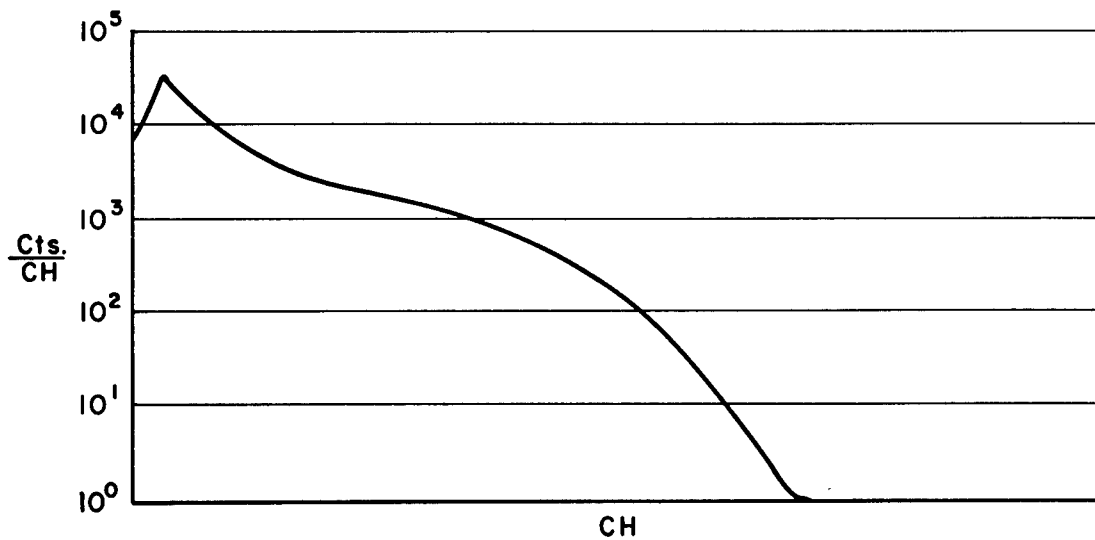


Fig. 4.25-- $^{60}\text{Co}$  Spectrum at a Distance to the Base of the Tower from the Detector of 750 Yd, Source Height of 1125 Ft, Collimator Acceptance Angle =  $30^\circ$ , with  $\theta$  Kept at  $0^\circ$  and  $\phi$  Kept at  $300^\circ$

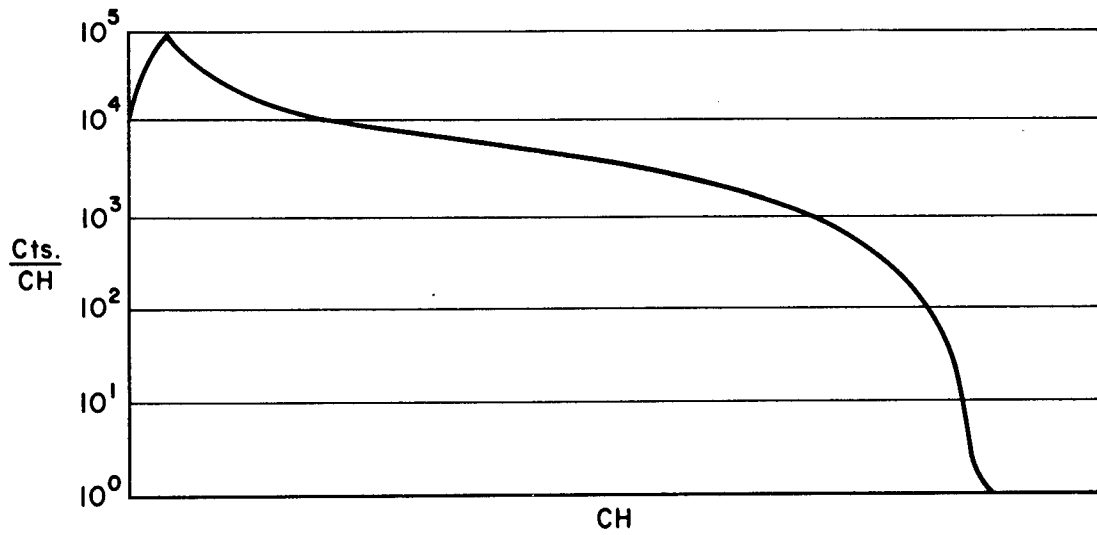


Fig. 4.26-- $^{60}\text{Co}$  Spectrum at a Distance to the Base of the Tower from the Detector of 750 Yd, Source Height of 1125 Ft, Collimator Acceptance Angle =  $30^\circ$ , with  $\theta$  Kept at  $0^\circ$  and  $\phi$  Kept at  $330^\circ$

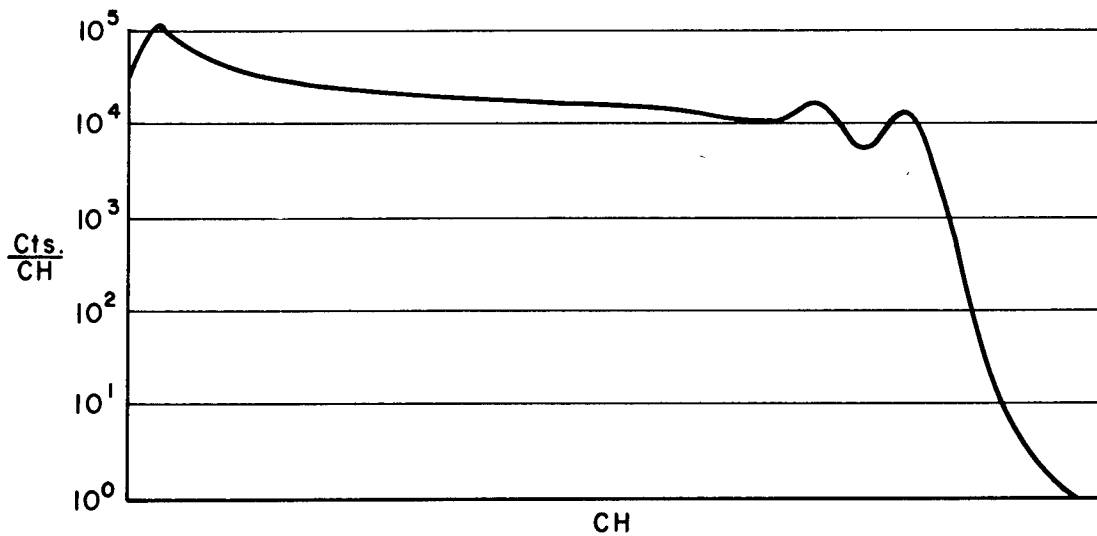


Fig. 4.27-- $^{60}\text{Co}$  Spectrum at a Distance to the Base of the Tower from the Detector of 750 Yd, Source Height of 1125 Ft, Collimator Acceptance Angle =  $30^\circ$ , with  $\theta$  Kept at  $0^\circ$  and  $\phi$  Kept at  $0^\circ$

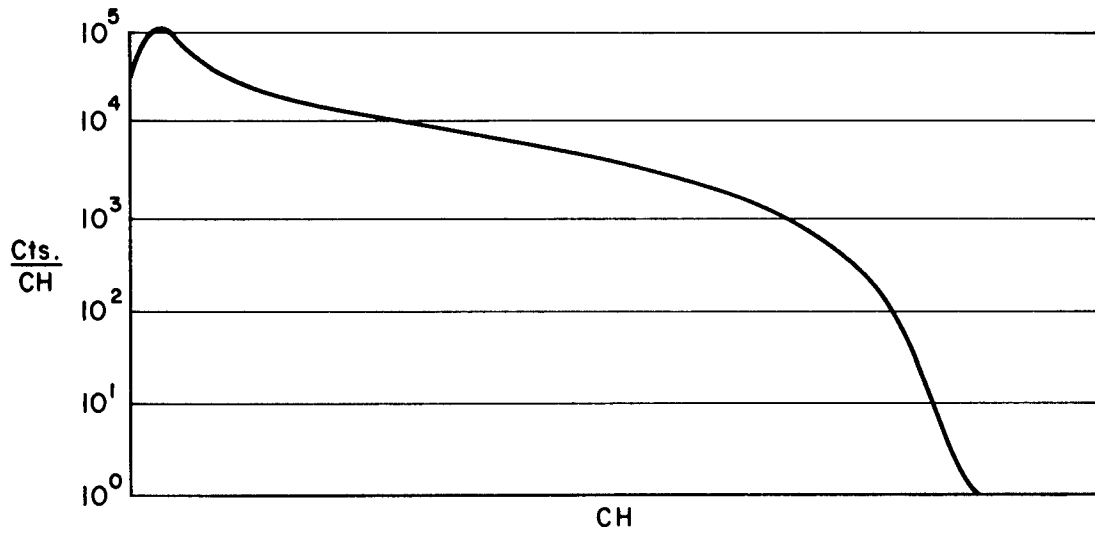


Fig. 4.28-- $^{60}\text{Co}$  Spectrum at a Distance to the Base of the Tower from the Detector of 750 Yd, Source Height of 1125 Ft, Collimator Acceptance Angle =  $30^\circ$ , with  $\theta$  Kept at  $0^\circ$  and  $\phi$  Kept at  $30^\circ$

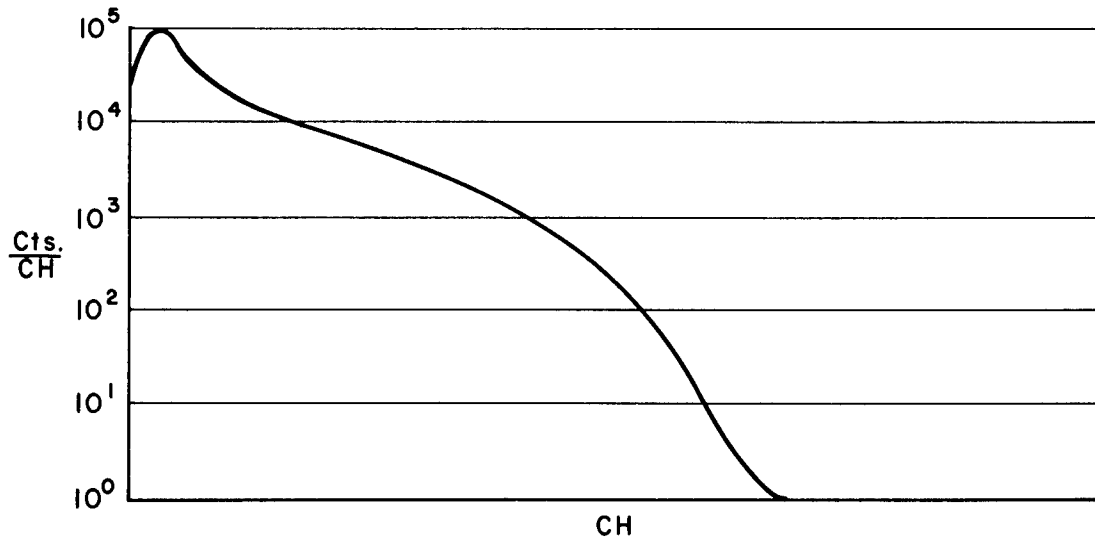


Fig. 4.29-- $^{60}\text{Co}$  Spectrum at a Distance to the Base of the Tower from the Detector of 750 Yd, Source Height of 1125 Ft, Collimator Acceptance Angle =  $30^\circ$ , with  $\theta$  Kept at  $0^\circ$  and  $\phi$  Kept at  $60^\circ$

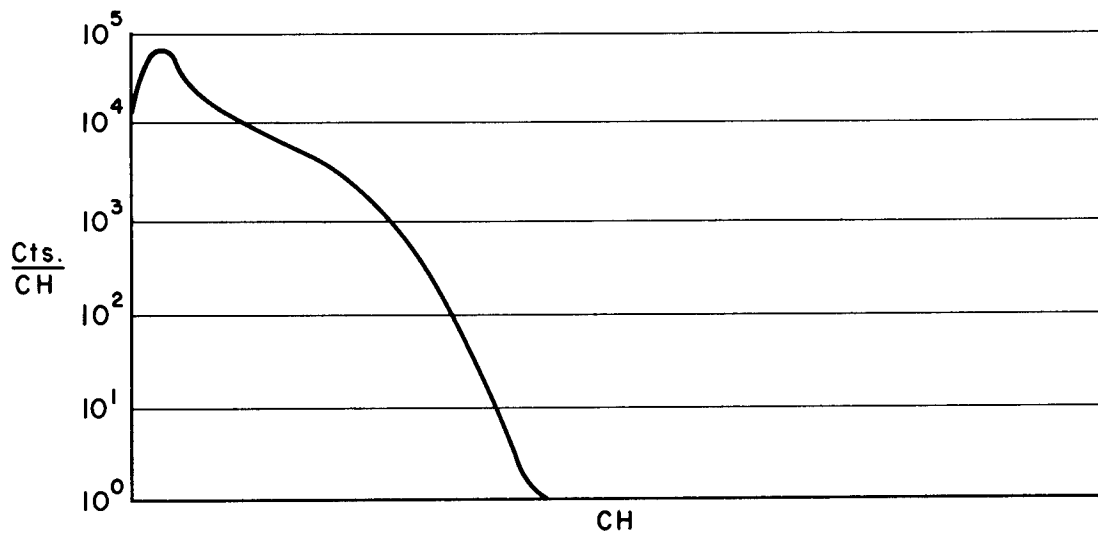


Fig. 4.30-- $^{60}\text{Co}$  Spectrum at a Distance to the Base of the Tower from the Detector of 750 Yd, Source Height of 1125 Ft, Collimator Acceptance Angle =  $30^\circ$ , with  $\theta$  Kept at  $0^\circ$  and  $\phi$  Kept at  $90^\circ$

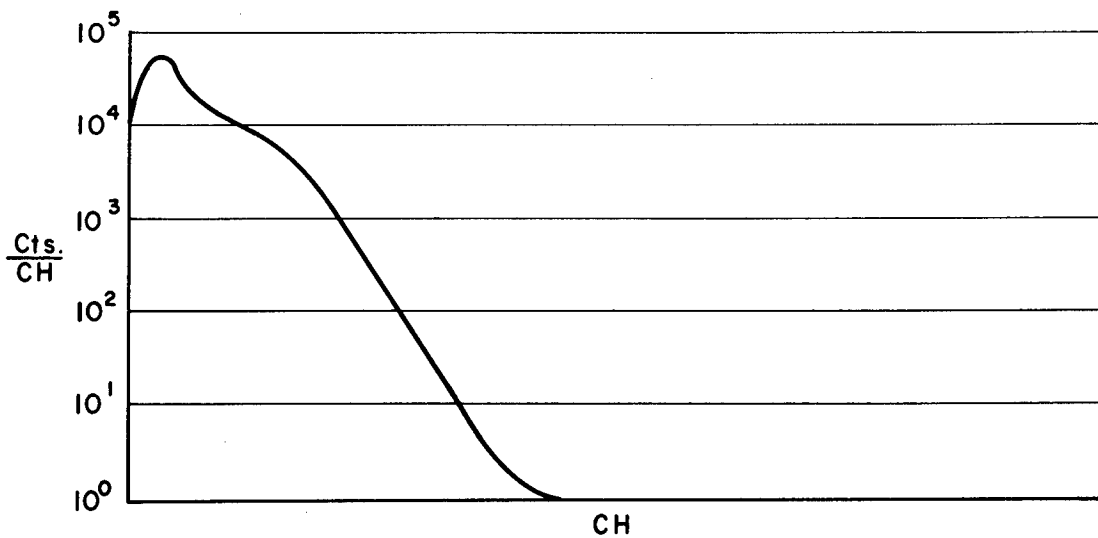


Fig. 4.31-- $^{60}\text{Co}$  Spectrum at a Distance to the Base of the Tower from the Detector of 750 Yd, Source Height of 1125 Ft, Collimator Acceptance Angle =  $30^\circ$ , with  $\theta$  Kept at  $0^\circ$  and  $\phi$  Kept at  $120^\circ$

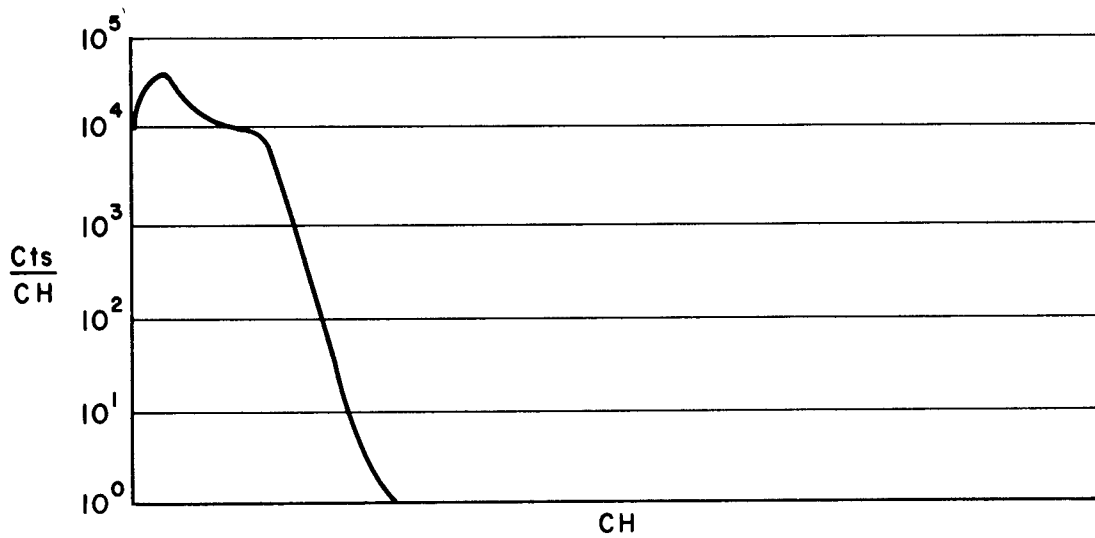


Fig. 4.32-- $^{60}\text{Co}$  Spectrum at a Distance to the Base of the Tower from the Detector of 750 Yd, Source Height of 1125 Ft, Collimator Acceptance Angle =  $30^\circ$ , with  $\theta$  Kept at  $0^\circ$  and  $\phi$  Kept at  $150^\circ$

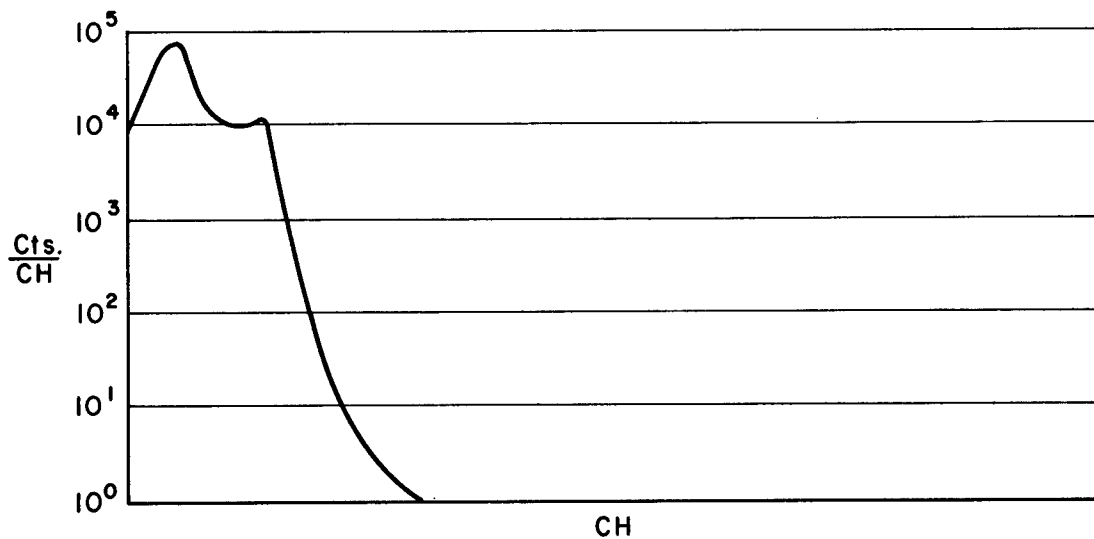


Fig. 4.33-- $^{60}\text{Co}$  Spectrum at a Distance to the Base of the Tower from the Detector of 750 Yd, Source Height of 1125 Ft, Collimator Acceptance Angle =  $30^\circ$ , with  $\theta$  Kept at  $0^\circ$  and  $\phi$  Kept at  $180^\circ$

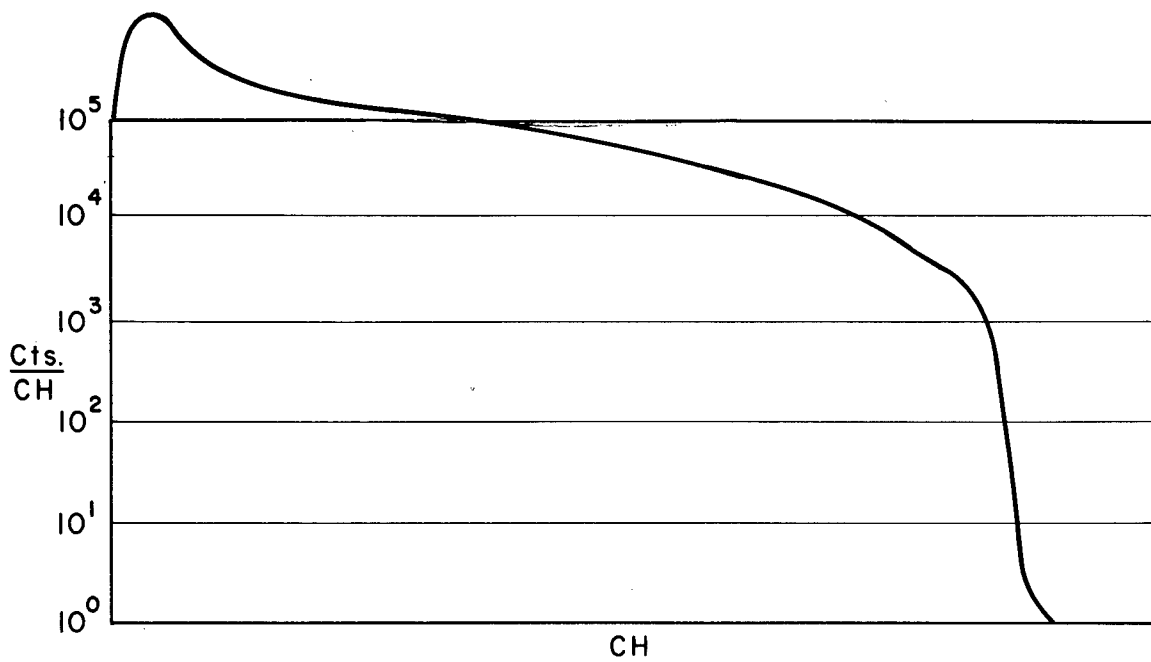


Fig. 4.34-- $^{60}\text{Co}$  Spectrum at a Distance to the Base of the Tower from the Detector of 750 Yd, Source Height of 1125 Ft, Collimator Acceptance Angle =  $30^\circ$ , with  $\phi$  Kept at  $0^\circ$  and  $\theta$  Kept at  $330^\circ$

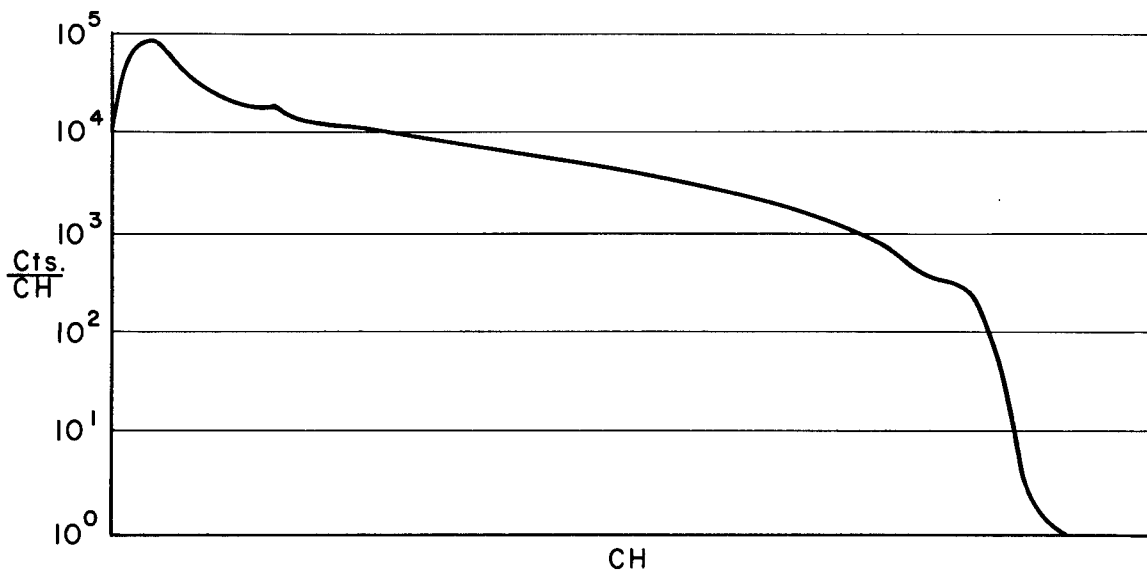


Fig. 4.35-- $^{60}\text{Co}$  Spectrum at a Distance to the Base of the Tower from the Detector of 750 Yd, Source Height of 1125 Ft, Collimator Acceptance Angle =  $30^\circ$ , with  $\phi$  Kept at  $0^\circ$  and  $\theta$  Kept at  $30^\circ$

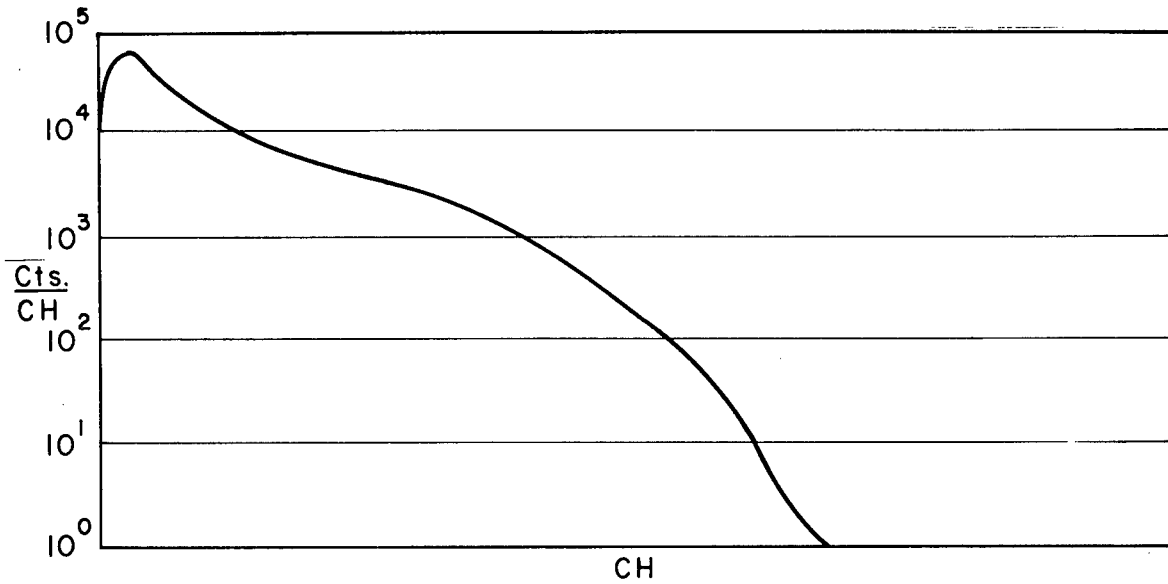


Fig. 4.36-- $^{60}\text{Co}$  Spectrum at a Distance to the Base of the Tower from the Detector of 750 Yd, Source Height of 1125 Ft, Collimator Acceptance Angle =  $30^\circ$ , with  $\phi$  Kept at  $0^\circ$  and  $\theta$  Kept at  $60^\circ$

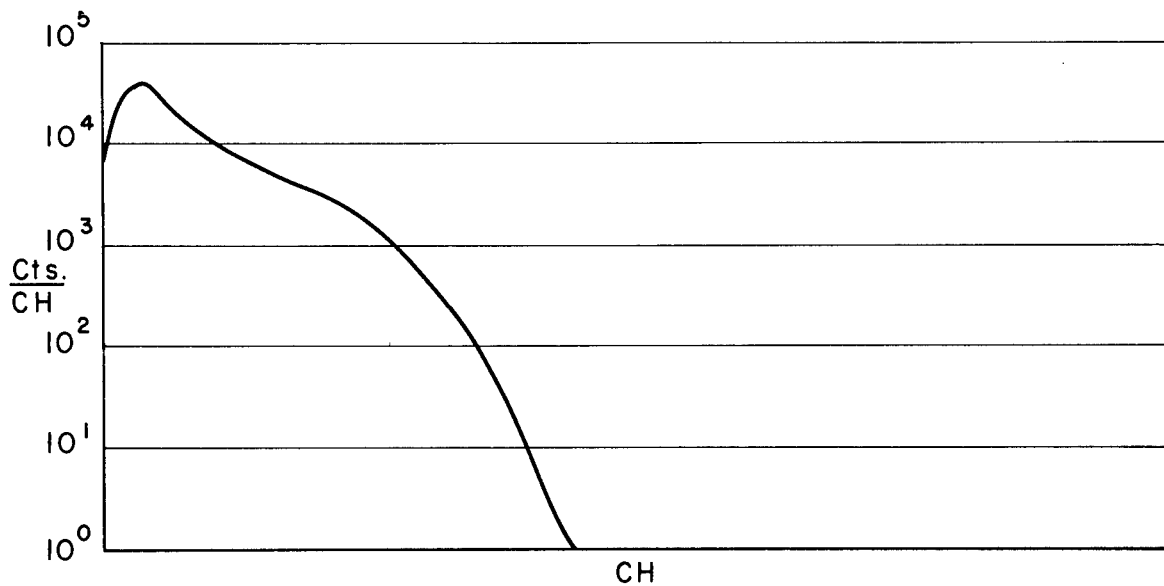


Fig. 4.37-- $^{60}\text{Co}$  Spectrum at a Distance to the Base of the Tower from the Detector of 750 Yd, Source Height of 1125 Ft, Collimator Acceptance Angle =  $30^\circ$ , with  $\phi$  Kept at  $0^\circ$  and  $\theta$  Kept at  $90^\circ$

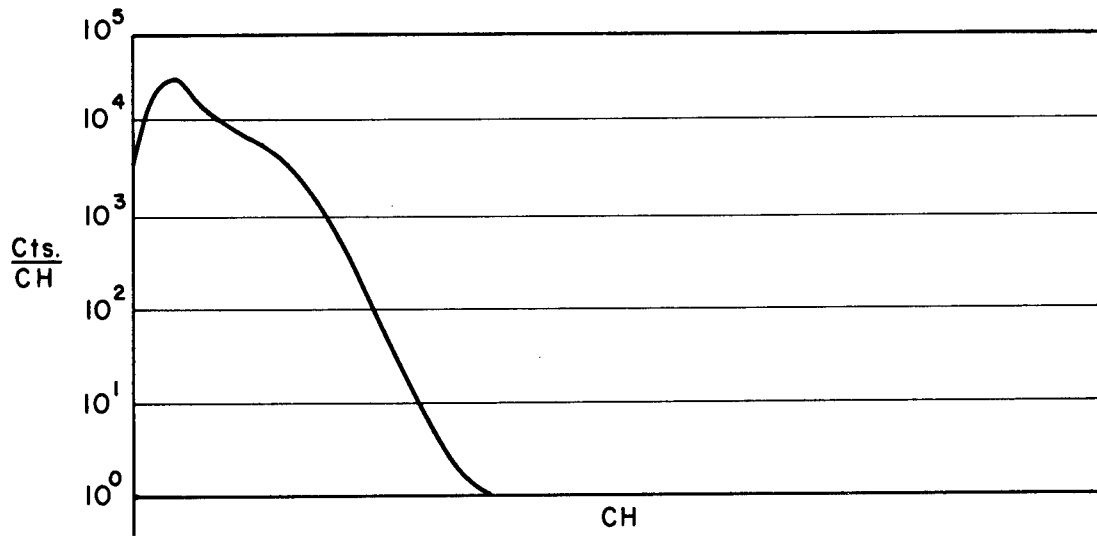


Fig. 4.38-- $^{60}\text{Co}$  Spectrum at a Distance to the Base of the Tower from the Detector of 750 Yd, Source Height of 1125 Ft, Collimator Acceptance Angle =  $30^\circ$ , with  $\phi$  Kept at  $0^\circ$  and  $\theta$  Kept at  $120^\circ$

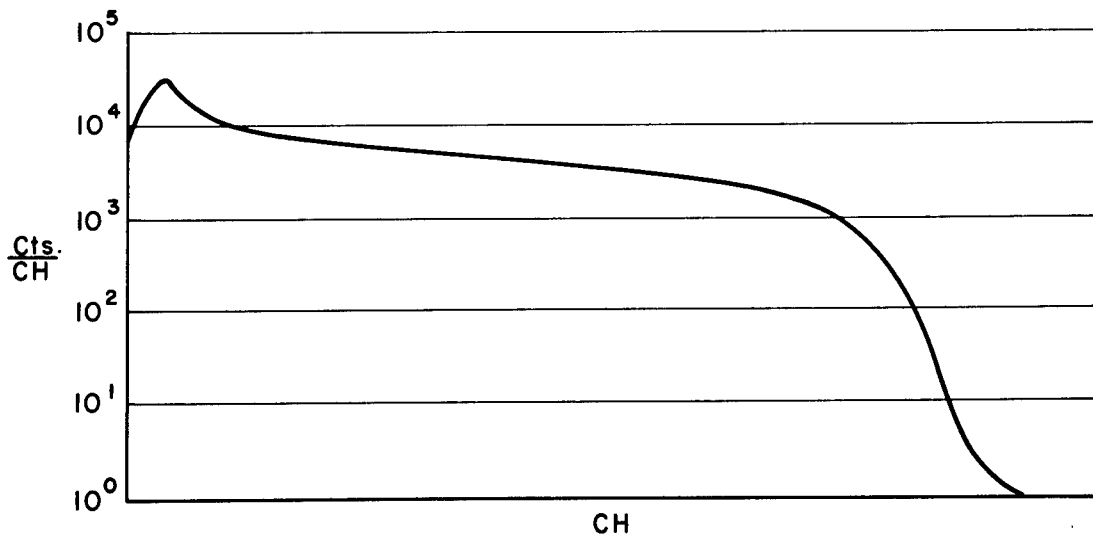


Fig. 4.39-- $^{60}\text{Co}$  Spectrum at a Distance to the Base of the Tower from the Detector of 750 Yd, Source Height of 1125 Ft, Collimator Acceptance Angle =  $10^\circ$ , with  $\theta$  Kept at  $0^\circ$  and  $\phi$  Kept at  $340^\circ$

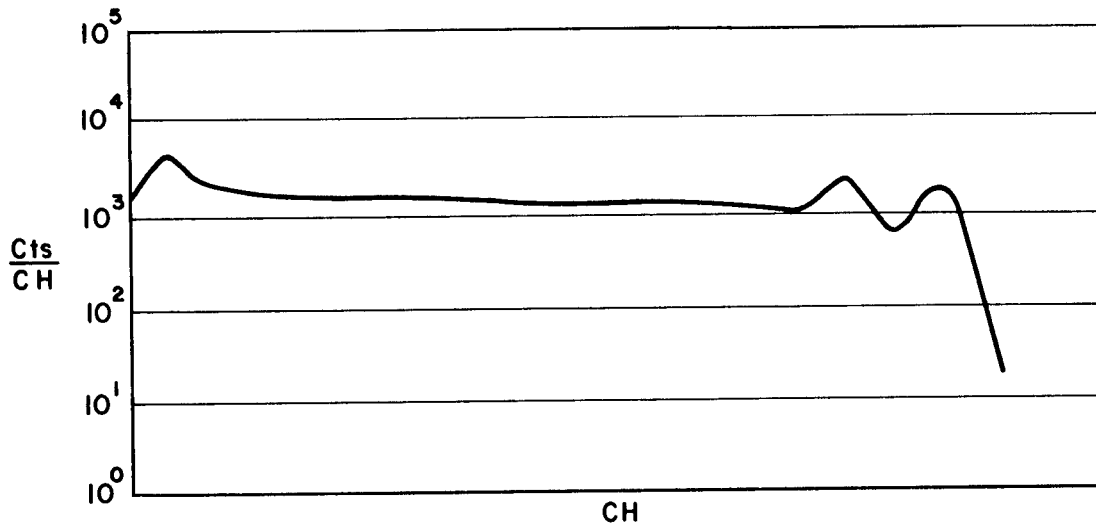


Fig. 4.40-- $^{60}\text{Co}$  Spectrum at a Distance to the Base of the Tower from the Detector of 750 Yd, Source Height of 1125 Ft, Collimator Acceptance Angle =  $10^\circ$ , with  $\theta$  Kept at  $0^\circ$  and  $\phi$  Kept at  $350^\circ$

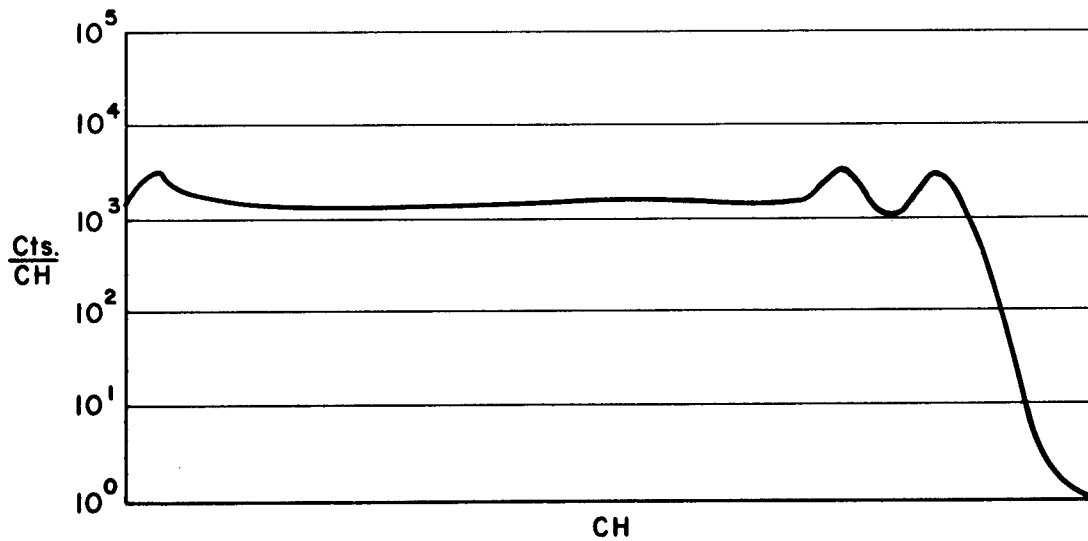


Fig. 4.41-- $^{60}\text{Co}$  Spectrum at a Distance to the Base of the Tower from the Detector of 750 Yd, Source Height of 1125 Ft, Collimator Acceptance Angle =  $10^\circ$ , with  $\theta$  Kept at  $0^\circ$  and  $\phi$  Kept at  $0^\circ$

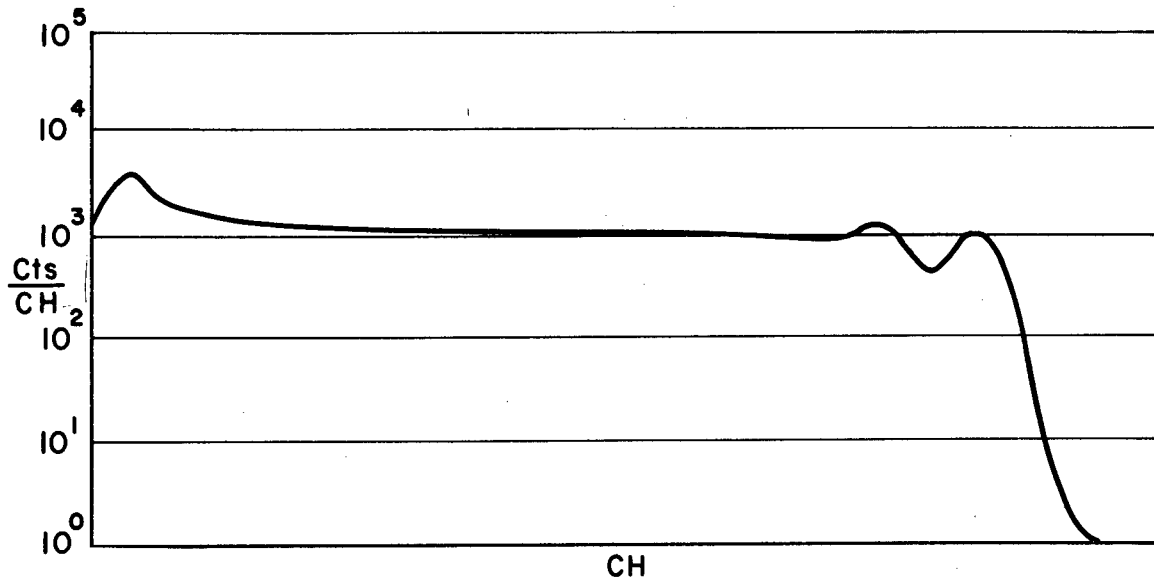


Fig. 4.42--<sup>60</sup>Co Spectrum at a Distance to the Base of the Tower from the  
 Detector of 750 Yd, Source Height of 1125 Ft, Collimator Acceptance  
 Angle = 10°, with  $\theta$  Kept at 0° and  $\phi$  Kept at 10°

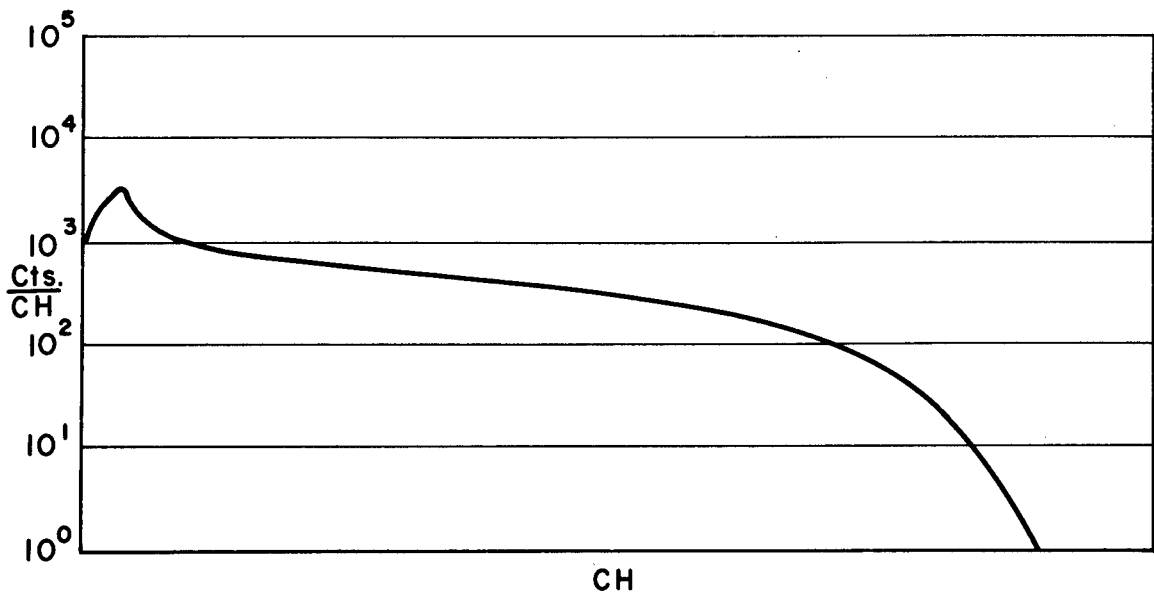


Fig. 4.43--<sup>60</sup>Co Spectrum at a Distance to the Base of the Tower from the  
 Detector of 750 Yd, Source Height of 1125 Ft, Collimator Acceptance  
 Angle = 10°, with  $\theta$  Kept at 0° and  $\phi$  Kept at 20°

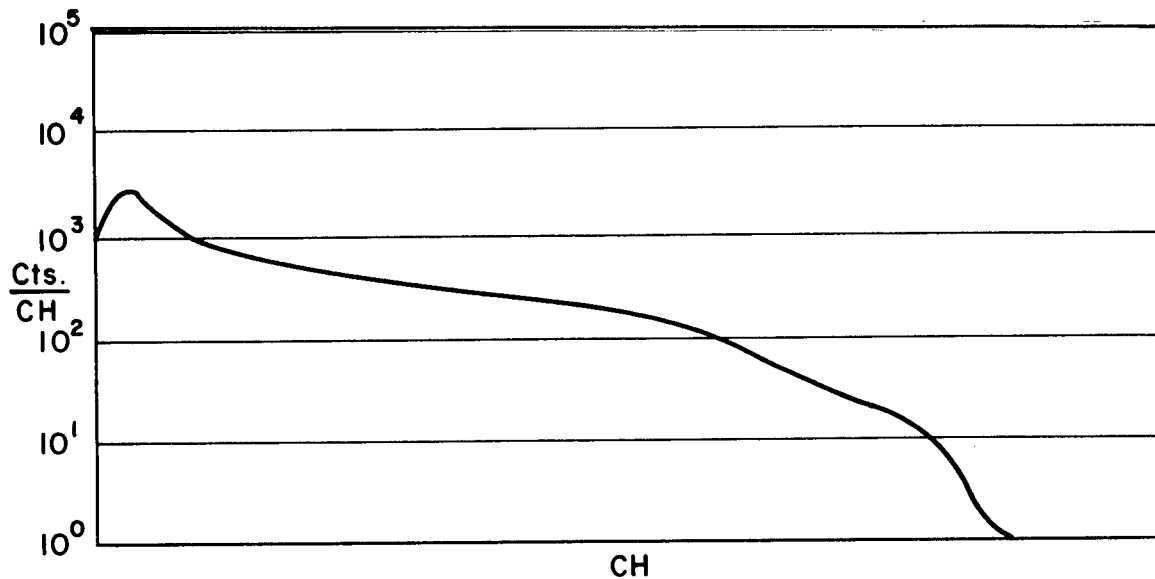


Fig. 4.44-- $^{60}\text{Co}$  Spectrum at a Distance to the Base of the Tower from the Detector of 750 Yd, Source Height of 1125 Ft, Collimator Acceptance Angle =  $10^\circ$ , with  $\theta$  Kept at  $0^\circ$  and  $\phi$  Kept at  $30^\circ$

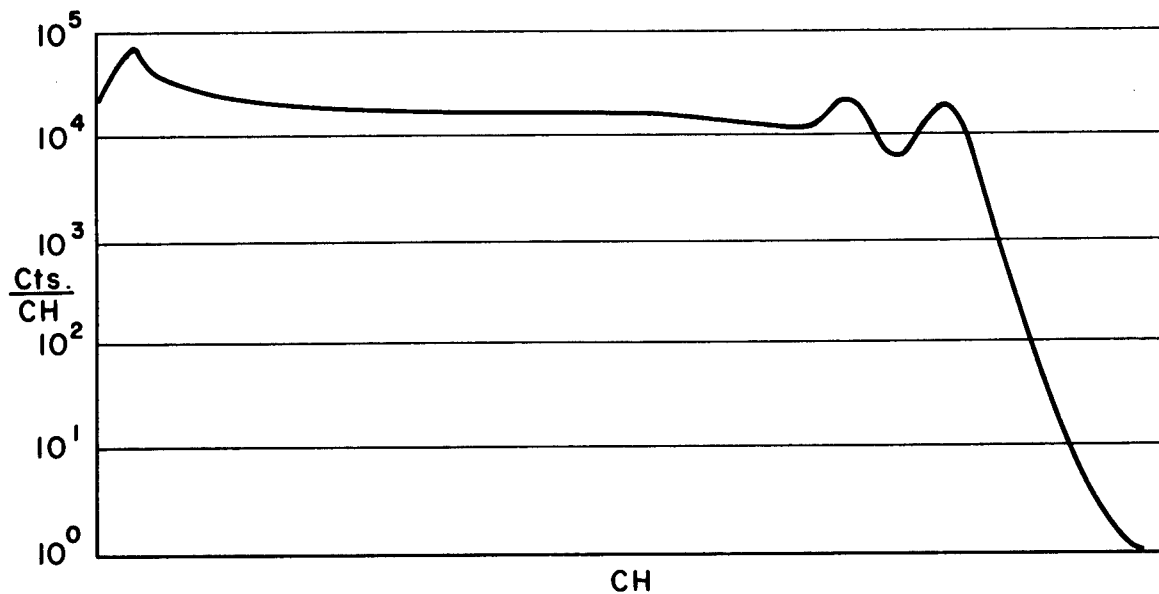


Fig. 4.45-- $^{60}\text{Co}$  Spectrum at a Distance to the Base of the Tower from the Detector of 1000 Yd, Source Height of 27 Ft, Collimator Acceptance Angle =  $30^\circ$ , with  $\theta$  Kept at  $0^\circ$  and  $\phi$  Kept at  $0^\circ$

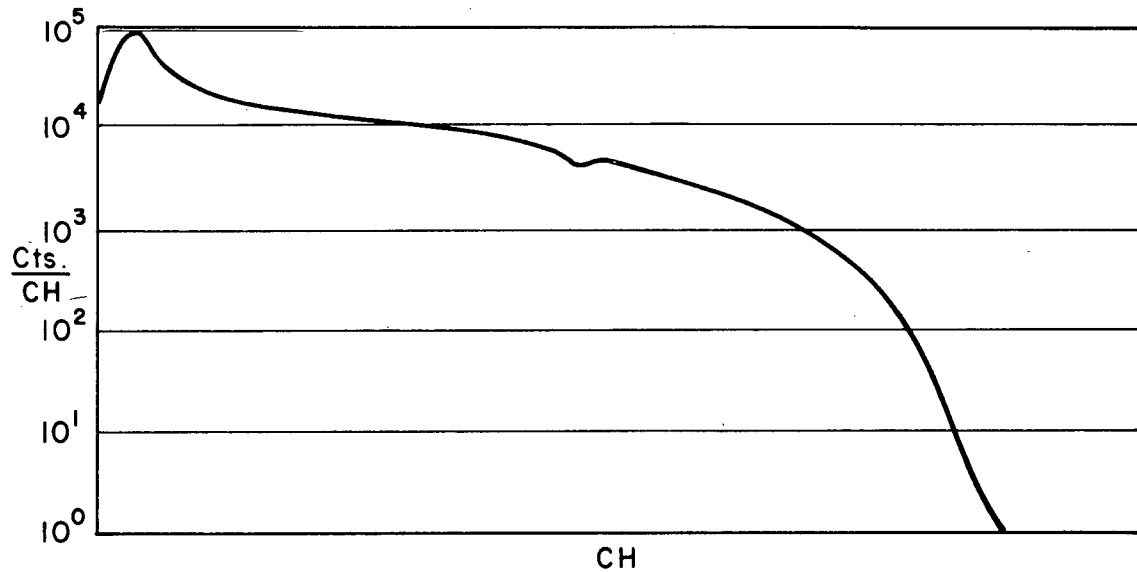


Fig. 4.46--<sup>60</sup>Co Spectrum at a Distance to the Base of the Tower from the Detector of 1000 Yd, Source Height of 27 Ft, Collimator Acceptance Angle = 30°, with  $\theta$  Kept at 0° and  $\phi$  Kept at 30°

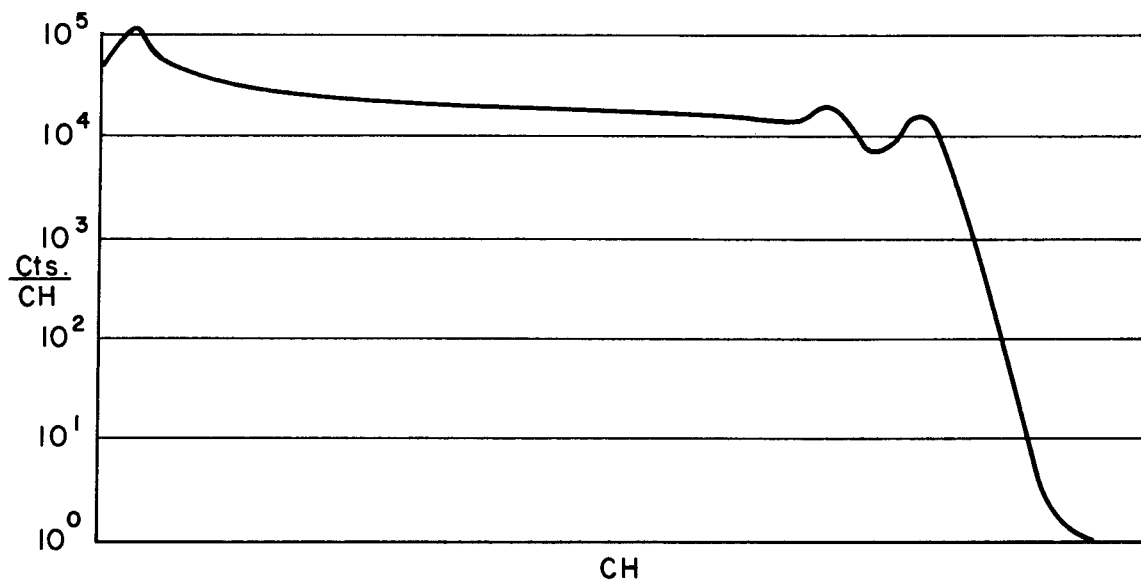


Fig. 4.47--<sup>60</sup>Co Spectrum at a Distance to the Base of the Tower from the Detector of 1000 Yd, Source Height of 300 Ft, Collimator Acceptance Angle = 30°, with  $\theta$  Kept at 0° and  $\phi$  Kept at 0°

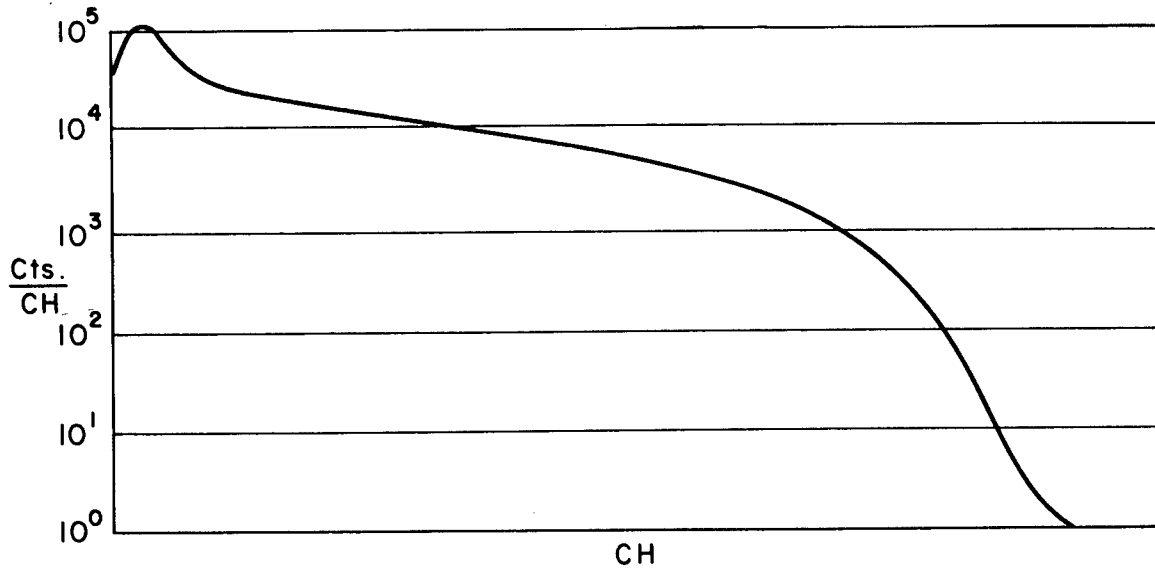


Fig. 4.48-- $^{60}\text{Co}$  Spectrum at a Distance to the Base of the Tower from the Detector of 1000 Yd, Source Height of 300 Ft, Collimator Acceptance Angle =  $30^\circ$ , with  $\theta$  Kept at  $0^\circ$  and  $\phi$  Kept at  $30^\circ$

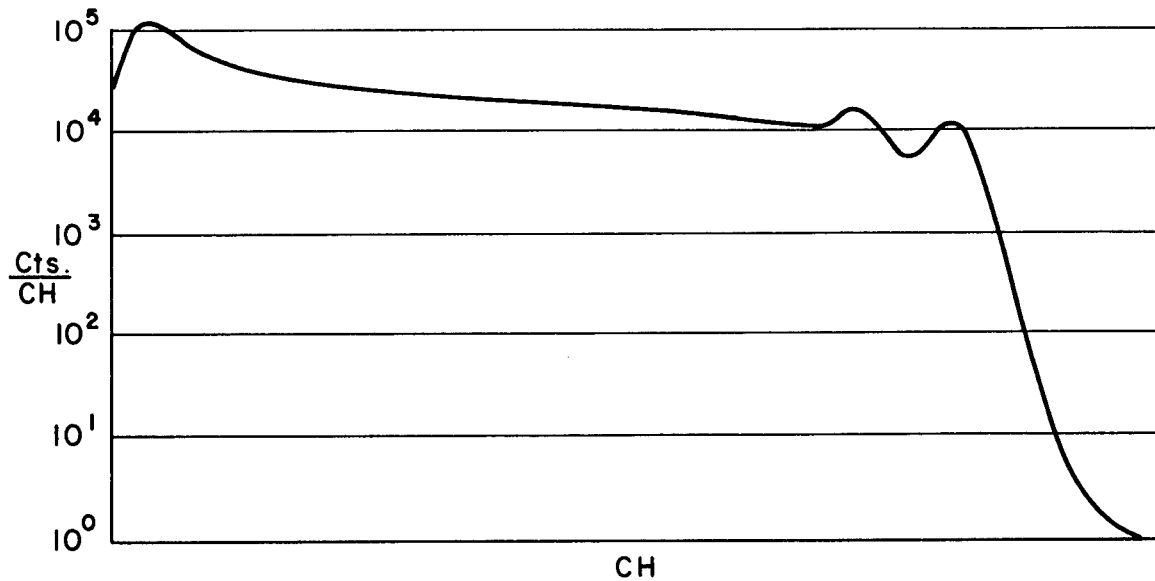


Fig. 4.49-- $^{60}\text{Co}$  Spectrum at a Distance to the Base of the Tower from the Detector of 1000 Yd, Source Height of 1500 Ft, Collimator Acceptance Angle =  $30^\circ$ , with  $\theta$  Kept at  $0^\circ$  and  $\phi$  Kept at  $0^\circ$

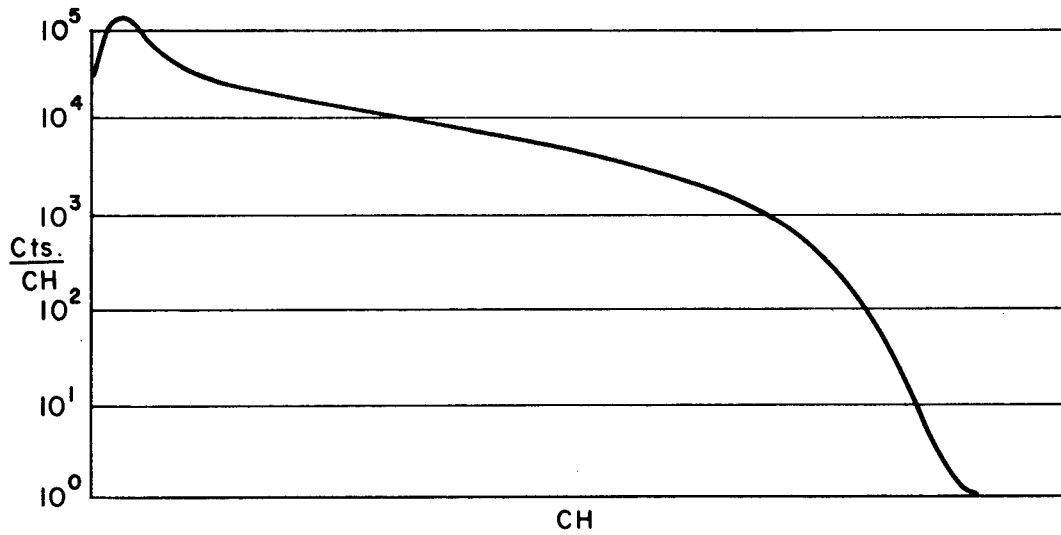


Fig. 4.50-- $^{60}\text{Co}$  Spectrum at a Distance to the Base of the Tower from the Detector of 1000 Yd, Source Height of 1500 Ft, Collimator Acceptance Angle =  $30^\circ$ , with  $\theta$  Kept at  $0^\circ$  and  $\phi$  Kept at  $30^\circ$

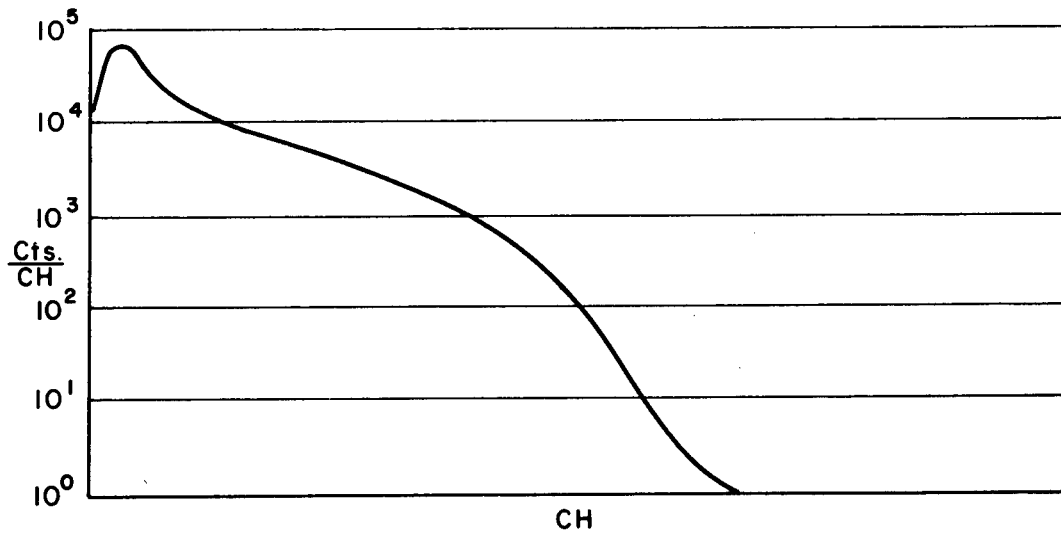


Fig. 4.51-- $^{60}\text{Co}$  Spectrum at a Distance to the Base of the Tower from the Detector of 1000 Yd, Source Height of 1500 Ft, Collimator Acceptance Angle =  $30^\circ$ , with  $\theta$  Kept at  $0^\circ$  and  $\phi$  Kept at  $60^\circ$

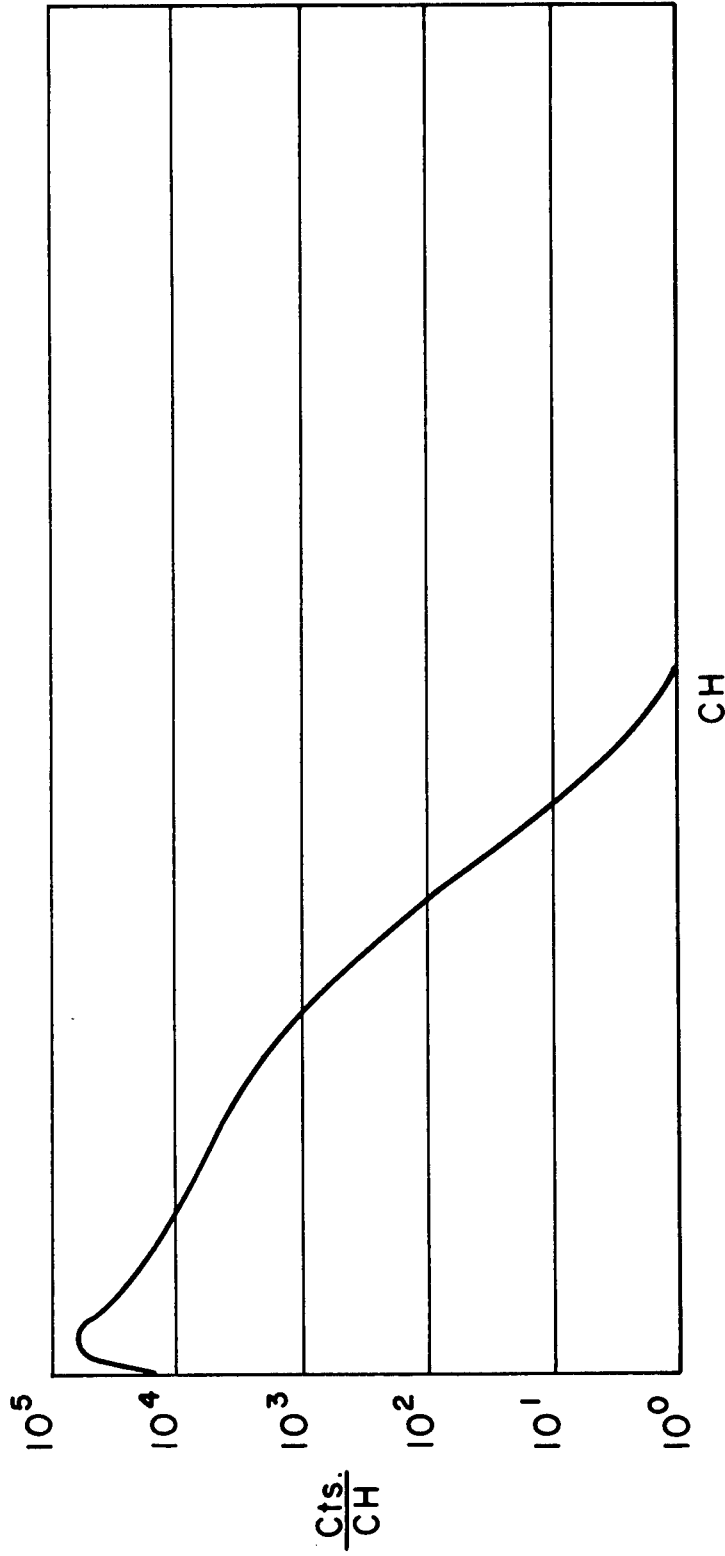


Fig. 4.52--<sup>60</sup>Co Spectrum at a Distance to the Base of the Tower from the  
 Detector of 1000 Yd, Source Height of 1500 Ft, Collimator Acceptance  
 Angle = 30°, with  $\theta$  Kept at 0° and  $\phi$  Kept at 90°

at this distance used a 30° collimator opening. With the source at 27 ft, the air-ground interface was intercepted for the  $\phi = 0^\circ$  run; all other points are above the interface.

#### REFERENCE

1. J. A. Auxier, F. F. Haywood, and L. W. Gilley, General Correlative Studies - Operation BREN, USAEC Report CEX-62.03, September 1963.

## Chapter 5

### CONCLUSION

The dose data obtained with the reactor as the source show that the radiation field is symmetrical about the zero angle except for angles at which the air-ground interface is intercepted. As a result, the radiation dose field can be described solely as a function of the polar angle for all angles which do not intercept the interface. The  $^{60}\text{Co}$  spectra measured as a function of angle verify these results.

An interesting comparison between the BREN gamma-dose angular distribution measurements and the weapons test data<sup>1</sup> can be made. While the neutron data were similar to that obtained from weapons tests, the reactor gamma-ray distribution measured during BREN is not as sharply peaked in the forward direction as the weapons data. A logical reason for this difference can be found if the two radiation sources are compared. For a weapon, the gamma-ray field consists primarily of gamma rays from fission products and neutron interactions with the air and with soil; during BREN, the reactor core retained products and thus provided shielding of the fission product gamma rays, but the gamma-ray field from neutron interactions was identical to that produced by a weapon. Because the air, as a radiation source, is a large volume or diffuse source, the angular dose distribution should be less peaked in the forward direction, as observed. On the other hand, the  $^{60}\text{Co}$  gamma rays are nearer to the mean energy of the fission-produced gamma rays so that the angular dose distribution should be sharply peaked in the forward direction, as with a weapon where a significant fraction of the gamma rays are produced by fission products. This is in good agreement with the dose distributions measured during BREN with the  $^{60}\text{Co}$  source.

Other interesting effects produced by the predominance of neutron-produced gamma rays on the BREN measurements are given in the reports concerning spatial distributions of the dose fields in air and in radiation analogs of Japanese houses.<sup>2,3</sup>

#### REFERENCES

1. R. H. Ritchie and G. S. Hurst, Penetration of Weapons Radiation: Application to the Hiroshima-Nagasaki Studies, Health Phys., 1: 390-404 (1959).
2. J. S. Cheka, F. W. Sanders, T. D. Jones, and W. H. Shinpaugh, Distribution of Weapons Radiation in Japanese Residential Structures, USAEC Report CEX-62.11, August 1965.
3. F. F. Haywood, J. A. Auxier, and E. T. Loy, An Experimental Investigation of the Spatial Distribution of Dose in an Air-over-Ground Geometry, USAEC Report CEX-62.14, October 1964.

## CIVIL EFFECTS TEST OPERATIONS REPORT SERIES (CEX)

Through its Division of Biology and Medicine and Civil Effects Test Operations, the Atomic Energy Commission conducts certain technical tests, exercises, surveys, and research directed primarily toward practical applications of nuclear effects information and toward encouraging better technical, professional, and public understanding and utilization of the vast body of facts useful in the design of countermeasures against weapons effects. The activities carried out in these studies do not require nuclear detonations.

The following is a partial list of all reports available from studies that have been completed. All reports listed are available, at \$3.00 each, from the Clearinghouse for Federal Scientific and Technical Information, U. S. Department of Commerce, Springfield, Va. 22151.

- CEX-58.1, Experimental Evaluation of the Radiation Protection Afforded by Residential Structures Against Distributed Sources, J. A. Auxier, J. O. Buchanan, C. Eisenhauer, and H. E. Menker, 1959.
- CEX-58.7, AEC Group Shelter, AEC Facilities Division, Holmes & Narver, Inc., 1960.
- CEX-58.8, Comparative Nuclear Effects of Biomedical Interest, C. S. White, I. G. Bowen, D. R. Richmond, and R. L. Corsbie, 1961.
- CEX-58.9, A Model Designed to Predict the Motion of Objects Translated by Classical Blast Waves, I. G. Bowen, R. W. Albright, E. R. Fletcher, and C. S. White, 1961.
- CEX-59.1, An Experimental Evaluation of the Radiation Protection Afforded by a Large Modern Concrete Office Building, J. F. Batter, Jr., A. L. Kaplan, and E. T. Clarke, 1960.
- CEX-59.7B (Pt. I), Experimental Radiation Measurements in Conventional Structures. Part I. Radiation Measurements in Two Two-story and Three One-story Typical Residential Structures Before and After Modification, Z. G. Burson, 1966.
- CEX-59.7B (Pt. II), Experimental Radiation Measurements in Conventional Structures. Part II. Comparison of Measurements in Above-ground and Below-ground Structures from Simulated and Actual Fallout Radiation, Z. G. Burson, 1964.
- CEX-59.7B (Pt. III), Experimental Radiation Measurements in Conventional Structures. Part III. The Attenuation of Air-scattered Radiation in a Basement, Z. G. Burson, 1965.
- CEX-59.13, Experimental Evaluation of the Radiation Protection Afforded by Typical Oak Ridge Homes Against Distributed Sources, T. D. Strickler and J. A. Auxier, 1960.
- CEX-59.14, Determinations of Aerodynamic-drag Parameters of Small Irregular Objects by Means of Drop Tests, E. P. Fletcher, R. W. Albright, V. C. Goldizen, and I. G. Bowen, 1961.
- CEX-60.1, Evaluation of the Fallout Protection Afforded by Brookhaven National Laboratory Medical Research Center, H. Borella, Z. Burson, and J. Jacovitch, 1961.
- CEX-60.3, Extended- and Point-source Radiometric Program, F. J. Davis and P. W. Reinhardt, 1962.
- CEX-60.5, Experimental Evaluation of the Fallout-radiation Protection Afforded by a Southwestern Residence, Z. Burson, D. Parry, and H. Borella, 1962.
- CEX-60.6, Experimental Evaluation of the Radiation Protection Provided by an Earth-covered Shelter, Z. Burson and H. Borella, 1962.
- CEX-61.1 (Prelim.), Gamma Radiation at the Air-Ground Interface, K. O'Brien and J. E. McLaughlin, Jr., 1963.
- CEX-61.4, Experimental Evaluation of the Fallout-radiation Protection Provided by Selected Structures in the Los Angeles Area, Z. G. Burson, 1963.
- CEX-62.01, Technical Concept—Operation BREN, J. A. Auxier, F. W. Sanders, F. F. Haywood, J. H. Thorngate, and J. S. Cheka, 1962.
- CEX-62.2, Nuclear Bomb Effects Computer (Including Slide-rule Design and Curve Fits for Weapons Effects), E. R. Fletcher, R. W. Albright, R. F. D. Perret, Mary E. Franklin, I. G. Bowen, and C. S. White, 1963.
- CEX-62.11, Distribution of Weapons Radiation in Japanese Residential Structures, J. S. Cheka, F. W. Sanders, T. D. Jones, and W. H. Shinpaugh, 1965.
- CEX-62.13, Post Pulse Gamma-radiation Spectrum—Operation BREN, J. H. Thorngate and E. T. Loy, 1966.
- CEX-62.14, An Experimental Investigation of the Spatial Distribution of Dose in an Air-over-Ground Geometry, F. F. Haywood, J. A. Auxier, and E. T. Loy, 1964.
- CEX-62.50, Neutron-field and Induced-activity Measurements—Operation BREN, F. M. Tomnovce and J. M. Ferguson, 1965.
- CEX-62.81 (Final), Ground Roughness Effects on the Energy and Angular Distribution of Gamma Radiation from Fallout, C. M. Huddleston, Z. G. Burson, R. M. Kinkaid, and Q. G. Klinger, 1964.
- CEX-63.3, Barrier Attenuation of Air-scattered Gamma Radiation, Z. G. Burson and R. L. Summers, 1965.
- CEX-63.7, A Comparative Analysis of Some of the Immediate Environmental Effects at Hiroshima and Nagasaki, C. S. White, I. G. Bowen, and D. R. Richmond, 1964.
- CEX-63.10, Design of a Shielded Source for the Irradiation of Natural Animal Populations, A. C. Lucas, Z. G. Burson, and R. E. Lagerquist, 1966.
- CEX-64.3, Ichiban: The Dosimetry Program for Nuclear Bomb Survivors of Hiroshima and Nagasaki—A Status Report as of April 1, 1964, J. A. Auxier, 1964.
- CEX-64.7, Neutron and Gamma-ray Leakage from the Ichiban Critical Assembly, J. H. Thorngate, D. R. Johnson, and P. T. Perdue, 1966.
- CEX-65.01, Feasibility Study: Intense 14-Mev Neutron Source for Operation HENRE, T. G. Provenzano, E. J. Story, F. F. Haywood, and H. T. Miller, 1966.
- CEX-65.02, Technical Concept—Operation HENRE, F. F. Haywood and J. A. Auxier, 1965.
- CEX-65.03, Operations Plan—Operation HENRE, Technical Director's Staff, 1965.
- CEX-65.4, Biological Tolerance to Air Blast and Related Biomedical Criteria, C. S. White, I. Gerald Bowen, and D. R. Richmond, 1965.